

Experimental and Numerical Investigation of Drilling
Performance in Anisotropic Formations and with Axial
Compliance at the Bit

by

© Abourawi Alwaar

A Thesis submitted to the

School of Graduate Studies

in partial fulfillment of the requirements for the degree of

Master of Engineering

Faculty of Engineering and Applied Science

Memorial University of Newfoundland

Abstract

As drilling performance is a key indicator of success in the oil and gas industry, numerous academic and industry organizations have been researching how to improve drilling with regard to time and efficiency. A study is done to determine rock isotropy by applying mechanical and physical measurements, along with oriented drilling, as anisotropy has a distinct impact in drill performance. Based on these findings, the study then performs drilling experiments on anisotropic rock in order to gauge the effect of anisotropy on drill efficiency. The tests employ a dual-cutter PDC bit, 35 mm, and use several different WOB under constant atmospheric pressure and water flow. In looking at relationships of WOB, ROP and DOC, it is clear that increasing the WOB leads to a subsequent increase in DOC and ROP. Furthermore, increasing the WOB also leads to increases in cutting sizes as well as material anisotropy. At Memorial University in Newfoundland, Canada, the Drilling Technology Laboratory (DTL) has developed a passive vibration-assisted rotational drilling (p-VARD) tool which enhances drill rates of penetration (ROP) in lab tests. Previous lab experiments, including simulations, point to axial vibrations having significantly improved ROP. These experiments are carried out by applying the Discrete Element Method (DEM) simulation, using the DTL p-VARD configurations tool. To gauge the tool's cutting efficiency, a PFC2D (i.e., particle flow code in two dimensions) numerical model is utilized in simulating micro-crack generation/propagation for the drill procedure on synthetic rocks. The pVARD tool compares the downhole vibration with the rigid drill configuration of conventional rotary drilling, using low, medium and high spring compliance. Next, output parameters for ROP, MSE, and DOC are analyzed for pVARD/ non-pVARD configurations. The overall results point to the pVARD tool having a positive impact in downhole drilling, showing improvements in DOC, MSE, and ROP.

Acknowledgement

I wish to extend my sincere thanks to the many people who have assisted me in my research endeavours.

First of all, I would like to thank my family for their love and support, which encouraged me to continue with this work to the very end.

As well, I wish to thank my graduate supervisor, Dr. Stephen Butt, for his support and encouragement as well as his deep insights into the thesis problem, which guided me to find appropriate solutions.

In addition, I thank my friend, Abdel Salaam, for his assistance in programming the simulations, and I also thank the Drilling Technology Laboratory group members for their ongoing support.

This work was done at the Drilling Laboratory Technology (DTL) at Memorial University of Newfoundland in St. John's, Canada. The project is funded by Atlantic Canada Opportunity Agency (AIF contract number: 781-2636-1920044), involving Husky Energy, Suncor Energy and Research and Development Corporation (RDC) of Newfoundland and Labrador. Financial support is also provided by the Ministry of Higher Education and Scientific Research, Libya,

Contents

Abstract.....	II
Acknowledgement	III
List of Tables	VIII
List of Figures.....	IX
List of Abbreviations, Nomenclature, and Symbols	XIV
Chapter 1	1
1.1 General.....	1
1.2 Scope and objectives of the work.	2
1.3 Organization of Thesis.	2
Chapter 2	4
Literature Review	4
2.1 Overview	4
2.2 Historical background.....	6
2.3 PDC Bit Penetration Mechanisms	9
2.4 Natural Vibrations of Single PDC Cutter Penetration.....	12
2.5 ROP and Drilling Efficiency	16
2.6 pVARD Tools.....	17
2.7 Distinct Element Method.....	17
2.8 Cutter-rock interaction.....	19

2.9. Impact of drill string vibrations on drilling efficiency during Penetration.....	20
2.10.1 Axial vibrations.....	23
2.11.2. Torsional vibrations	24
2.12.3. Lateral/transverse vibrations.....	25
2.13 Impact of Bottom-Hole Cleaning during Rock Penetration.	30
2.14. Impact of Axial Compliance on Drill String.	32
2.15 Impact of Stiffness, Damping, and Compliance in Down-hole Vibration and Drilling Performance.....	34
2.15. Brief explanation of anisotropic rocks.....	34
Chapter 3	39
Baseline development of rock anisotropy investigation utilizing empirical relationships between oriented physical and mechanical measurements and drilling performance	39
3.1. Introduction	40
3.2. Test Procedure And Apparatus.....	41
3.3 Sample Preparation.....	42
3.4. Conducted Tests	42
3.5. Physical Properties’ measurements	43
3.6. Mechanical Tests	47
3.6.1. UCS test	47
3.1.2 PLI test.....	49

3.6.3 IT test	51
3.6.4. Drilling Tests	53
3.7. Summary.....	57
Chapter 4	59
Laboratory Investigation on Directional Drilling Performance in Isotropic and Anisotropic Rocks	59
4.1. Introduction	60
4.2. Experimental Equipment And Procudre.....	62
4.2.1 Physical measurements	62
4.2.3 Mechanical measurements	68
4.2.4 Lab. Drilling experiments	71
4.2.4.1 Lab drilling apparatus.....	71
4.2.4.2 RLM and R-Shale samples preparation for drilling experiments	71
4.2.4.3 Drilling cuttings' collection	73
4.3. Lab experiments results	74
4.3.1 Drilling performance.....	74
4.3.1.1 WOB vs. ROP and DOC	74
4.3.1.2 Cutting size analysis.....	75
4.6. Conclusions	78
Chapter 5	80

PFC-2D Numerical study of the influence of passive vibration assisted rotary drilling tool (pVARD) on drilling performance enhancement	80
5.1. Introduction And Background.....	81
5.2. Description Of Pvard	83
5.3. Studied Parameters	83
5.4. Results	86
5.4. Double parameter analysis	88
5.5. Multiple parameter analysis	92
Chapter 6 Conclusion and Future Work.....	99
6.1. Conclusion	99
6.2. Future Work.....	100
References	101

List of Tables

Table 1. Effects of Drill String Vibration According to Vibration Mode (Mohammed Fayez 2012).....	27
Table 2. Simulation results of the AGT and Hydropulse tool without and with the shock tool (Gharibiyamchi 2013)	32
Table 3. Summary of number of samples, type of tested conducted, and the orientation of tests.	42
Table 4. Mean values of Vp, Vs and UCS for the standard samples of UCS test.....	49
Table 5. Test matrix of lab oriented drilling experiments including WOB, ROP, and DOC....	55
Table 6. Calculated ROP for RLM and Red Shale.....	57
Table 7. Mean values of oriented Vp, Vs, density, and dynamic elastic moduli of RLM	64
Table 8. Mean values of oriented Vp, Vs, and density of two R-Shale samples1, and 2, respectively.....	65
Table 9. All and mean values of the measured Vp and Vs of several R-Shale samples in directions parallel to bedding in various locations.....	66
Table 4.10 contains the estimated UCS values of R-Shale samples obtained by point load perpendicularly to bedding. The mean value of the PLI = 2.7MPa.	70
Table 11. Summary of PLI test values of R-Shale samples	70
Table 12. Drilling parameters of WOB, ROP and DOC for RLM and R-Shale	74
Table 13. Summary of PFC-2D parameters and their magnitudes.....	84
Table 14. Summary of DOC result in PFC-2D and laboratory work.	87

List of Figures

Figure 1. Smith standard 6-inch Mi 711 1 (Schlumberger 2017).....	10
Figure 2. Conditions and components o 1 (Khorshidian et al.,2012).....	14
Figure 3. Spectrum of vertical velocity at horizontal speed of 1.5 m/s and vertical load of 125 KN (Khorshidian et al 2012).....	14
Figure 4. Spectrum of cutter vertical force at vertical load of 125 kN (Khorshidian et al. (2012)	15
Figure 5. Spectrum of cutter vertical position at vertical load of 125 kN (Khorshidian et al., (2012)	15
Figure 6. Axial vibration and “bit bounce” (Ashley et al 2001).....	24
Figure 7. Torsional vibrations and “stick-slip” (Ashley et al 2001).....	25
Figure 8. Lateral vibrations of drill strings (Ashley et al 2001).	26
Figure 9. Li’s experimental results of vibration assisted rotary drilling ROP & WOB.	29
Figure 10. ROP curves vs. WOB and rotary speed for ideal and actual drilling conditions (Maurer model)	30
Figure 11. Effect of shock tool in drilling performance of the AGT (BHP = 1000 psi, WOB = 60 kN and sinusoidal force amplitude of 19.25 kN) (Gharibiyamchi 2013).....	33
Figure 12. Effect of shock tool in drilling performance of the Hydropulse tool (BHP = 1000 psi, WOB = 60 kN and pulse amplitude of 198.5 kN) (Gharibiyamchi 2013).	34
Figure 13. Apparatus used for Vp and Vs measurement.	44
Figure 14. Sample of the recorded waves	44

Figure 15. Vp, Vs, and Density of all samples of Axial and Block PLI tests in different orientations	45
Figure 16. Mean values of measured Vp and Vs of standard UCS test in different orientations	45
Figure 17. Mean values of the measured Vp and Vs of samples of Axial and Block-PLI test in different directions.	46
Figure 18. Mean values of P-wave, S-wave, and Elastic Moduli in three orientations.....	46
Figure 19. Mean of Lamé' Constant and Bulk Modulus in three orientations	47
Figure 20. Mean value of Poisson's ratio in three orientations	47
Figure 21 . Samples of UCS test cored in different orientations	48
Figure 22. Mean values of UCS	48
Figure 23. Samples of Axial and Block tests with PLI tester.....	49
Figure 24. UCS Vs. Is.....	50
Figure 25. UCS values by PLI using different "c" factors.	50
Figure 26. Mean Values of UCS values by different tests.	51
Figure 27. IT strength of the tested samples and their densities.....	52
Figure 28. Estimated strength by IT and PLI tests	52
Figure 29. Tested Samples by IT test.	52
Figure 30. Top: LTS and grooved rotating plate for rpm calculation and bottom: recorded spikes by LTS to calculate rpm. For this run, RPM= 280.....	54
Figure 31. Sample of the recorded data used to calculate ROP. For this run, the slope = ROP of 8.00 (m/hr).....	54

Figure 32. WOB Vs. ROP for three different flow rates and three different orientations	55
Figure 33. Some samples of drilling tests with PDC drill bit.....	56
Figure 34. Drilling performance through RLM (top) and Red Shale (bottom).....	56
Figure 35. Oriented density and wave velocity measurements of RLM	63
Figure 36. The oriented dynamic elastic moduli of RLM	63
Figure 37. Oriented density and wave velocity measurements of R-Shale-1.....	64
Figure 38. Oriented density and wave velocity measurements of R-Shale-2.....	65
Figure 39. All and mean values of Vp and Vs measured in parallel direction to R-Shale bedding.	67
Figure 40. Multi measurements of Vp and Vs in two sets of parallel faces in parallel direction to R-Shale bedding.....	67
Figure 41. Mean values of oriented (σ) of RLM by splitting test.	68
Figure 42. RLM samples before and after test and splitting test apparatus.....	69
Figure 43. R-Shale samples for oriented physical characterization and point load test.....	70
Figure 44. Lab scale conventional drill rig.....	71
Figure 45. RLM and R-Shale samples after drilling in different orientations.....	72
Figure 46. RLM samples before and after drilling	72
Figure 47. Cutting samples and cutting sieving apparatus	73
Figure 48. Oriented relationship between WOB and ROP of RLM.....	75
Figure 49. Oriented relationship between WOB and ROP of R-Shale	75

Figure 50. Cutting size analysis with the increase of WOB in drilling RLM in the three orientations 0°, 45°, and 90°. Figures show matching distribution confirming isotropy of RLM.	77
Figure 51. Cutting size analysis with the increase of WOB in drilling RLM in the three orientations 0°, 45°, and 90°. Figures show mismatching distribution confirming isotropy of RLM	78
Figure 52. Description of the numerical study of the drilling process using PFC-2D, including weight on bit in case of PVARD.....	85
Figure 53. One set of PFC-2D output using rigid drilling for different BHP and same WOB=2354.4N.	86
Figure 54. One example of data comparison between simulation and experimental work using the 3rd pVARD configuration.....	88
Figure 55. ROP vs. DOC for simulated pVARD 1	89
Figure 56. ROP vs. DOC for simulated pVARD 2	89
Figure 57. ROP vs. DOC for simulated pVARD 3	90
Figure 58. ROP vs. DOC for simulated RIGID.....	90
Figure 59. ROP vs. MSE for simulated pVARD1.	91
Figure 60. ROP vs. MSE for simulated pVARD 2.....	91
Figure 61. ROP vs. MSE for simulated pVARD 3.....	92
Figure 62. ROP vs. MSE for simulated RIGID.....	92
Figure 63. Compared experimental ROP in all drilling modes of pVARD and rigid.	93
Figure 64. Compared simulated ROP in all drilling modes of pVARD and rigid.	93
Figure 65. Compared experimental DOC in all drilling modes of pVARD and rigid.	94

Figure 66. Compared simulated DOC in all drilling modes of PWARD and rigid.94

Figure 67. Compared experimental MSE in all drilling modes of pWARD and rigid.....95

Figure 68. Compared simulated ROP in all drilling modes of pWARD and rigid.95

Figure 69. Compared result of ROP for all drilling modes of experimental work vs. PFC-2D
numerical work.....96

Figure 70. Compared result of MSE for all drilling modes of experimental work vs. PFC-2D
numerical work.....96

List of Abbreviations, Nomenclature, and Symbols

Ach	Chamfer area
a	Repression angles
BHP	Bottom-Hole Pressure
BHA	Bottom Hole Assemblies
BHC	Bottom-Hole Cleaning
C	Damping Ratio
CCS	Confined Compressive Strength
CFD	Computational Fluid Dynamic
DEM	Distinct Element Method
DTL	Drilling Technology Laboratory
DOC	Depth of Cut
DTL	Drilling Technology Laboratory
d	Depth of cut
E	Drilling specific energy
FEM	Finite Element Method
Fcs	Horizontal force on cutter
Fcn	Vertical force on cutter v_i
Fc	Face cutter force
Fch	Chamfer force
Fb	Back cutter force
GPM	Gallon per Minute
g	Gravity
IADC	International Association of Drilling Contractors

IT Indirect Tensile

IS Indirect shear

J Energy

K Spring Stiffness

Kf Bulk modulus

LWD Logging while drilling

MWD Measurement while Drilling

MRR Material Removal Rate

MSE Mechanical Specific Energy

M Mass

PDC Polycrystalline Diamond Compact

pVARD Tools Passive Vibration Assisted Rotational Drilling (VARD) Tools

PFC Particle Flow Code

PLT Point Load Strength Index

PDC Polycrystalline Diamond Compact

POOH pull-out-of-hole

R Ball radius

ROP Rate of Penetration

RPM Revolution per Minute

RLM Rock Like Material

R Ball radius

S Drilling strength

SEM Scanning Electron Microscope

TOB Torque on Bit

UCS	Unconfined Compressive Strength
U_n	Amount of overlap
V_s	Shear Wave Velocity
V_p	compressional velocity
WOB	Weight on Bit
X_i	Position vector
XRD	X-ray diffraction
Θ	Back rake angle
μ	Coefficient of friction
ρ	Density
ζ	Intrinsic specific energy
ψ	Interfacial friction angle
μ	Coefficient of friction
γ	Bit constant
l	Contact length
σ	Contact strength
σ_0	Hydrostatic stress in crushed material
ω_d	Relief angle
ρ	Density

Chapter 1

1.1 General

Rocks are considered to have anisotropic features if their thermal, seismic, hydraulic, and mechanical properties are directionally variable. Anisotropy is considered such an important characteristic in rock engineering that applications which overlook anisotropic features in the rock being studied end up with errors (Amadei, 1997). In fact, rock engineering and any type of rock mechanics cannot proceed without the engineer having a basic understanding of the anisotropy of the rock or rocks at issue.

The anisotropic features of rocks depend largely on their origins, such as sedimentary rock stratification and metamorphic rock mineral foliation, along with rock mass discontinuities. In rock engineering, knowing the anisotropy type and extent is crucial in measuring stress, particularly when applying the over-coring approach. Knowing the anisotropy type and extent is also critical for preventing damage caused by excavation and for displacement control (Amadei, 1996). Furthermore, anisotropy should be taken into consideration in applying the equivalent continuum method for rock masses, due to significant deformations which may occur in the discontinuities. Overall, then, mechanical rock anisotropy forms an integral part of rock engineering, and operations should not be proceeded until the anisotropy (typically defined according to the elastic modulus ratio) has been determined (Cho et al., 2012).

In materials, anisotropic elastic behavior can be deduced by determining the contributions of 21 elastic constants as well as symmetry (Lekhnitskii, 1963). In general, a material's symmetric inner composition will reflect in the symmetry of the material's elastic properties. Of the numerous types recorded for elastic symmetry, transversely isotropic models are usually applied

in rock mechanics. The transversely isotropic planes are related to rock stratification and foliation, as well as rock discontinuity (Lekhnitskii, 1963).

1.2 Scope and objectives of the work.

The present work aims to find the best approach to achieving optimal drilling performance by increasing both the Weight on Bit (WOB) and rate of penetration (ROP) in anisotropic formation and with axial compliance at the bit. The conducted experiments include physical measurements, mechanical measurements, and drilling tests followed by oriented drilling (i.e. 0°, 45° and 90°). also conducted drill cuttings analysis with comparison to artificial rocks (RLM). The relationships between the drilling data were evaluated including drilling rate of penetration (ROP), depth of cut (DOC), and the mechanical specific energy (MSE) and corresponding effective WOB. The investigations will be carried out across a broad range of conditions, with and without the use of pVARD technology. Factors such as extreme flow rate, extreme bottom-hole pressure (BHP), extreme WOB will be simulated on a variety of rocks under parameters that would not be possible in real-world conditions

1.3 Organization of Thesis.

The thesis is organized in six chapters.

Chapter 1. Introduce the background to the problem, the need for research, objectives, and scope of the study.

Chapter 2. Provides a literature review, exploring recently published work on enhancement of drilling performance through simulations and modeling. Highlighted topics of the review cover aspects such as ROP, WOB, MSE, PDC bits penetration mechanisms, and cut depth.

Chapter 3. baseline development of rock anisotropy investigation utilizing empirical relationships between oriented physical and mechanical measurements and drilling performance.

Chapter 4. laboratory investigation on directional drilling performance in isotropic and anisotropic rocks.

Chapter 5. Pfc-2d numerical study of the influence of passive vibration assisted rotary drilling tool (pVARD) on drilling performance enhancement

Chapter 6. a summary of the whole study is presented, contains conclusions and recommendations for future work. Optimization of drilling productivity is one of the main subjects to be discussed in this chapter.

Chapter 2

Literature Review

2.1 Overview

Drill string vibrations are one of the main problems in drilling, particularly for applications in directional wells or horizontal wells, where the weight on the bit can not be properly controlled. This can lead to a reduction in the penetration rate due to the twist-offs in the drilling string and as a result of fishing time. Premature downhole failure of measurement while drilling (MWD) systems has a negative impact on the stability of the wellbore and reduces the life of the joint between tool joints. However, it is possible to reduce the total cost of the operation by reducing the vibration of the drill string (Reich, 1995).

Drill strings are tubes of varying lengths made up several different tools, bits, etc including stabilizers, drill collars and pipes. The primary purpose of this collective system is to transfer the rotary motion created by the rotary table to the drill bit located downhole. Additionally, the drill strings can generate the axial force needed to pulverize rock and forcefully enter into the formation. This type of force is called weight-on-bit (WOB) and is usually created through the weight of the drill string, although it can also develop at the hydraulic cylinders, uphole. Drill strings can be either short or long, depending on what they are being used for. So, for instance, in drilling oil wells, strings can be several thousand meters long and comprise stabilizers, drill pipes and collars, whereas in drilling blast holes, the system is generally quite short and is made up only of drill pipes attached to a drill bit. Whether the system is long or short, the collars and pipes feed the drill string during ground boring (Aminfar, 2008)

The complicated dynamic behavior of the drill string system, the difficulty of the drilling process, and the lack of homogeneity in formation all contribute to create the drilling string vibrations (Schmalhorst, 1999). There are three modes of vibration that exist during the drilling process: axial, torsional and lateral. These modes of vibration-related phenomena cause bit bounce in axial vibration mode, stick/slip in torsional mode and a whirling effect in lateral mode. All of these make it hard, even impossible in fact, to predict precisely the optimum parameters of drilling (Schmalhorst, 1999). However, hard materials such as rock can be simulated using a variety of approaches and models.

One of the best of these is the distinct element method (DEM), a modeling approach which is especially useful in dynamic situations that include high deformation and strain. Given its superiority, DEM will be applied in the present work for examining the performance level of drilling operations through the creation of a toolkit. The aim here is to include in the kit all of the main factors that comprise a drilling operation as a means to accurately replicate currently accessible experimental tests. Itasca Inc (IC. 2008) created a tool that uses software to simulate rock-cutting activities. The tool helps to investigate the dynamic process as well as the physical mechanics, that occur during cutting. The model is constructed using PFC2D software and features three standing walls which have no friction from the sides or bottom. The model also shows rock ringed by a cutter in addition to the walls. For the PFC2D in this case, the rock material is indicated by particles. Furthermore, the cutter's speed is fixed horizontally as well as vertically, along with a fixed depth. In the course of the cutting procedure, a variety of different parameters, including energy, force and velocity, are monitored.

This section explores the interconnections of rate of penetration (ROP) and drilling efficiency and includes summaries on published work dealing with vibration drilling that applies axial forces to enhance drilling efficiency. Work carried out by the Drilling Technology Laboratory Group (DTL) at Memorial University in Newfoundland is highlighted. A representative selection of down-hole systems currently in development and/or use that apply vibrational energy for increasing ROP are also included in this section.

2.2 Historical background

A number of researchers have looked into the viability of increasing drilling performance by adopting different approaches. Recently, Ledgerwood (2007) examined the impact of crushed particles, suggesting that these particles, when under hydrostatic pressure, exhibit ultra-high strength. In fact, Ledgerwood (2007) posited that the particles' lowest strength would be equal to the strength found in virgin rock. Ledgerwood's (2007) findings also pointed to the formation rock's potential to be drilled when subjected to hydrostatic pressure, which showed how the rock material's inelastic properties exert a greater influence in ROP than, for instance, more elastic properties like the friction angle. A few years later, Li et al (2010) examined the impact of bit vibration in relation to the rate of rotary drilling penetration for laboratory rotary core drilling. In this case, the laboratory core drill underwent certain modifications to make it suitable for drilling in various conditions such as WOB and different axial vibration amplitudes (Li et al, 2010). The researchers tested rates of 300 RPM as well as 600 RPM without applying vibrations, and then tested vibration rates of 60 Hz with amplitudes ranging from 0.09 to 0.29 to 0.44mm. The test outcomes indicated that when the WOB measured below the founder point, the ROP rose in proportion to the vibration's amplitude, with a few of the outcomes indicating that rises in ROP were higher toward the ROP-WOB curve peak (Li et al., 2010).

Around the same time, Yusuf, (2011) published a paper entitled several tests were conducted to gauge the impact of using different vibration frequencies as well as different amplitudes. Additionally, the researchers applied a lab drill rig on sample materials of predetermined unconfined compressive strength (UCS), utilizing water as a drilling fluid and measuring indicators like amplitude and frequency of vibration /rotary speed, flow rate, torque, ROP, and WOB (Yusuf, 2011). They found that vibration rotary drilling with a diamond drag bit under controlled frequency conditions showed markedly higher ROP than traditional rotary drilling.

At the same time, Akbari et al, (2011) published a paper entitled, “Dynamic Single PDC Cutter Rock Drilling Modeling and Simulations Focusing on ROP Using Distinct Element Method.” The researchers used a rock-cutting strategy simulating WOB along with rotary speed, carefully monitoring the penetration rates. The simulation outcomes indicated that, for specific frequencies, there was a notable rise in penetration rate when they superimposed an oscillatory WOB (Akbari et al, 2011). The researchers also looked into the phenomena of drill string vibration and instabilities which occurred as a result of cutter rock interaction, along with some potential causes of hazardous scenarios. Additionally, how bottom hole pressure impacts the surface of rock materials was examined. Their findings indicated drops in ROP in proportion with bottom hole pressure logarithms as well as a lessening in the positive effect of force oscillations on ROP when the bottom hole pressure was boosted (Akbari et al., 2011).

A year later, Khorshidian et al, (2012) published their work analysing how natural vibrations affect the penetration mechanism in polycrystalline diamond compacts (PDCs). When drilling is carried out using a PDC bit, vertical oscillations are generated which impact penetration rates. Khorshidian et al, (2012) used a single PDC cutter-rock interaction simulation to examine how the cutter’s inertia affects vertical oscillations and discovered that the cutter’s horizontal speed

can increase the penetration rate, while the value of Mechanical Specific Energy (MSE) is boosted by the interactions of the cutter's horizontal speed and vertical vibrations.

A few years after that, Khorshidian et al. (2014) published a follow-up work entitled “The Influence of High Velocity Jet on Drilling Performance of PDC Bit Under Pressurized Conditions.” in which they demonstrated how raising the confining pressure can lower ROP. At the same time, Mozaffari (2014) created a simulation for analyzing Portland Cement-based synthetic rocks. His PFC2D model was tested to determine the impact of gap on a range of factors, including but not limited to “Young's Modulus, Poisson's ratio, friction angle vs. Confined Compressive Strength CCS, failure behaviour, tensile strength, and minimum particle size” (Mozaffari, 2014). Meanwhile, Gharibiyamchi (2014) applied the discrete element method (DEM) for simulating Axial Oscillation Generator Tool (AGT) and the hydropulse tool, with test outcomes pointing to major increases in drill performance, especially for AGT.

A year later, Reyes et al, (2015) analyzed performance rates of rotary drilling penetration mechanisms based on “rock characteristics, drill rig parameters and operational parameters”. The work highlighted the passive vibration-assisted rotary drilling (pVARD) tool, which aims to improve penetration by using rock bit interaction for building axial vibrations. Along with finding correlations between parameters such as ROP and WOB to cutting size distribution, the researchers developed a novel particle size distribution bar diagram for comparing cuttings samples. Following on the heels of Reyes and colleagues' (2015) work, Rana et al, (2015) also looked at the role of pVARD in improving ROP through utilizing PDC drill bits. The researchers investigated the responses of a pVARD prototype through using concrete samples with a UCS of around 50 MPa, finding average ROP increases of 50% to 100% over non-pVARD tools.

More recently, Zhong et al. (2016) experimented on a range of DEM simulations, aiming to improve ROP through the application of vibration. These investigations are part of a wider exploration of ways and means to improve ROP. At the Drilling Technology Laboratory (DTL) at Memorial University in Newfoundland, for instance, pVARD technology is being used as one of the main tools in their cutting-edge research in the field. Accordingly, the present work explores DEM simulations of PDC bit penetration as well as comparative drilling with and without pVARD, investigating factors such as frequency and amplitude. The outcome of the Memorial DTL experiments thus far indicates a significant improvement in drilling performance when measured by MSE, material removal rate (MRR) and depth of cuter (DOC), among other key gradients.

2.3 PDC Bit Penetration Mechanisms

Over the years, extensive changes have been introduced to drag bits (also known as fixed cutter bits) with the intention of enhancing drill performance. Steel blades have given way PDC bits, with an eye to enabling faster and longer rounds of drilling. Steel blade bits were once ideal for shallow and soft drill sites, but harder site material necessitated hardier bits, and so steel was replaced with diamond, leading to a significant increase in bit life as well as a major drop in drilling costs. Figure 1 illustrates a PDC bit that is commonly used today (Schlumberger 2017). Bits can range in size and configuration, as well as in number and cutter size.



Figure 1. Smith standard 6-inch Mi 711 1 (Schlumberger 2017).

According to Glowka (1989), PDC bit design should, to a large extent, be determined by how cutter forces come into contact with the material to be cut, and that cutter forces are primarily defined by how cross-sectional areas interact with the rock-cutting device. Furthermore, Detournay et al (1962) explained that drilling specific energy ($E=T/d$) and drilling strength ($S=W/d$), share a linear relationship in the drilling process. Shortly after making this discovery, Detournay et al (2008) further explained that bit response can also be impacted by characteristic contact length, as well as contact strength (σ). Contact length indicates the bit's wear rate (>1 mm is optimal), while contact strength indicates "the maximum normal stress transmitted by the cutter flat rock interface." Sellami et al (1989) suggested how existing or forced stresses might aid in the creation of tensile cracks during cutting, but neither situation leads to enhanced ROP in PDC bits, mainly because of the bits, extreme negative rake angle. Moreover, Sellami et al. (1989) discovered in the course of their lab experiments, that in-situ stresses have very little impact on ROP, but that increasing mud pressure serves only to slow ROP increases in BHP also have the same effect. They also found that there are two forces affecting PDC bits: the first one (cutting force) is the force needed to break the rock or other material to be cut, and the

second one (frictional force) emerges as a consequence of normal forces working against wear flat.

Gerbaud et al (2006) brought in a new approach to rock-cutter interaction that considers the impacts of back cutter force (from rock deformation), cutter face crushed material edge, and chamfer size /shape. Earlier approaches worked on the assumption that the cutting force and cutting surface were proportional, but this is valid only for sharp bits that feature a low back rake angle. A higher back-rake angle or a chamfered cutter results in higher force value. We can see this clearly in Figure 2, which shows how back / side rake angles are impacted by the cutting face edge of crushed materials. As can be seen, the cutter inclination is determined by the back-rake angle (ω_c) and side rake angle and exerts a strong influence on the cutting force. Gerbaud et al. (2006) listed three distinct forces that have an effect on the PDC bit: 1) the force that affects the cutting face surface, which they termed “F_c” 2) the force that affects the chamfer surface, termed “F_{ch}”; and 3) the force that affects the back-cutter surface, termed “F_b”.

$$F = F_c + F_{ch} + F_b \quad (2-1)$$

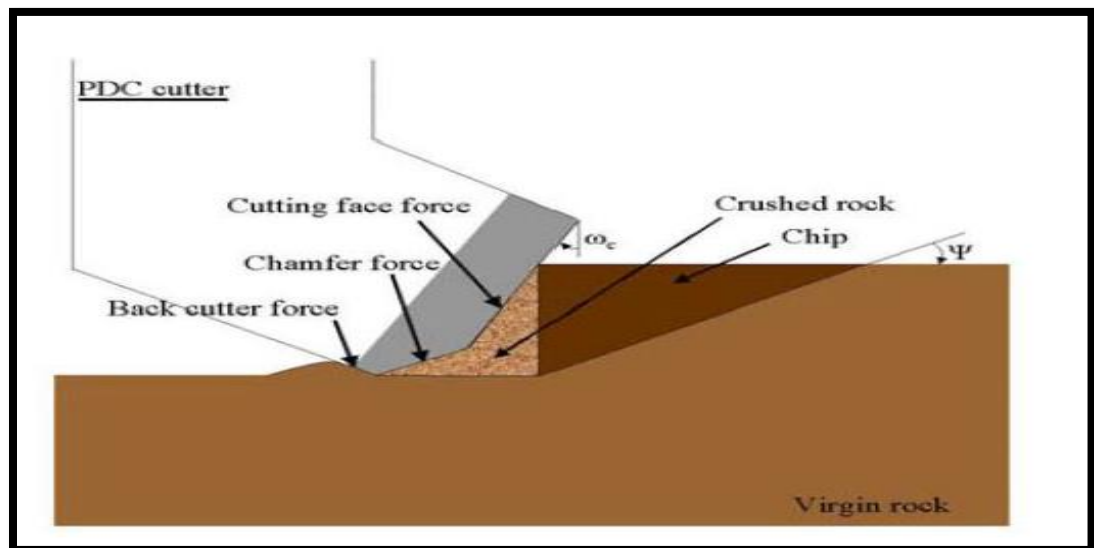


Figure 2. Forces acting on PDC cutter 1 Gerbaud et al. (2006)

In general, cutting force is nothing more or less than “pure force” intended to compromise a hard substance (in this case, rock). Figure 2.1 shows how the “pure force”, when used against the cutting face, has been applied against the rock at the edge of the crushed materials. The force results in rock chips having a failure angle (ψ) independent from PDC orientation. Thus, we can see the impacts of back side angles through the frictional contact of hard (e.g., rock) surface and chipped crushed material.

2.4 Natural Vibrations of Single PDC Cutter Penetration

When drilling using PDC bits, vertical oscillation invariably occurs and can have a range of impacts on ROP and overall drilling efficiency levels (Dupriest 2005). DEM can be used to simulate a single PDC cutter-rock interaction to explore drilling parameters (e.g., load on cutter, cutter mass on drilling responses like vertical vibration, DOC and MSE, or cutter force components) (Glowka 1989). The force working against both the bit cutter face and wear flat create cutter and drill string vertical vibration. In most instances, cutting occurs when an adequate load is applied to the cutter and is then pushed toward the cut direction. Chip generation results from oscillations of the force components moving against the cutter (Akbari et al 2011).

Daniyevsky et al (1993) and Dubinsky et al (1992) argued that bit and drill string interactions (due to, for instance, pipe and drill string stiffness or mass of Bottom Hole Assemblies (BHA) with the material being drilled can cause a range of dynamic effects. Richard et al (2002) agreed and suggested that torsional or vertical vibrations are controllable through modifications of RPM and WOB. Along the same lines, McCray et al (1959) pointed to the benefit of magnetostriction vibratory drilling, which they claimed can double the ROP simply by adding a vibration to the roller cone bits (Kolle 2004). This approach, however, is better suited to depths only up to 100 meters, as deeper wells would have a negative impact on ROP as a consequence

of chip hold down and less than ideal bit cleaning. Another innovative tool (a hydraulic actuator) uses the vibratory force on the bit through the creation of pressure pulsation, succeeding in boosting the ROP up to 33% in simulations (using a BHP of 20 MPa), but falling far short of this rate in real-world tests (Kolle 2004). According to Akbari et al (2011), rock fractures can be expanded by using vibratory forces on PDC bit cutters, but such fracturing approaches should not be used under high pressure conditions. Pessier et al., (2011) demonstrated how a so-called hybrid bit (roller cone bit and PDC bit in one) boosts ROP due to vertical movement, and Khorshidian et al (2012) modeled single-cutter penetration with DEM (see Figure 3). According to Khorshidian and colleagues lowering the DOC can result by lowering the cutter's vertical load, but no impact on the DOC was observed by simply altering the cutter's mass, as only the cutter's inertia is altered. However, raising the cutter's load results in raising the mechanical specific energy (MSE), defined as "the amount of energy (J) spent removing a unit volume of rock, V_{rock} , (m^3)" resulting in (J/m^3) (Tutluoglu, 1984). The MSE is also considered the rock's strength compromised (through penetration) by the bit. Rises in MSE might result from a variety of circumstance at the well, including friction or inadequate cleaning (Khorshidian, 2012). The cutter's horizontal movement when undergoing cutting action corresponds to vertical oscillations in vibrations in the cutter's force components, velocity and position (Khorshidian, 2012).

Khorshidian et al., (2012) argued that crushed particles lodged in the cutter and ramp were the primary cause of cutter vertical vibration. These particles, retained in place by confining pressure in the bottom-hole, are able to shift upwards only until the creation of the next chip or the cutter's vertical load measures greater than upward-trending forces in the particles.

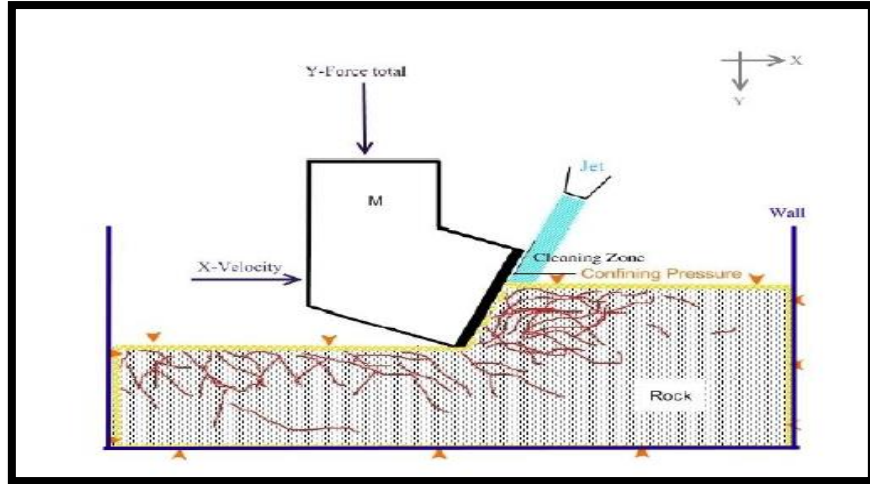


Figure 3: Conditions and components o 1 (Khorshidian et al.,2012)

Figure 4 illustrates Khorshidian et al.'s model of vertical velocity across a variety of cutter mass values. The figure demonstrates how the vertical velocity peak amplitude increases in lower cutter mass. Increased acceleration occurs due to increased excitation that results from the cutter's vertical load and the cutting actions' vertical force. Figures 5 and 6 also show how amplitudes in lower mass cutters resulting in higher peaks. It is worth noting that while Khorshidian et al. used a single small PDC bit with constant light mass in their tests, the combined impacts of bit type, geometry and mass were not studied.

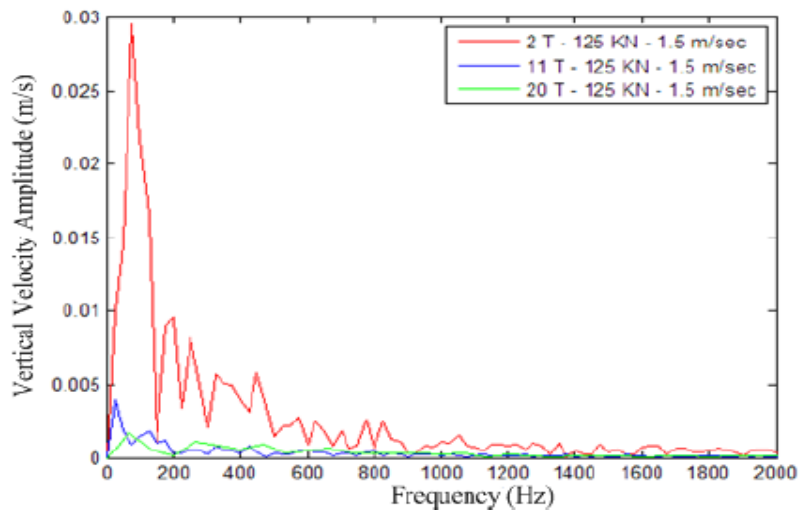


Figure 4. Spectrum of vertical velocity at horizontal speed of 1.5 m/s and vertical load of 125 KN (Khorshidian et al 2012)

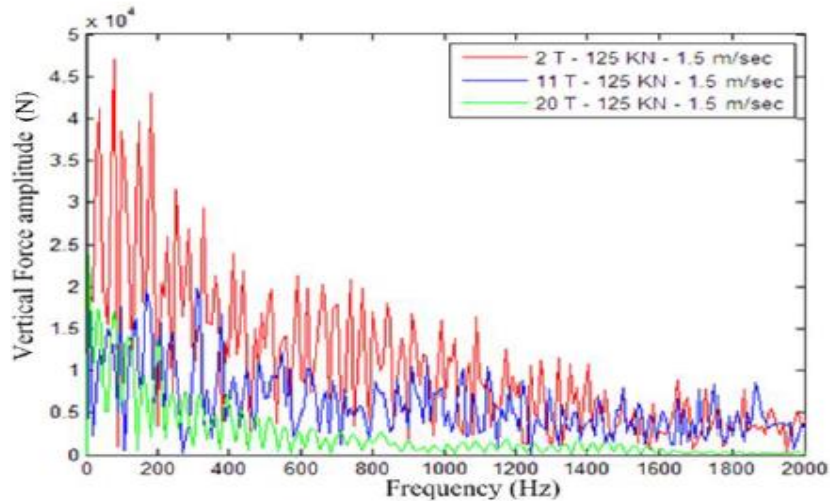


Figure 5. Spectrum of cutter vertical force at vertical load of 125 kN (Khorshidian et al. (2012))

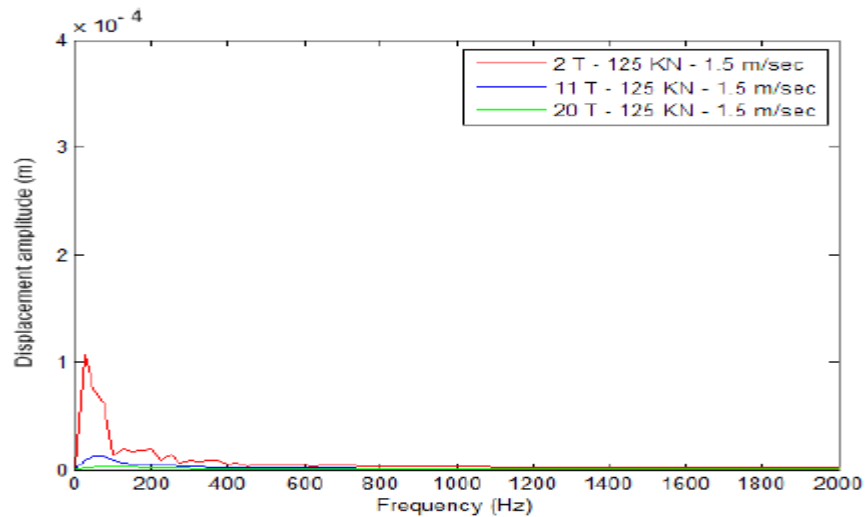


Figure 6: Spectrum of cutter vertical position at vertical load of 125 kN (Khorshidian et al., (2012))

Along with the investigations mentioned above with colleagues, Khorshidian et al., (2012) worked solo on a number of drilling trials that examined bit performance of rock penetration, which Khorshidian found to be notably less when subjected to borehole pressure. Similarly, Khorshidian's tests also found that cutting accumulations negatively impacted flow intensity, particularly under high borehole pressure conditions. These findings led him to suggest that properly tuned Bottom-Hole Cleaning (BHCs) could boost the performance of drill bits simply by clearing away the surplus cutting materials. Unfortunately, at the same time, removing the

cuttings could potentially cause an unwanted increase in hydraulic horsepower, leading to an adverse effect on bit performance through the creation of nozzle jet impact forces working against the WOB (Khorshidian et al.,2014).

2.5 ROP and Drilling Efficiency

Taylor et al., (1996) argued that most findings on drilling efficiency highlight its connection with ROP. Because of this perceived interconnection, drilling efficiency and ROP are typically seen as two sides of the same coin in that ROP is the primary parameter affecting drilling efficiency. However, field results indicate that ROP might be just one of several different factors affecting drilling efficiency. For instance, Wilmot et al., (2010) argued that drilling efficiency is contingent on a number of operational parameters or performance qualifiers (PQ), not just ROP. These parameters include but are not limited to vibration control, durability, footage drilled per BHA, down-hole tool life, borehole quality as well as ROP. Thus, while ROP is certainly a factor in drilling efficiency, any enhancement of ROP should not come at the expense of any other PQ.

In a general sense, ROP can be defined as “drilling advancement per unit time when the drill bit is on bottom and drilling ahead”, with the majority of the elements that impact ROP during drilling also affecting the other PQs. Some of the factors are listed below, divided into the three categories of planning, environment, and execution (Elnahas, 2014).

1. Planning factors include: hole size, casing depths, well profile, bit drive mechanism, BHA, drilling fluid type and properties, flow rate, hydraulic horse power per square inch (HSI), and hole cleaning (Elnahas, 2014).

2. Environmental factors include: lithology types, formation drillability (hardness, abrasiveness), pressure conditions and deviation tendencies (Elnahas, 2014).

3. Execution factors include: WOB, RPM, and drilling dynamics (Elnahas, 2014).

The two basic kinds of ROP are instantaneous (ROPi) (measured in finite time / distance during drilling) and average (ROPav) (measured as total interval drilled from running-in-hole [RIH] to pull-out-of-hole [POOH] stages) (Elnahas, 2014).

2.6 pVARD Tools

The DTL at Memorial University, Newfoundland, developed a passive VARD (pVARD) tool for enhancing ROP and drilling efficiency, along with decreasing the volume of penetrated rock energy usage. Lab and field tests have validated the usefulness of pVARD in boosting drill performance. Because ROP declines as BHP grows, pVARD technology dampens the increases in pressure, resulting in greater efficiency in drilling and in overall expenditures. Furthermore, as the springs in the axial-compliant part deliver requisite compliance, the VARD technology can then administer the ideal amount of axial displacement, and, in so doing, give full ROP. The Appendix provides in-depth details (e.g., calibrations, etc.) on the VARD technology used in the DTL experiments (Zhong 2016).

2.7 Distinct Element Method

The distinct (or sometimes referred to as discrete) element method (DEM) is a popular numerical strategy used in tabulating both the effects and movements of mass amounts of small particles (Wikipedia Shi, G 1989). While similar to molecular dynamics, DEM also includes aspects of complex geometries, rotational degrees-of-freedom, and stable contact (Wikipedia Shi, G 1989).

DEM is usually applied when dealing with engineering issues in granular flows as well as powder and rock mechanics. The approach occasionally now also includes thermodynamics and coupling to Computational Fluid Dynamics (CFD) and Finite Element Method (FEM), in which case it is called the extended distinct element method. DEMs are generally computationally rich, so they often engage in parallel processing, using distributed or shared systems. This enables them to increase both the particle number and simulation length (Zhong 2016).

Another approach to dealing with the large operational canvas is to view each particle as unique and thus to take an average of all the particles, thereby viewing the process as a continuum. For granular behaviours in soil mechanics, the so-called continuum strategy regards all materials as being either elastic-plastic or simply elastic, building a simulation using the mesh-free or finite element method. For gas-like granular flow, viewing the material as a continuum enables the application of computational fluid dynamics. There are, however, flaws in applying the continuum strategy that should be looked into prior to adopting the method for lab or field use (Mozaffari 2013)

In order to explore the fracture process more deeply, Xia et al (2009) used uniaxial compression tests to examine failure patterns in rocks, weighing their findings against outputs produced by DEM compression. The results indicated how DEM-generated models of rock failures and published data were generally in agreement. In fact, the fracture patterns generated in the simulations were similar to fractures observed in lab trials. Potyondy et al (2004) generated sandstone DEM models from non-uniform size particles. The simulations did a reasonably good job of capturing the samples stiffness evolution. Hentz et al (2004) used DEM models for simulating oversized strains by combining straining particle bonds and thereby circumventing the more complicated approaches that allow FMD and FDM simulations of oversized strains.

Akbari (2011) demonstrated in his thesis research that implicit FEM is mostly inefficient and thus not suitable for the present work. At the same time, the literature reviewed above clearly shows that the DEM approach is the most suitable strategy for numerical simulation methods that simulate failure processes due to bit cutter penetration. So, we chose Itasca Consulting Group's 2-dimensional particle flow code (PFC2D) to be the DEM software in the present study. Numerous published research studies have shown that PFC2D is well able to simulate force distribution across a broad range of rock behaviours such as crack distribution, contacts, strain rates, high deformation, etc. (Mendoza et al 2010). At the same time, DEM's calculation formulation strategy is explicit instead of implicit, which indicates a higher level of efficiency in problems (such as failure or collapse) that feature non-linear behaviour, along with dynamic response and large strain. Adopting such an approach allows for the occurrence of dynamic simulations, where data moves in speeds in accord with the particle stiffness and mass. Hence, a critical time step is developed in keeping with the system's features (i.e., the least amount of time needed for stress waves movement from particle to particle) and dynamic equations of motion can be formulated and resolved easily, after which the new contact forces can be reprogrammed according to the tabulated displacements (Strack, et al. 1979).

2.8 Cutter-rock interaction

DEM and fracture mechanics can be used to develop a numerical simulation of rock-cutting, with the dual aims of 1) determining the cutter's mechanical characteristics in the rock cutting process, and 2) determining the cutter's peak force reactions before they occur. These factors are critical, since rock cutting has an impact on the drill bit's stability. In his study, Ranman (1985) determined that the cutter's peak force can be twice the average force. Copur et al (2003) likewise carried out numerous tests on different samples, while Bilgin et al, (2006) investigated

more than 22 types of rock material. The researchers found a clear relationship connecting the cutter's force and the rock's compressive and tensile strengths, along with static elastic and dynamic moduli (Bilgin et al., 2006). Expanding on the work of these researchers, Evans (1984) and Goktan (1997) developed a cutter model to simulate cutter rock interaction, building on the assumption that the cutter's tensile stress determines the degree, quality, and speed of rock-breaking. Their model is based on rock and rock-like material's mechanical properties as well as the cutter's parameters. Today, the approach is the predominant strategy used in rock-breaking enterprises around the world.

A closer inspection of the above studies reveals that the cutter's reaction forces are determined by the mechanical characteristics of the rocks under study, which then influenced the cutter parameters. Connections to average peak force reactions that were made via theoretical speculation, simulations and lab/field experiments were compared using linear regression analysis. The findings clearly show that linear correlation coefficients of numerical results accord with Goktan's (1997) theory, which indicates that this particular numerical model can in fact effectively be used in rock cutting simulations.

2.9. Impact of drill string vibrations on drilling efficiency during Penetration.

The industry is looking into ways to lessen the vibration factor, as vibrations can have a significant impact on drilling direction, ROP and WOB. It can also have a devastating effect on the life of drilling tools like cutters, bearing, bottomhole assemblies (BHAs), and measurement-while-drilling (MWD) tools (M, Fayez 2012). Vibrations can even lower the efficacy of the entire drilling system process by preventing the total energy from being transmitted downhole (Omid 2008).

As we say earlier, drill string and bit vertical oscillations that occur in the drilling process can adversely affect penetration (Aadnoy 2009). These oscillations are primarily caused by a variety of forces working against the polycrystalline diamond compact (PDC) bit cutters (Aadnoy 2009). Yet, there is also evidence suggesting that bit vibrations might also positively increase PDC bit performance within certain conditions (Dupriest 2005).

In (Pixton 2010), a model created utilizing PFC2D demonstrated almost no connection between applied vibration and MRR. Babatunde (Yusuf, 2011) arrived at the contrary conclusion, using in his atmospheric drilling UCS at 50MPa and a 1.25-inch diameter PDC bit with vibration (in his case, a shaking table) (Yusuf, 2011). Three vibration levels (high, medium, and low) were applied at frequencies of 45Hz, 55Hz and 65Hz and several different WOBs (Yusuf, 2011). Although Yusuf (2011) concluded beyond a doubt that vibration does in fact increase drilling rates, optimal conditions are difficult to determine. Concerning to Yusuf, however, was the worrying trend of improvements in ROP up to a certain level of vibrations, after which there was a decided decrease in improvements (Yusuf, 2011).

Dunayevsky et al (1993) found that bit-formation interaction caused the dynamic components of the force, while Dubinsky et al (1992). pointed to dynamic forces being the cause of bit and string interaction with the drilled material and subsequent vibrations at the bit. Furthermore, bit and drill string vibrations share a connection with the pipe's vertical stiffness as well as the BHA mass. Force changes in the cutting direction could potentially lead to bit stick-slip and subsequent BHA failure, not to mention reduced ROP (Payne 1995). Richard et al (2002) demonstrated the interrelationship of PDC bit vertical and torsional vibrations and that bit oscillations might potentially be reigned in simply by altering velocity and WOB.

McCray (1995) investigated magnetostriction vibratory drilling technology, in which an electromagnetic transducer creates vibrations through the introduction of an alternating electric current in the solenoids around a laminated core. The device, which vibrates at a frequency of 230 Hz, more than doubled the ROP when used at depths less than 100 m and in conjunction with star-type roller cone bits. Pessier (2011) created then hybrid next-generation bits through combining PCD cutters and roller cones. These bits can fracture the hardest of rocks while increasing MSE and ROP. Meanwhile, Kollé (2004) fashioned a hydraulic actuating device that created pulses at the bit, resulting in a decrease in pressure drop on the drill string. Despite lab tests indicating a 33% spike in ROP (when using BHP at 20 MPa), real-life field trials showed next to no ROP improvement.

In their research work, Pixton (2010) employed a mud-actuated hammer on a PDC bit, along with tiny jets on the PDC cutters. Their device was dubbed the PHAST (pulsed jet hammer-assisted shearing technology) bit and appeared promising in lab simulations, but ultimately, under higher BHP conditions that replicated real-life field conditions, showed next to no improvement. Akbari et al (2011) used vibratory forces in the cutter to make larger rock fractures, but this fracturing approach was not feasible in high-pressure conditions.

Given this situation, a thruster device is currently being used in some BHAs to mitigate the impact of vibrations on the BHA. This device works by controlling the bit tracking and thereby stabilizing conditions (Schmalhorst 1999). Drill string vibration, however, is formed as a result of the bit, BHA and other factors working together, which makes it more complicated to deal with. Drill string vibration happens at the outset of penetration, when the bit comes into contact with the formation. In addition to other issues, drill string vibrations create problems with measurements while drilling (MWD), which could then cause faulty readings of sensitive

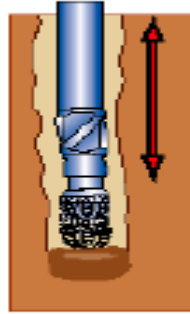
parameters. Moreover, drill string vibrations can cause damage to bits, lost potential energy, and wellbore instability (Fayez 2012). Drill collars and their adjacent drill pipes are impacted the most, but every vibration model shows a slightly different impact on drilling operations. The following section outlines the three type of vibrations that are most common, along with the areas they most affect.

2.10.1 Axial vibrations

Drill string axial vibrations create vibrations along the axis of the drill string in the wellbore direction (see Figure 7). Axial vibrations are in large part the result of movements within the chain of the drill string in either direction and can also cause bit bounce. Bit bounce occurs if weight-on-bit fluctuations are larger than usual and result in the bit being lifted off the bottom over and over again, vertically along the drill string. The bit is then dropped and affects the formation. The typical results of bit bounce are listed below (Omid 2008):

1. Bit and BHA damage or even destruction, which might then cause downhole tools to fail.
2. Lessening of ROP.
3. If severe, BHA vibrations can also result.
4. String flexing can cause axial and lateral shocks, which can subsequently damage the drill string.
5. Shallow wells may experience damage to their hoisting equipment.
6. Hook load weight may experience fluctuations.

Bit Bounce



“Axial”

Figure 7: Axial vibration and “bit bounce” (Ashley et al 2001)

2.11.2. Torsional vibrations

Torsional vibrations are defined as twisting motions in the drill string. The primary cause of these kinds of vibrations is stick-slip. Torsional vibrations develop when the bit and drill string are either accelerated or decelerated (which they occasionally do) as a result of frictional torque on the BHA and bit (see Figure 8). Additionally, torsional vibrations can cause unusual downhole rotations. Such rotations can develop when the bit is temporarily stationary, as this makes the string torque up and spin free. The extent of the stick-slip in large part determines the duration of the bit's stationary period as well as the rotational acceleration speed when the bit is freed. The downhole RPM can grow to several times the measurement of surface RPM. Some of the unwanted results of stick-slip are listed below (Omid 2008).:

1. Lessening of ROP.
2. Wearing out of stabilizer and bit gauges.
3. Damage to PDC bit.
4. Unwanted variations in surface torque readings (averaging >15%).
5. Interferences of mud pulse telemetry.

6. Connection over-torque.
7. Twist-offs of back-off and drill string.

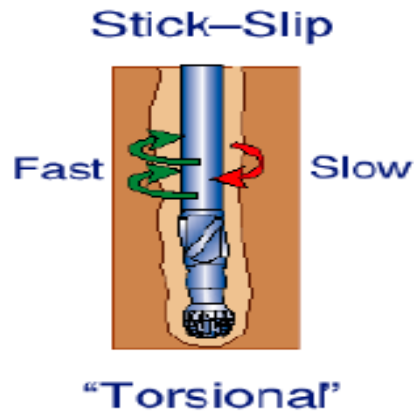


Figure 8: Torsional vibrations and “stick-slip” (Ashley et al 2001)

2.12.3. Lateral/transverse vibrations

The third major type of vibrations is lateral vibration. As shown in Figure 9, this type of vibration occurs as side-to-side motions in a transverse direction to the string. The vibration mode is mainly created by whirl, which is eccentric rotation of either the drill string or a portion of it around a point that is not the geometric center of the borehole. This movement happens only if there is sufficient lateral movement in the BHA for it to curve outwards and come into contact with the borehole wall. In extreme instances, bit whirl can even lead to axial and torsional vibrations or mode coupling. Typical impacts of bit whirl are (Omid 2008).:

1. Extreme shock and vibrations in the BHA.
2. Downhole electronic failure due to lateral shocks.
3. Destruction of or damage to bit-cutting structure.
4. Destruction of or damage to stabilizer and tool joint.
5. Extreme bending stress that can damage or destroy drill collar connections.

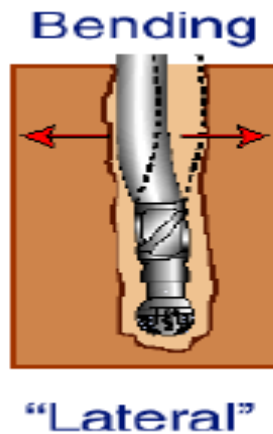


Figure 9: Lateral vibrations of drill strings (Ashley et al 2001).

One of the main reasons for drill string-related failures is the vibrations produced by drilling. Drill string vibrations can have a wide variety of causes, including the cutting action of the drill bit, misalignment, bends, kinks, mass imbalance, rotor wobbling, and friction (e.g., between the bit and the drilling surface or the column and borehole wall). However, regardless of how they are caused, vibrations in the drill string are damaging to the drilling process and equipment, as the vibrations could lead to one or more of the following issues (Azar 2007).

- Unusual wear and tear of the equipment, causing mechanical overloads and failures due to equipment fatigue (Azar 2007).
- Reduced penetration by the equipment, raising operational expenditures due to longer completion times (Azar 2007).
- Damage to measurement equipment as well as disruptions to the measurements made throughout the drilling project (Azar 2007)
- Significant energy loss (Azar 2007)
- Decreased BHA stability and directional control (Aza 2007)

- Drill pipe rupturing, drill-bit weakening, screw connection fissures, and damage to downhole tools, all caused by stress corrosion cracking (SCC) (Azar 2007).

Research indicates that the worst types of vibrations in drilling operations are those affecting the drill collars and adjacent drill pipes. However, every vibration model shows varying degrees of impact on operations.

Table 1 shows issues related to drill string vibration, according to mode.

Vibration Mode	Type	Effect
Axial	Bit Bounce	BHA failures, compromised/worn bits Decreased ROP Causes problems with additional vibration modes
Torsional	Stick/Slip	Fatigue failure or damage to bit-cutting components due to changing RPM and cutter loads Decreased ROP Early failure/fatigue of downhole tools, BHA and drill string Twist-offs & washouts Replacements & fishing trips Higher costs
Lateral	Whirl	Decreased ROP Early bit-wear Wear to string stabilizer BHA washouts & twist-offs Larger boreholes Lateral problems causing additional vibrations

Table 1. Effects of Drill String Vibration According to Vibration Mode (Fayez 2012).

While recent research has clearly shown the wide range of impacts that downhole vibrations can cause to the functionality of polycrystalline diamond compact (PDC) bits, the majority of the research on the downhole dynamics of roller-cone bits has been on axial vibration. One such research is Chen, et al (2002) study, “Effects of Stick-Slip, Lateral, and Whirl Vibrations on Roller-Cone Bit Performance of Field Investigation.” According to Chen et al (2002), although a stick-slip vibration is not detrimental to a bit’s ROP, fluctuations in WOB and TOB during stick-slip cause the bearing/seal system and cutting structure to endure significant shock loads. As a result, the bit lateral vibration substantially decreases ROP, while also shortening bearing/seal life because of the massive changes in the size and direction of loads on the cones. Dubinsky et al (1992) suggested that bit vibrations are caused by dynamic forces resulting from bit and string interaction with rock. They also suggested that both bit and drill string vibrations are strongly dependent on the pipe’s vertical stiffness as well as the bottom-hole assembly’s mass. Furthermore, variations in forces in the cut direction could lead to bit stick-slip. As well as increasing the risk of BHA failure, it can also cause a decrease in the ROP. Li et al (2010) studied how vibration can affect bit performance and enhance ROP by using a P-VARD experimental set-up to record the effects. This study indicated in Figure 10 that the ROP increases with increases in WOB, and keeps rising to the founder point, at which time the ROP declines along with additional increases in WOB. This increase is the standard pattern for conventional rotary drilling – namely, that increases in ROP are proportional to those in rotary speed. Moreover, ROP increases with increases in vibration amplitude. This increase is more or less linear up to the point of peak ROP, at which time the rise in ROP is significantly higher.

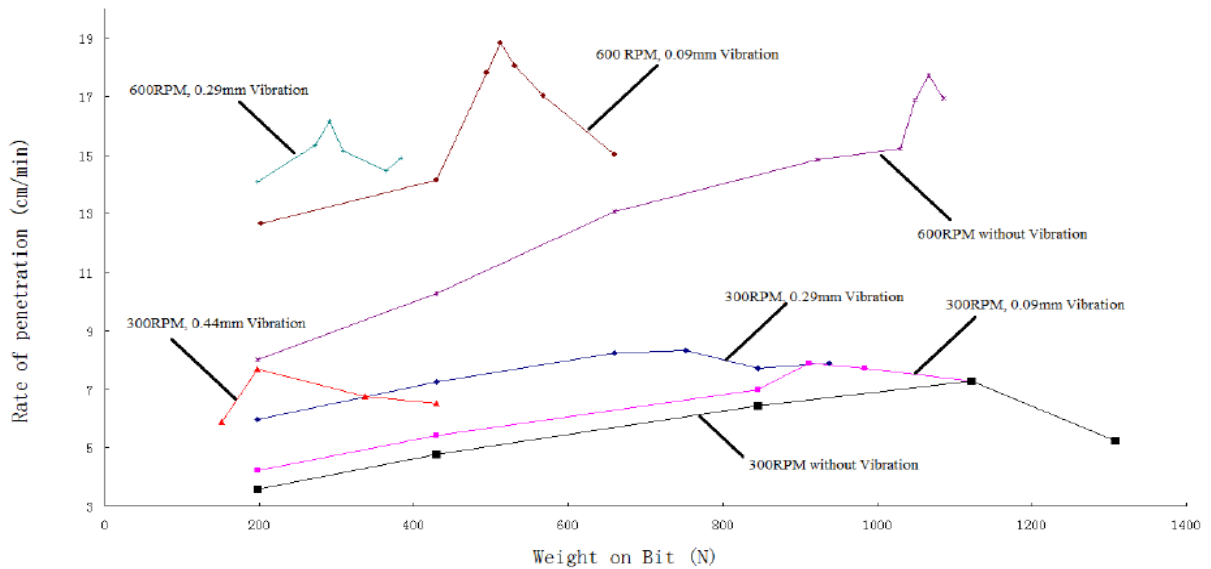


Figure 10- Li’s experimental results of vibration assisted rotary drilling ROP & WOB Li et al (2010)

Research suggests that there is optimal value for rotary speed and WOB vibration amplitude, such that ROP will decline in tangent with higher vibration amplitudes. Schen, et al., (2005), in their study “New Small Vibration Logging Tool to Optimize of Bit Drilling Performance”, showed that a novel component could increase roller cone bit stability when fitted with lug pads. Schen et al., (2005) also investigated how to reduce WOB in order also to reduce stick-slip in PDC Bit drilling. They found that although the reduced WOB dealt with the stick-slip, it made the lateral vibration issue worse. Nevertheless, and despite negatively impacting the drilling performance, the researchers were encouraged by their findings, as these indicated precisely what the problem was and where it was occurring. The findings also pointed to the dynamic activities that were happening. In another study on bit vibration, Richard et al, offered a novel approach to discerning the causes of stick-slip vibration, indicating that torsional and vertical vibrations of a PDC bit are coupled, and that the bit fluctuations can be controlled by variations in velocity and WOB.

2.13 Impact of Bottom-Hole Cleaning during Rock Penetration.

The simple definition of bottom-hole cleaning (BHC) is the removal of rock cuttings generated as part of the drill process. The removal is mainly accomplished by introducing fluid circulation at the hole bottom to flush any unwanted cuttings off the rock face and move the fragments above ground (Bourgoyne 1986). The BHC process can also serve to lubricate the drill string and drill bit, cool down the bit, and decrease overall wear and tear of the affected equipment (Bourgoyne 1986). The introduction of drilling fluid into the wells also creates bottom-hole pressure that is required for well control and bore-hole stability. Here, however, we will mainly explore how BHC impacts ROP. In his early work, Maurer (1962) examined how BHC impacts ROP during rotary drilling. His findings pointed to ROP being a function of WOB, rock strength, bit diameter, and other factors. Figure 11 depicts how drilling at high rotary speed and WOB necessitates BHC, and that without adequate BHC, the drilling process is inefficient (e.g., the bit will attempt to re-drill any left-over cuttings). Thus, effective BHC results in efficient ROP.

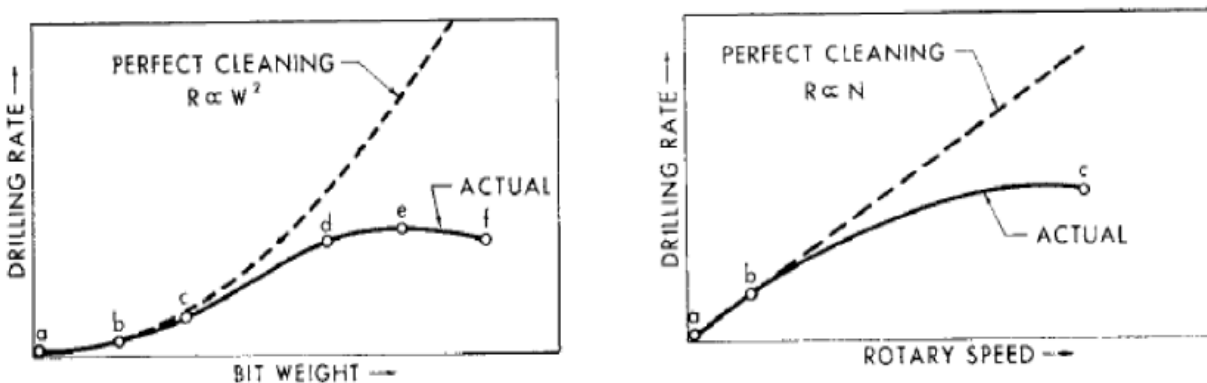


Figure 11. ROP curves vs. WOB and rotary speed for ideal and actual drilling conditions (Maurer model)

BHC also inhibits bottom-hole balling, according to Garner (1967). Specifically, without effective BHC, the crushed particles might become lodged in the bit cutters and significantly reduce both ROP and bit efficiency. Again, what is needed is effective BHC that includes the

flushing away of fine particles both in the hole itself and on the equipment. Rabia (1989) agreed that good BHC prevents bit balling while ultimately increasing ROP. However, Rabia studied only Gulf Coast shale and did not investigate any connection between BHC and BHP. Wells et al (2008) also looked into ways to avoid bit balling of PDC bits, stating that HSI's impact on ROP is mostly confined to soft rocks (e.g., shale), and that the effect of these factors on harder rock was nearly nonexistent. Meanwhile, Speer (1959) in seeking the most effective drilling technique, stated that the BHC is mostly just useful for clearing away crushed materials and cuttings, but does not have any significant impact on ROP. The published literature reviewed in the present study points to bit hydraulics being more effective in roller cone bits more than PDC bits due mainly to the nozzle position in the penetration area. Furthermore, PDC bit nozzles tend to be positioned directly near any outflow of fluid, which then covers the PDC cutters and inhibits bit balling. In contrast, in roller cone bits, the jet nozzles are directed towards the cone teeth. Tutloughlu (1984) examined rock cutting mechanics using a single cutter subjected to fixed DOC and certain atmospheric conditions. He asserted, from his findings, that the crushed materials in front of the cutter were the primary reason for reduced performance levels and ROP, and that cleaning the materials away resulted in notable enhancement in penetration. Tutloughlu's findings accord well with those of Mozaffari, (2013) who discovered in his simulations that the majority of the cutter's energy is lost to particle friction instead of rock-breaking. Again, like Tutloughlu, Mozaffari (2013) recommended that the best way to increase ROP as well as MRR (material removal rate) was to ensure effective BHC. Overall, then, the literature is nearly unanimous in its conclusion that the best way to enhance ROP is through efficient BHC.

2.14. Impact of Axial Compliance on Drill String.

In examining the impact of axial compliance on penetration mechanisms, including ROP, a Gharibiyamchi (2014) carried out a number of simulation tests using a shock tool. Specifically, he modeled two hydraulic pulsing drilling tools – AGT and hydropulse – both with and without using his chosen tool. AGT and hydropulse are similar in some regards, but AGT forms pressure pulses through limiting a fluid’s flow area, whereas hydropulse employs sporadic total stoppage of the flow. Additional differences include that the output pressure profile of AGT is depicted as sinusoidal instead of impact profile. In viewing the outcome of his tests, Gharibiyamchi (2014) asserted that the impact of the shock tool was more pronounced when utilized together with AGT instead of hydropulse technology and suggested that positioning the shock tool over the hydraulic pulse tools might enhance the penetration mechanism.

The table2 below lists the values for MRR and MSE in hydraulic pulsing tools both with and without shock tool technology. The BHP in all simulations was equivalent to 1000 psi (Gharibiyamchi 2014).

AGT without Shock Tool		AGT with Shock Tool	
MSE (KJ/m ³)	MRR (10 ⁻³ m ³ /s)	MSE (KJ/m ³)	MRR (10 ⁻³ m ³ /s)
338000	0.08	6880	4.01
Hydropulse Tool without Shock Tool		Hydropulse Tool with Shock Tool	
MSE (KJ/m ³)	MRR (10 ⁻³ m ³ /s)	MSE (KJ/m ³)	MRR (10 ⁻³ m ³ /s)
5870	2.99	5680	4.88

Table 2: Simulation results of the AGT and Hydropulse tool without and with the shock tool (Gharibiyamchi 2014)

As can be seen in the table, MSE values declined after applying the shock tool, but MRR values rose. Gharibiyamchi. attributed this to axial compliance added by the shock tool (Gharibiyamchi 2014). In this case, the shock tool, which functioned as an oscillatory system, was an axially spring-loaded mandrel positioned between the annulus and drill pipe pressure. The tool makes an open pump area that enables hydraulic pulse tools to function and the mandrels to move in an upward and downward motion (Bellville springs). In short, Gharibiyamchi's shock tool changes the pressure pulses into mechanical force as well as motion.

Figures 12 and 13 depict the AGT and hydropulse cutting process, carried out, respectively, with and without the shock tool. Figure 12 clearly shows that when the AGT functions without the benefit of the shock tool, the performance registers as sub-par. The ROP is ultra-low because the sinusoidal force cannot damp upwardly, leaving the entire assembly bouncing unrestrainedly (Gharibiyamchi 2014). However, the introduction of the shock tool immediately raises the DOC, enabling the cutter to process the rock-cutting faster and smoother, with little to no bounce.

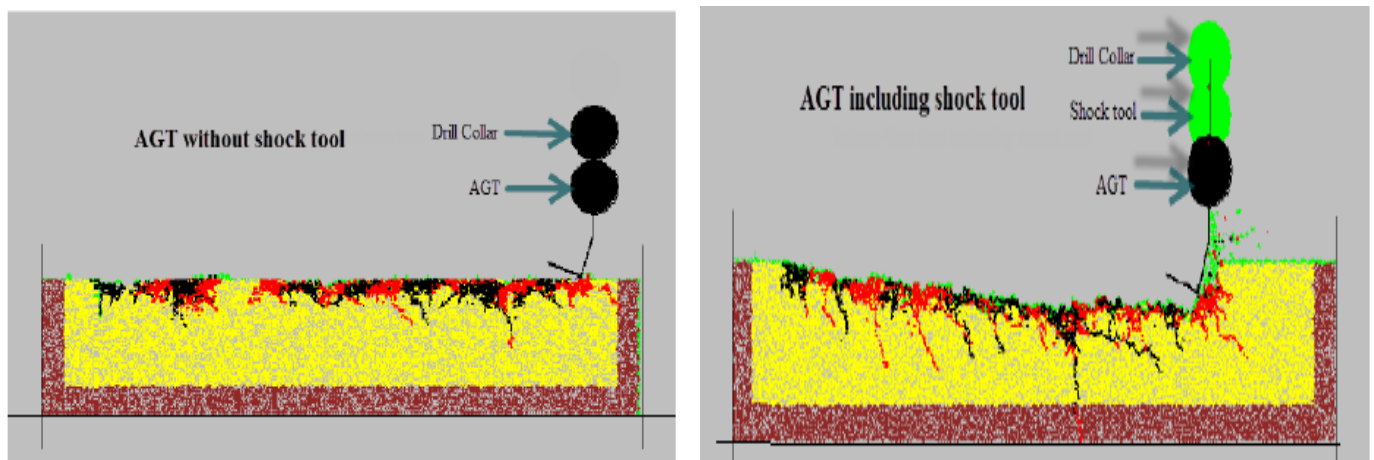


Figure 12. Effect of shock tool in drilling performance of the AGT (BHP = 1000 psi, WOB = 60 kN and sinusoidal force amplitude of 19.25 kN) (Gharibiyamchi 2014).

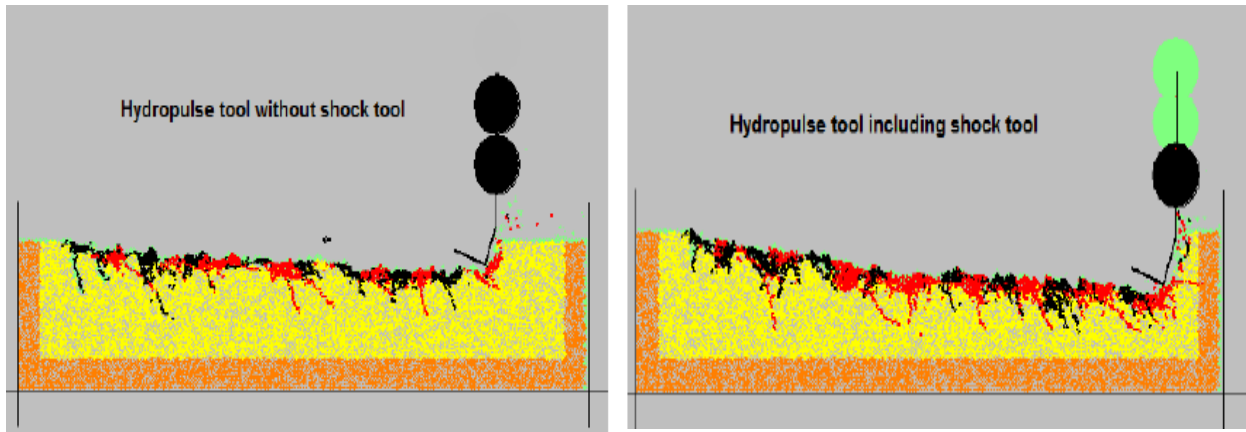


Figure13: Effect of shock tool in drilling performance of the Hydropulse tool (BHP = 1000 psi, WOB = 60 kN and pulse amplitude of 198.5 kN) (Gharibiyamchi 2014).

2.15 Impact of Stiffness, Damping, and Compliance in Down-hole Vibration and Drilling Performance

As mentioned earlier in the reviews of Dunayevsky et al.'s (1993) and Dubinsky et al.'s (1992) research, there are clear connections among BHA, pipe and drill string stiffness, and vibrations plaguing bits. At the same time, we also saw how dynamic components in forces impacted the cutter are derived from drill string and bit interactions with the material being drilled. A number of complex down-hole devices have been developed to reduce BHA vibrations in order to raise the level of ROP. The next section presents these devices and explores how they have an impact on both ROP and down-hole vibrations.

2.15. Brief explanation of anisotropic rocks

The oil and gas drilling industry are known for its extensive testing of rocks for their specific anisotropy. This is because whether in horizontal, extended reach or deviated wells, anisotropic formation can have significant effects. For instance, it can impact the rate of penetration (ROP), initiate instability in the well bore, and add to borehole wander and deviation of the planned trajectory of a well.

Two primary categories of anisotropy are induced and intrinsic anisotropy. Induced anisotropy occurs due to strain from fractures, applied stress, and diagenesis. This type of anisotropy aligns fractures, cracks, grains and pores, such that rock which previously was isotropic turns into seismically anisotropic material. On the other hand, intrinsic anisotropy occurs from preferential orientation of sediment pore and grain, and involves grain shape and size, compaction, deposition, and overall sediment composition. In rocks which are sedimentary in feature, intrinsic anisotropy assumes a transverse isotropic form. Shale, for instance, is almost always intrinsically transversely isotropic Melaku (2007).

Furthermore, with regard to variations within rock material, anisotropy presents as one of only a handful of indicators which can be investigated using wavelengths that exceed the scale of the variations' lengths. In other words, anisotropy can be observed if the wavelength applied for the observation is no smaller than the elements which created the anisotropy. So, for instance, we can use seismic scale (at frequencies of around 500 to 900 kHz) for reservoir beds, and ultrasonic scale for detecting anisotropy for centimetre scale Melaku (2007).

There are two different kinds of material alignments in anisotropy: vertical alignment, which features a horizontal axis of symmetry and is termed vertically transverse isotropy (VTI), and horizontal alignment, which features a vertical axis of symmetry and is termed horizontally transverse isotropy (HTI). Two models were developed to show the elastic characteristics of these anisotropical alignments (e.g., stiffness, velocity). These and other parameters can be useful in better understanding the concepts of vertical and horizontal permeability anisotropy and in laying the groundwork for hydraulic fracture jobs. Waves in VTI typically are faster-moving along the horizontal rather than the vertical alignment. It is important to both identify and measure VTI anisotropy, as it is necessary as a correlating factor for finding variations in

amplitude, as well as for seismic and bore-hole imaging and for comparisons of sonic logs found in vertical or deviated wells. Similarly, it is important to detect and quantify HTI waves, which move in the direction of the fracture inside the rock and also move faster than the wave which crosses the fracture. The main purpose for detecting and quantifying HTI anisotropy is to obtain data on the orientation and density of the fracture, along with data related to the overall rock stress Rezapour (2015).

Anisotropic rock material has been the subject of several lab studies recently Dan et al, (2012). In Nasseri et al, (2003). carried out a procedure on schistose rocks, aiming to measure and analyze their deformational response and strength. The tests were conducted for material in the uniaxial and triaxial states and for the whole orientation angle range. In a similar work, Tien et al, (2001) investigated artificial material aiming to find strength criteria and failure mechanisms in rock which was transversely isotropic.

According to most tests carried out over the past half century, the majority of sedimentary rocks are characterized by anisotropy in both deformation and strength Unlu et al, (2004). Moreover, the extent of the anisotropy is generally dissimilar among the sedimentary rocks, with some significantly more anisotropical compared to other formations as a result of bedding planes which are well-defined Chappell, (1990). In other recent research, the correlation between drilling ROP and anisotropy has also been looked at. In Brown et al, (1977) investigated how rock anisotropy can impact ROP and hole deviation tendencies.

Another feature of anisotropy which has been looked at is its strength across different rock types. Sandford et al, (1974) used slate to carry out triaxial tests, while Gatlin et al, (2013) measured directional characteristics for two shale varieties by applying auxiliary stress-strain measuring devices and triaxial compression cell equipment. Meanwhile, Unlu et al, (2004) evaluated

anisotropic intact rock strength by incorporating data obtained in tests measuring indirect tensile (i.e., Brazilian) and compressive (i.e., uniaxial/triaxial) characteristics. In a similar investigation, Nasser et al. (2003) looked at failure patterns in several anisotropic schistose rocks both for the micro and macro scales, using confined and unconfined triaxial compression as testing methods.

A long list of other experiments has also been carried out in the field. Halidou et al. (1994) found that plastic deformation in rocks usually occurs together with damage from micro-cracks caused by strain softening. Chen et al. (2010) developed a model representing potential damage incurred by anisotropic materials, built on the conclusions of Pietruszczak et al (2002) plastic model that looked at induced damage resulting from micro-cracks. Additionally, when analyzing various types of geostructures, the material's directional dependence of strength must be considered, which necessarily involves the development of models that measure structural anisotropy. Duveau et al. (1998) conducted a comprehensive review of research which explored plastic deformation and general failure criteria.

In other work, Vernik et al. (1997) discovered that, in shale, thermal maturity and velocity anisotropy were related, as were kerogen orientation and content and velocity anisotropy, while Nur et al. (1992) measured values for anisotropy that exceeded 50% in North Sea black shale. A few years later, Johnston et al. (1995) used velocity in combination with measurements from Scanning electron microscope (SEM) observations and X-ray diffraction (XRD) to find possible correlations between clay mineral orientation and velocity anisotropy. By employing an X-ray diffraction approach, the researchers used orientation indices, discovering positive correlations between orientations for velocity and grains of chlorite and illite (Johnston et al. 1995). This led

the researchers to propose that anisotropy at elevated pressures was caused by preferred mineral orientation instead of crack alignment (Johnston et al.1995).

A few years after that, Hornby (1998) looked at how elasticity is affected by pore fluids by measuring shear and compressional wave velocities (< 80MPa) for fluid-saturated shale. Using two samples (one from a bore-hole in the North Sea, and another from elsewhere undersea and stored organically in its own fluid), the researcher measured the cores perpendicular and parallel to the bedding. He found that anisotropy values reached 48% in shear wave velocity and 26% in compressional velocity, and that these values reduced as the pressure increased. Hornby (1998) concluded that decreases in porosity had greater impacts on anisotropy compared to increases in mineral alignments under greater pressure.

Wang (2002) investigated a novel approach to obtaining anisotropies, velocities, and elastic constants from shales in multiple adjacent core plugs that featured a variety of orientations. By employing transversely isotropic rock, the researcher formulated calculations for three different plugs (perpendicular, parallel, and $\pm 45^{\circ}$ to symmetry axes). From these formulations, he then was able to find five independent elastic constants. Wang (2002) indicated that the benefit of using the three-plug approach was the calculation redundancy for the five elastic constants, as three velocity readings were obtained for every core plug formulation.

Yet another strategy for exploring the various mechanical behaviors in rock is the numerical simulation approach. Lisjak et al. (2014) applied FEM/DEM to modeling anisotropy in Opalinus Clay, while Debecker et al. (2013) investigated slate's fracture behavior by applying the universal distinct element code (UDEC). In the researchers performed article-based DEM simulations to study fractured rock mass anisotropy, using a series of smooth joint contact to indicate the macro fractures' mechanical properties.

Chapter 3

Baseline development of rock anisotropy investigation utilizing empirical relationships between oriented physical and mechanical measurements and drilling performance

This chapter is the paper “Baseline development of rock anisotropy investigation utilizing empirical relationships between oriented physical and mechanical measurements and drilling performance”. A. Abugharara and A. Alwaar concerted and conducted the experiment, analysed the data, and wrote the paper and C. Hurich, S. Butt, suspended the research and edited the paper. It was published in the International Conference on Ocean, Offshore and Arctic Engineering (OOAE), June 19-24, 2016, Busan, South Korea. The Figure numbers and references are altered to coordinate the designing rules set out by Memorial University of Newfoundland as compared with the original manuscript published in the conference proceeding.

Abstract

This paper describes a baseline investigation to confirm the isotropy of rocks material through physical and mechanical measurements followed by oriented drilling. This baseline is intended to evaluate drilling experiments in anisotropic rock materials to determine the significance of the anisotropy on drilling performance. The conducted tests include oriented measurements of compressional and shear wave velocities (V_p and V_s , respectively), density, Elastic Moduli, Point Load Strength Index (PLI), Indirect Tensile (IT) strength, and Unconfined Compressive Strength (UCS). The oriented laboratory drilling experiments were conducted under various

pump flow rates and several weights on bit (WOB). In this work, an isotropic rock like material (RLM) was developed using Portland cement and fine-grained aggregate. The tested RLM specimens were of medium strength of ~50 MPa. The RLM samples were cored in different orientations and then, tested and drilled according to these orientations. (e.g. 0°, 45° and 90°, representing horizontal, diagonal and vertical directions, respectively). Two main sets of lab tests were performed including pre-drilling and drilling tests. For the predrilling lab experiments, two main sets of tests were conducted to determine the physical and mechanical properties of samples (as outlined above) including PLI, IT, UCS, V_p , V_s , density, and corresponding isotropic Dynamic Elastic Moduli. For the drilling tests, a vertical lab scale drilling rig was used with a 35-mm dual-cutter polycrystalline diamond compact “PDC” bit. The drilling parameters involved were flow rates, nominal rotary speed of 300 rpm, and various WOB under atmospheric pressure. The relationships between the drilling data were analyzed including drilling rate of penetration (ROP), depth of cut (DOC), and corresponding effective WOB. The results of all mechanical, physical, and drilling measurements and tests show consistent values indicating the isotropy of the tested rock material. This consistency verifies that the drilling tests are free of bias associated with drilling orientation.

3.1. Introduction

Rocks can be characterized as isotropic, where material properties are independent of orientation, or anisotropic, where they are not. Special cases of rock anisotropy include vertical transverse isotropic (VTI) or horizontal transverse isotropic (HTI), where the properties are uniform in either the vertical or horizontal plane, respectively, and different in the perpendicular direction. Anisotropy is an important character of rocks in oil and gas drilling operations, and it is known that anisotropy of the formation drilled in deviated, extended reach and horizontal

wells can impact the rate of penetration (ROP), contribute to borehole deviation and wander from the intended well trajectory, cause well bore instability. This is being investigated further in a parallel study to the one outlined in this paper and will be reported in future publications. However, to determine the influence of material anisotropy on drilling penetration, a baseline investigation of drilling penetration in an isotropic material was needed first. The proposed isotropic material is RLM composed of Portland cement and millimeter sized aggregate (essentially a fine-grained concrete) and which an unconfined compressive strength (UCS) of ~ 50 MPa. This paper describes the characterization of the RLM to confirm its isotropic material properties and oriented drilling experiments. The conducted experiments include physical measurements, mechanical measurements, and drilling tests. For the physical measurements, V_p and V_s are measured to determine the velocity anisotropy index (VA) as proposed by Tsidzi. (1997) for ultrasonic waves and by Brich. (1961) for description of seismic waves. For the mechanical tests, the unconfined compressive strength anisotropy index ($I_{\sigma C}$) given by Ramamurthy. (1993) and point load strength anisotropy I_a (50) proposed by (ISRM, 1981) and (ISRM, 1985) were determined. In addition to those measurements, a drilling evaluation based on drilling performance in isotropic and anisotropic rocks is included. The drilling performance was evaluated by calculating the ROP. All tests were conducted in three different orientations (e.g. 0° , 45° and 90° , representing horizontal, diagonal and vertical directions, respectively). Recorded data evaluated results, and work summary are reported.

3.2. Test Procedure and Apparatus.

In this section, the procedure of sample preparation, conducted physical and mechanical measurements as well as the drilling tests and apparatus used are described.

3.3 Sample Preparation

In this work, the tested RLM samples were cast using Portland cement and fine-grained rock aggregates (grain size < 2mm). All samples were fan air dried for 48-hours, after which all measurements were taken. Samples were prepared according to ASTM D4543-08. (2008). Before conducting the mechanical tests (e.g. UCS, PLI, and IT), Vp and Vs were measured for all samples. The samples and type of conducted tests are summarized in Table 3.

Number of samples	Test Type	Orientation	Direction representation	Sub-test Type	num. of samp.
110	PLI	90-Degree	Vertical	Axial	19
				Block	24
		45-Degree	Diagonal	Axial	13
				Block	15
		0-Degree	Horizontal	Axial	17
				Block	22
24	IT	90-Degree	Vertical		24
7	UCS	90-Degree	Vertical		2
		45-Degree	Diagonal		1
		0-Degree	Horizontal		4
21	Drilling	90-Degree	Vertical		7
		45-Degree	Diagonal		7
		0-Degree	Horizontal		7
VP and VS were measured for all samples of PLI and UCS tests.					Total =162

Table 3. Summary of number of samples, type of tested conducted, and the orientation of tests.

3.4. Conducted Tests

Three sets of different tests were conducted on the RLM samples. The purpose of these tests is to determine the anisotropy percentage of the rock by measuring the Vp and Vs, and then utilizing the measured velocities and density in determining the dynamic elastic moduli.

3.5. Physical Properties' measurements

Ultrasonic Method: This method is used to measure V_p , V_s , and to determine, with measured densities the corresponding dynamic elastic moduli (DEM) according to ASTM D-2845-08. (2008). Comparing to the available methods of sound velocities (e.g. low frequency sonic wave method and the frequency resonant method), the high frequency ultrasonic method is the more reliable and practical. The main influence for adopting the ultrasonic method in determining the wave velocities is the associated non-destructive test procedure, low cost, and more importantly high precision. This method is applied for measuring V_p , V_s and the elastic constants are calculated then using the measured velocities and the bulk density. V_p and V_s can be affected by the inner structure of the tested material. Such factors include mineralogy, grain's size and distribution, density, porosity's percentage and type, weathering, water content, stress level, and temperature Soroush et al. (2003). As the ultrasonic wave velocities increase with the increase of rock strength Onyia. (1988), the work of this paper, exhibit that the measured V_p and V_s were found to be in same range in all orientations confirming using same rock of same strength of RLM. The measurements show small differences; though, due to the nature of experiments. Figure 14 shows the ultrasonic method equipment utilized in measuring V_p and V_s . The equipment includes TDS 1002B Two Channel Digital Storage Oscilloscope, Square Wave Pulsar/Receiver Model 5077PR, and two Panametrics shear-wave sensors. Shear wave coupling was used to ensure complete contact between sensors and rock samples.

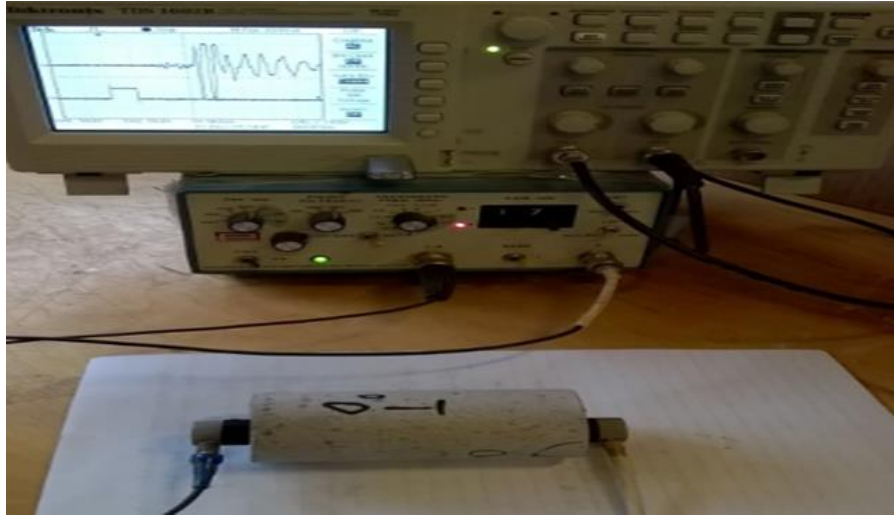


Figure 14. Apparatus used for V_p and V_s measurement.

One sample of the recorded ultrasonic waves is shown in Figure 15.

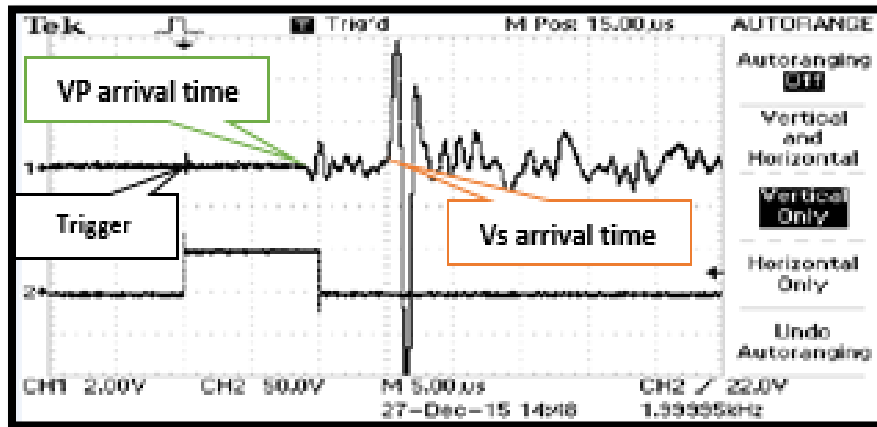


Figure 15. Sample of the recorded waves

The measured V_p and V_s and their relationship with density of all prepared samples for Axial and Block-PLI test in different directions are shown in Figure 16.

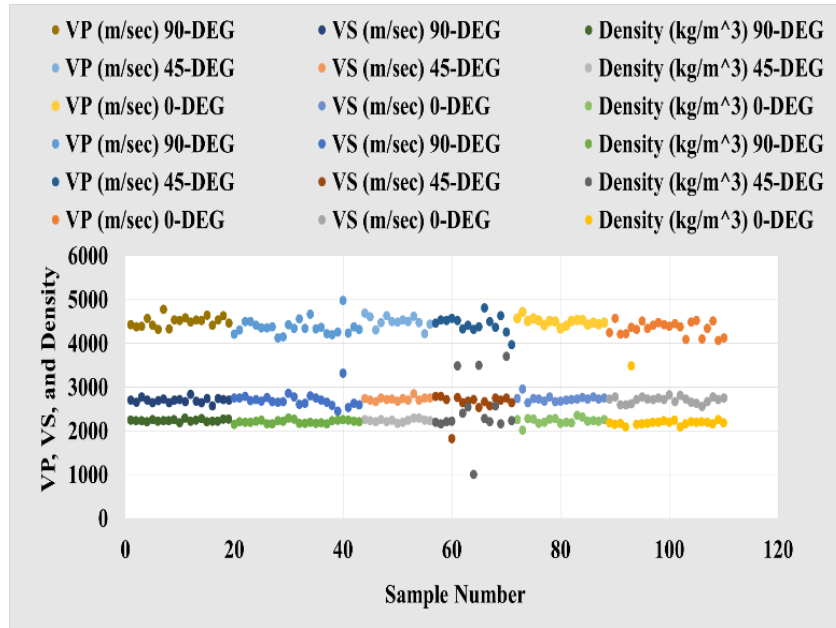


Figure 16. Vp, Vs, and Density of all samples of Axial and Block PLI tests in different orientations

The mean values of the measured Vp and Vs from the prepared samples for standard UCS test in different directions are shown in Figure 17

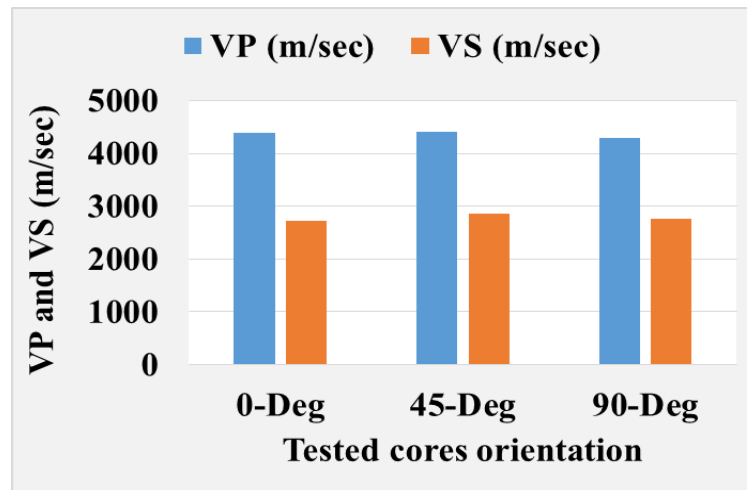


Figure 17. Mean values of measured Vp and Vs of standard UCS test in different orientations

The mean values of the measured Vp and Vs from the prepared samples for Axial and Block-PLI test in different directions are shown in Figure 18.

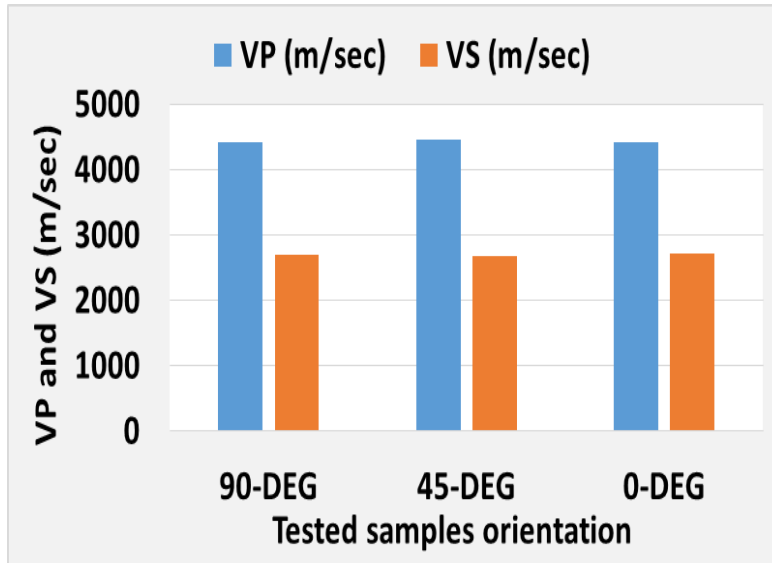


Figure 18. Mean values of the measured Vp and Vs of samples of Axial and Block-PLI test in different directions.

DEM were calculated based on measured velocities and densities. Figures 19, 20, and 21 show the mean values of the calculated Compressional Wave Modulus, Shear wave Modulus, Elastic Modulus, Lamé constant, Bulk Modulus, and Poisson’s ratio respectively. Based on velocity anisotropy index, VA proposed by Tsidzi. (1997), the VA of the RLM of his investigation is 0.0278 (%) < 2 confirming the isotropy of the tested material.

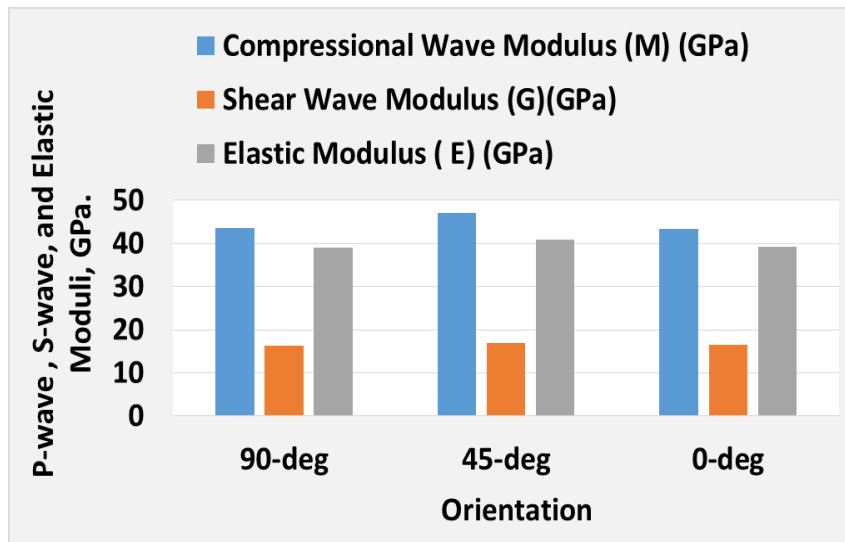


Figure 19. Mean values of P-wave, S-wave, and Elastic Moduli in three orientations

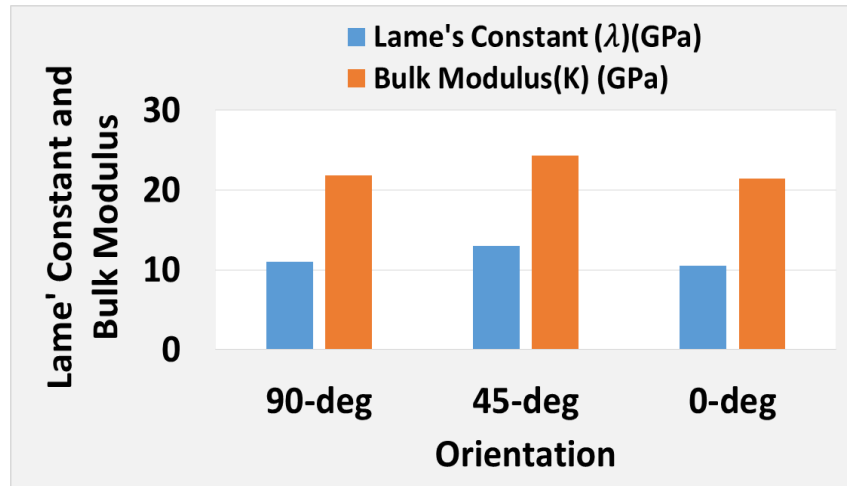


Figure 20. Mean of Lamé's Constant and Bulk Modulus in three orientations

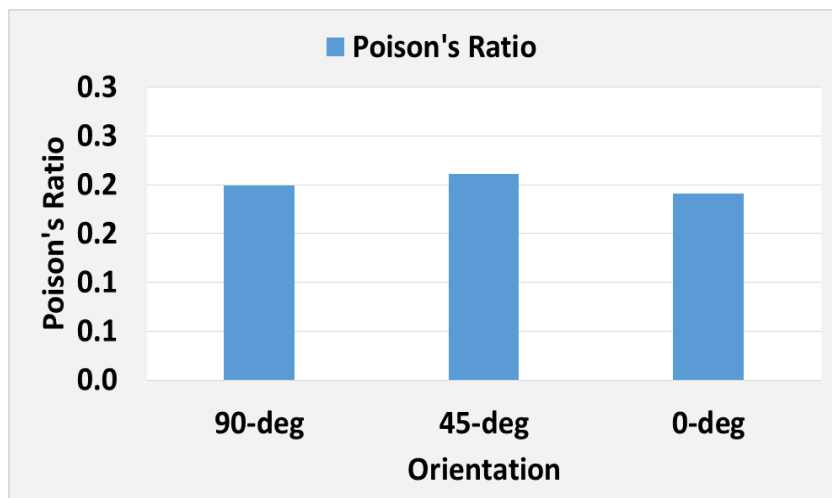


Figure 21. Mean value of Poisson's ratio in three orientations

3.6. Mechanical Tests

3.6.1. UCS test: For this test, many standard NQ cores were obtained by using cylindrical coring bit with outer diameter of 47.6 mm. Grinder was used to ensure parallel ends. ASTM D4543-08. (2008) was followed for ensuring appropriate sample preparation. Before conducting the mechanical tests, all measurements of V_p , V_s , and Density were taken for the samples. Figure 22 shows the samples cored in three different orientations to be tested for UCS.

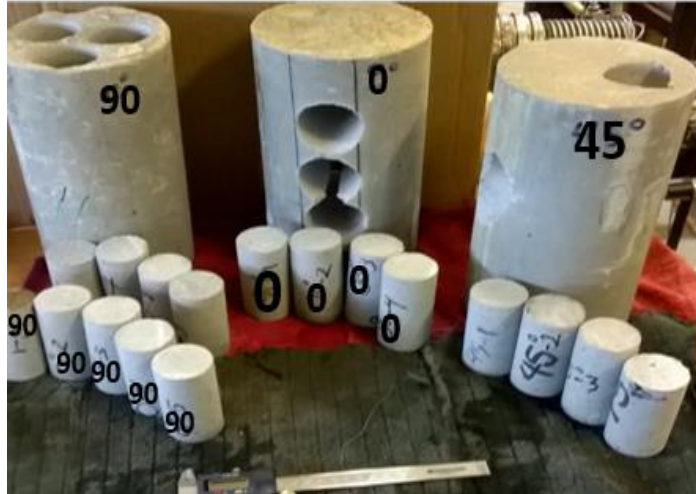


Figure 22 . Samples of UCS test cored in different orientations

UCS was conducted for cores according to ASTM D7012- 14. (2014). The UCS anisotropy of RLM of this paper was determined to be (1.059). This value falls between 1 and 1.1 using the method suggested by Ramamurthy. (1993) determining the isotropy of RLM. The mean values of the results of UCS tests are shown in Figure 23.

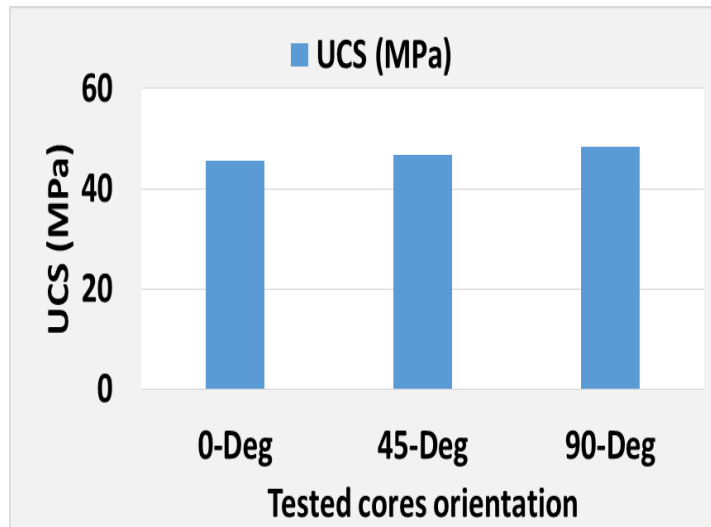


Figure 23. Mean values of UCS

Table 4 summarizes the recorded data for the standard cores for UCS test including V_p , V_s , and UCS.

Orientations	AVG. density (kg/m ³)	VP (m/sec)	VS (m/sec)	UCS (MPa)
0-Deg	2338.5	4384.1	2718.5	45.6
45-Deg	2252.9	4404.1	2853.9	46.7
90-Deg	2408.6	4283.2	2766.7	48.3

Table 4. Mean values of Vp, Vs and UCS for the standard samples of UCS test.

3.1.2 PLI test: In this test, two main types of samples were prepared for Axial and Block tests. ASTM D5731-08. (2008) was followed for test procedure. Type of samples including Axial and Block tests' samples, orientation representation, and PLI tester are shown in figure 24.



Figure 24. Samples of Axial and Block tests with PLI tester

The obtained result by this test followed the same trend of the previous tests in confirming the rock isotropy. However, some variations due to the nature of the test were observed. Such concern was highlighted by Bowman et al. (2007) and Bowden et al. (1998). Bowman proposed due to unrealistically high UCS estimating specific conversion factor” value in determining

UCS, especially for weak rocks in the laboratory. Therefore, “C” was determined for rocks tested in this paper to be “10.3” which gave reasonable UCS values comparing to using the standard “C” value of 24. Figure 25 shows the relationship between UCS values obtained by IT and Is (50). Such relationship provides a correlation that results a “C” factor equals 10.3. Applying this factor using the equation (UCS = 10.3 Is), provides UCS values that are in the strength range of the tested samples by other methods. Figure 26 shows the UCS of PLI using different “C” factors.

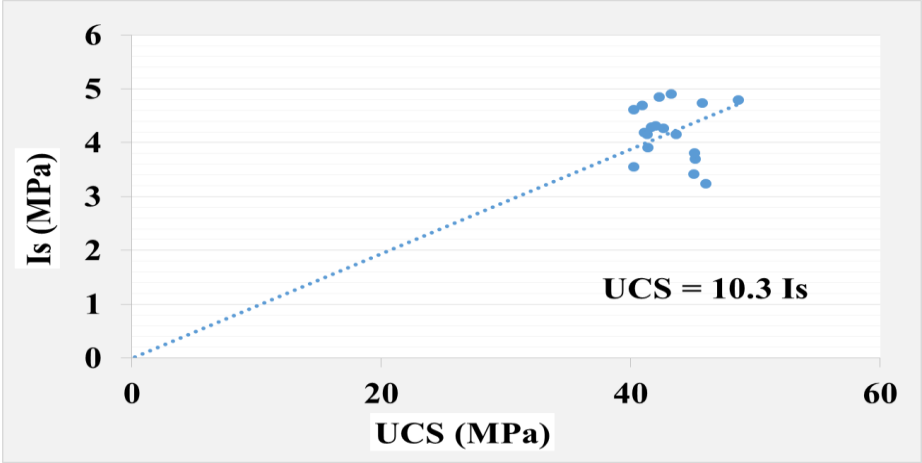


Figure 25. UCS Vs. Is

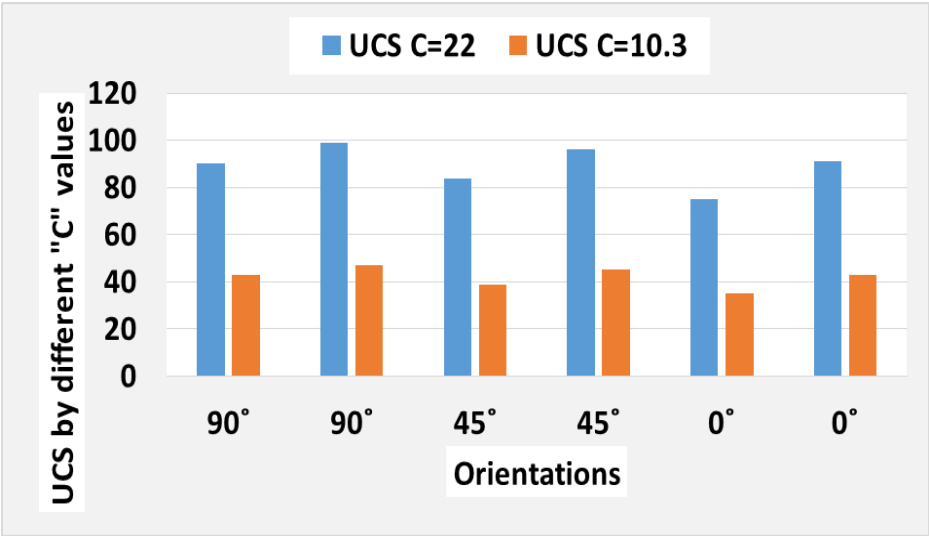


Figure 26. UCS values by PLI using different “c” factors.

Comparison between the mean values of the obtained UCS by different methods is shown in Figure 27. This representation of the data shows close correlation between the UCS values determined by different testing methods (UCS and IT) and the PLI using C factor of 10.3.

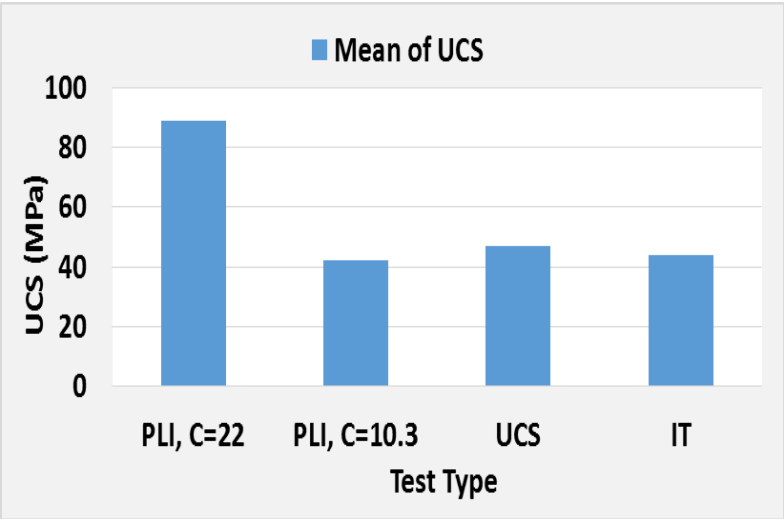


Figure 27. Mean Values of UCS values by different tests.

3.6.3 IT test: In this section, another practical, fast, and cheap, but reliable test was conducted. This test is the indirect tensile test (IT). It was performed in accordance to ASTM D6931-12. (2012). This test provided results of strength of the tested rock that is in the same range and compatible with strength results obtained from other testes reported in other sections of this paper. IT strength of the tested samples and their densities are shown in Figure 28. Figure 29 shows the relationship between the estimated strength by IT and PLI tests. The tested samples by IT are shown in Figure 30.

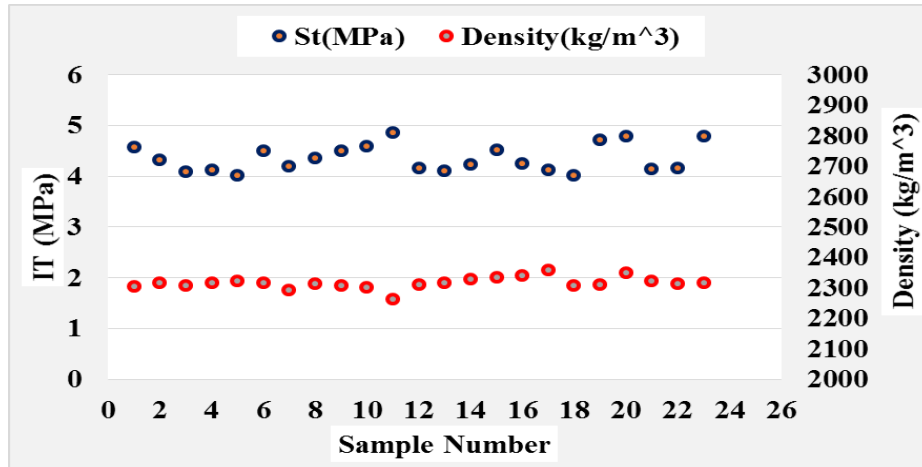


Figure 28. IT strength of the tested samples and their densities

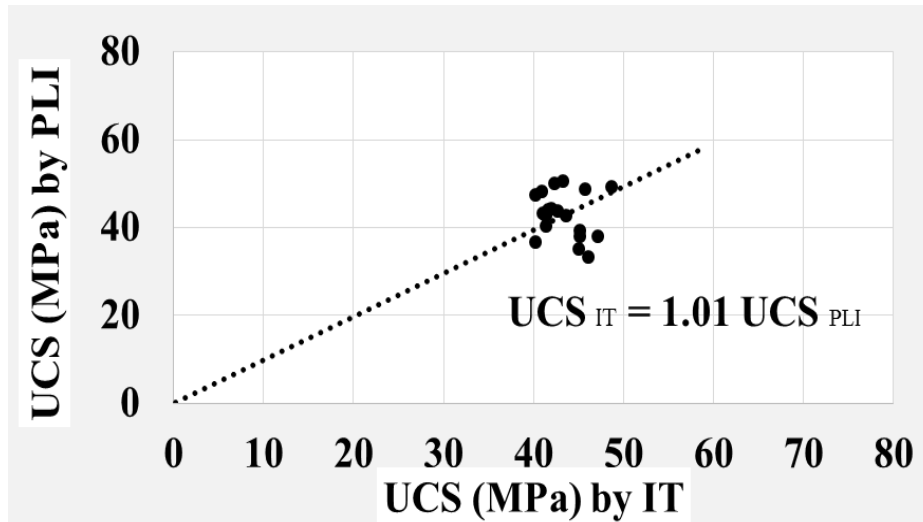


Figure 29. Estimated strength by IT and PLI tests



Figure 30. Tested Samples by IT test.

3.6.4. DRILLING TESTS

In this section, drilling performance is evaluated based on oriented drilling in isotropic (RLM) and anisotropic rocks (Red Shale). For drilling experiments, a vertical laboratory drilling rig was used. The applied drilling parameters included inputs of five different WOB, three flow rates, and three orientations. The laboratory drilling rig used for these tests was described by Rana et al (2015). The hydraulic configuration of the drill bit used in these tests was previously fully examined by Khorshidian et al. (2014). In order to evaluate the drilling efficiency of the conducted drilling tests for the work of this paper, the depth of cut (DOC), (mm/rev.) of the cutters was calculated. A laser triangulation sensor (LTS) was used to calculate the actual DOC. In all runs, DOC, which is equal to (ROP/rpm) , was found to be greater than the chamfer of the drill bit cutter that is 0.15 mm. Figure 31 shows LTS and the grooves made on a rotating plate and a sample of the LTS recorded data, top and bottom respectively. ROP is calculated using the numerical recorded data shown in Figure 32. Then relationships between the calculated ROP and WOB as function of flow rates and drilling orientations were constructed. Figure 32 shows the relationships between ROP and WOB using three different flow rates and in three different orientations. The results showed consistent trend in the three drilled directions. The results confirm that drilling was conducted through isotropy rocks. Drilled RLM samples grouped with respect to their drilling orientation are shown in Figure 33.

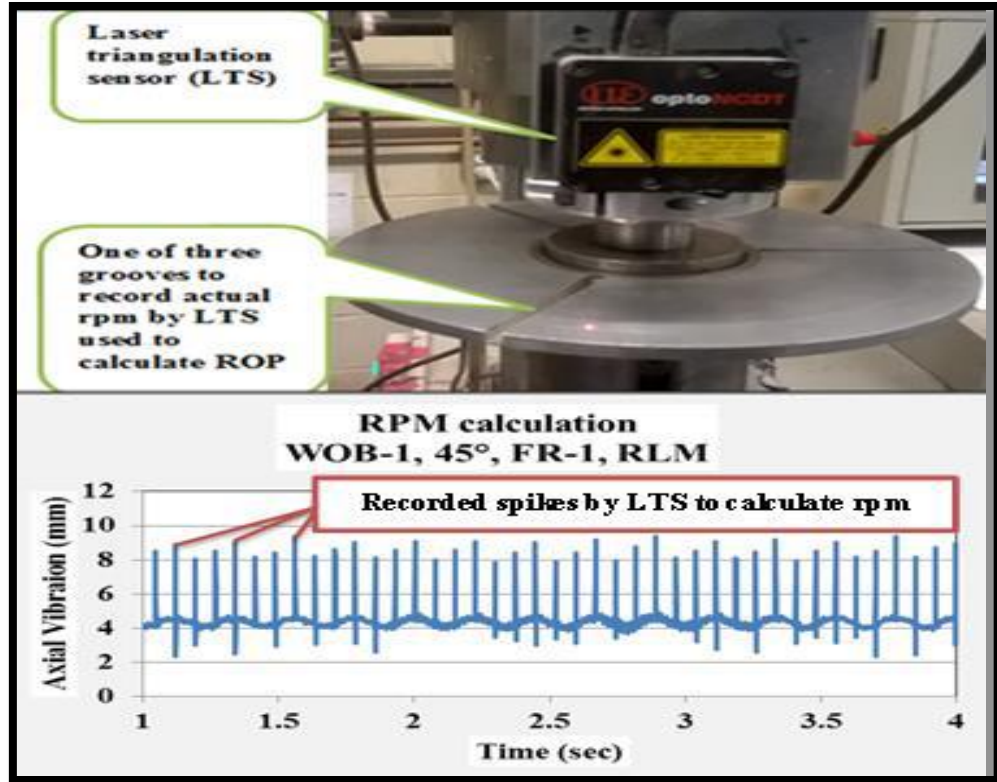


Figure 31. Top: LTS and grooved rotating plate for rpm calculation and bottom: recorded spikes by LTS to calculate rpm. For this run, RPM= 280.

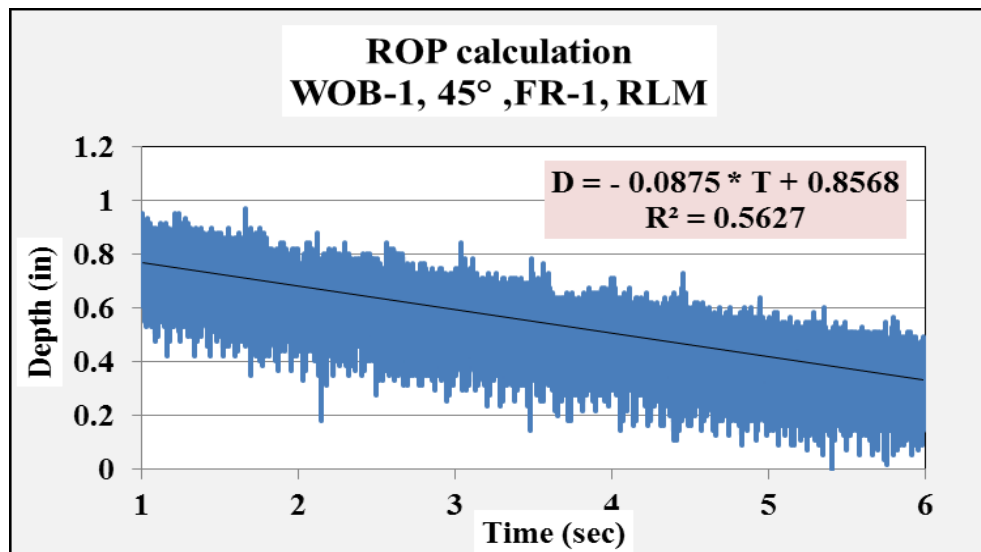


Figure 32. Sample of the recorded data used to calculate ROP. For this run, the slop = ROP of 8.00 (m/hr).

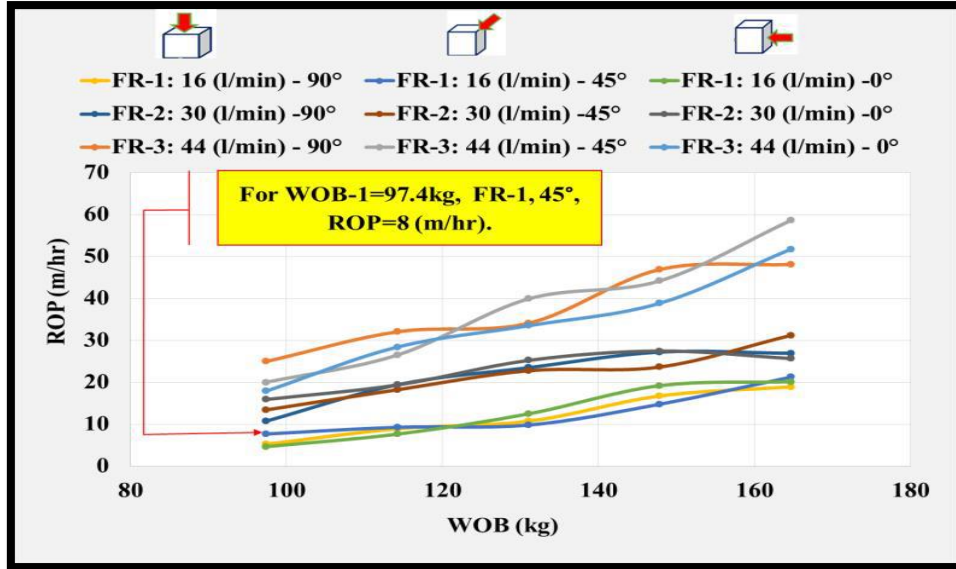


Figure 33. WOB Vs. ROP for three different flow rates and three different orientations

All data of lab drilling tests under different conditions of flow rates, orientations, and WOB are shown in Table 5.

Data of lab drilling tests (45 test runs in total)						
Flow rate and orientation	WOB (KG)	1	2	3	4	5
FR-1: 16 (l/min) - 90°	ROP (m/hr)	5.25	8.94	10.73	16.75	18.93
	DOC (mm/rev)	0.40	0.68	0.74	1.16	1.26
FR-1: 16 (l/min) - 45°	ROP (m/hr)	8.00	9.28	9.81	14.78	21.23
	DOC (mm/rev)	0.46	0.68	0.68	1.03	1.42
FR-1: 16 (l/min) - 0°	ROP (m/hr)	4.67	7.65	12.48	19.21	20.14
	DOC (mm/rev)	0.34	0.56	0.87	1.33	1.34
FR-2: 30 (l/min) - 90°	ROP (m/hr)	10.76	19.44	23.50	27.21	26.91
	DOC (mm/rev)	0.81	1.43	1.63	1.89	1.79
FR-2: 30 (l/min) - 45°	ROP (m/hr)	13.44	18.24	22.77	23.64	31.20
	DOC (mm/rev)	1.02	1.34	1.58	1.64	2.08
FR-2: 30 (l/min) - 0°	ROP (m/hr)	15.91	19.37	25.23	27.47	25.68
	DOC (mm/rev)	1.21	1.42	1.75	1.91	1.71
FR-3: 44 (l/min) - 90°	ROP (m/hr)	24.98	32.06	34.10	46.90	48.11
	DOC (mm/rev)	1.89	2.43	2.37	3.26	3.21
FR-3: 44 (l/min) - 45°	ROP (m/hr)	20.02	26.52	39.92	44.19	58.64
	DOC (mm/rev)	1.52	1.95	2.77	3.07	3.91
FR-3: 44 (l/min) - 0°	ROP (m/hr)	17.92	28.42	33.50	38.86	51.77
	DOC (mm/rev)	1.32	2.09	2.33	2.70	3.45

Table 5. Test matrix of lab-oriented drilling experiments including WOB, ROP, and DOC.

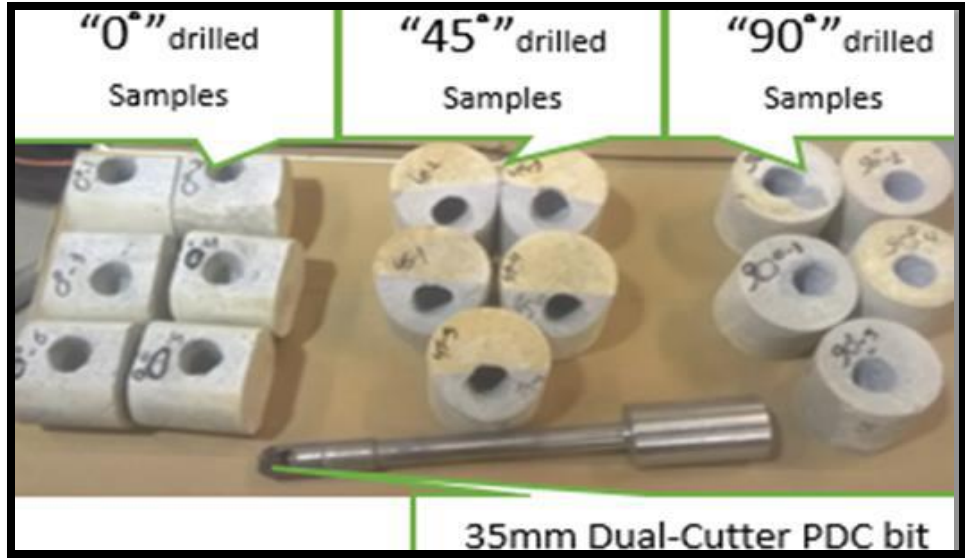


Figure 34. Some samples of drilling tests with PDC drill bit.

For comparison study between oriented drilling performance in RLM as isotropic rocks and Red Shale as anisotropic rocks, Figure 34 shows results from drilling in both materials. Such results are a part of study done by Abugharara et al. (2016) conducted on RLM and Red Shale and Table 6 includes the numerical data corresponding to the plots in Figure 35.

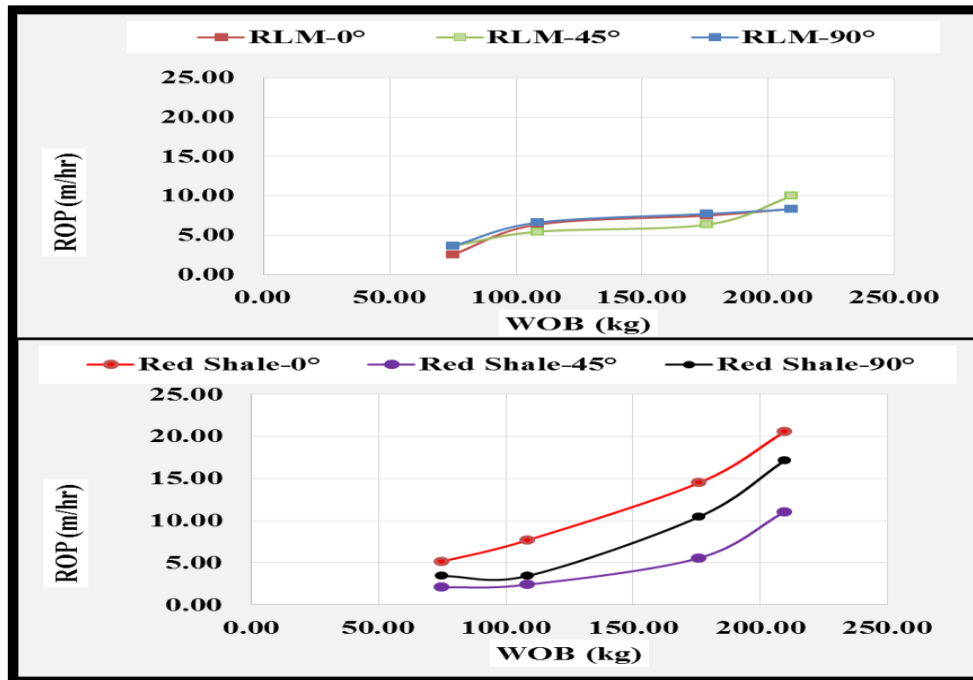


Figure 35. Drilling performance through RLM (top) and Red Shale (bottom)

Oriented Drilling in RLM (Isotropic) and Red Shale (Anisotropic) rocks						
Conditions: atmospheric pressure and flow rate of ~ 18 (L/min)						
Rock Type	Rotation	WOB(kg)	75.00	108.61	175.85	209.46
RLM	0°	ROP (m/hr)	2.55	6.35	7.49	8.35
	45°		3.63	5.44	6.35	9.98
	90°		3.63	6.60	7.71	8.29
Red Shale	0°	ROP (m/hr)	5.13	7.68	14.48	20.54
	45°		2.06	2.40	5.55	11.03
	90°		3.43	3.43	10.44	17.12

Table 6. Calculated ROP for RLM and Red Shale

3.7. SUMMARY

The work of this paper covers a set of selective physical, mechanical, and drilling measurements and tests, which can be summarized as follows:

- The physical measurements included calculating Vp, Vs, and DEM.
- The mechanical measurements included estimating the unconfined compressive strength of the rock by different methods.
- The drilling tests involved evaluating the penetration rate as a drilling performance indicator by applying various conditions of WOB, flowrates and orientations.
- The work was conducted on a medium strength concrete in three different orientations representing horizontal “0°”, diagonal “45°”, and vertical “90°” directions.
- The analysed result showed consistency confirming the isotropy structure of the tested rock in almost all the applied tests.
- A small degree of variation in the recorded measurements, in particular in PLI test was observed. The reason of the variation can be related to the change of the diameters of the tested samples with respect to the aggregates’ size (e.g. <2 mm).

- The effect of the diameter in PLI test (ASTM D5731-08) is a dimension effect. However, the effect of the ratio between sample diameter and aggregates size has been observed. A related research focusing on such effect has been started and will be further investigated for future publications
- Drilling performance evaluation can be emphasized as a new testing method for material anisotropic investigation along with the other testing methods included in this paper to determine the tested material anisotropy type and (%).
- The methodology of the selective tests performed in this paper can be taken for examining rocks' anisotropy parallel to other available methods.

Chapter 4

Laboratory Investigation on Directional Drilling Performance in Isotropic and Anisotropic Rocks

This chapter is the paper “Laboratory Investigation on Directional Drilling Performance in Isotropic and Anisotropic Rocks A. Abugharara and A. Alwaar concerted and conducted the experiment, analysed the data, and wrote the paper and C. Hurich, S. Butt, suspended the research and edited the paper. It was published in American Rock Mechanics Association in Houston, TX, CA, USA, 26-29 June 2016. The Figure numbers and references are altered to coordinate the designing rules set out by Memorial University of Newfoundland as compared with the original manuscript published in the conference proceeding.

ABSTRACT:

Successful drilling through shale with the optimal performance requires intensive research on controlled laboratory oriented drilling. The work of this paper is to evaluate oriented drilling, representing directional drilling in shale using a lab-scale drilling rig. Comparison study between drilling in shale and synthetic rock-like materials (RLM) of similar strength is included. The samples of shale and RLM were prepared to be characterized and drilled in different orientations (i.e. 0°, 45° and 90°) with respect to bedding for shale-samples and to the corresponding selected axis for RLM-samples. Physical measurements and mechanical tests were conducted to characterize the rocks and determine their anisotropy. Laboratory drilling experiments were performed using a 35mm dual-cutter PDC bit. Various weights on bit (WOB) were applied with constant water flow rate under atmospheric pressure. Drilling cuttings were collected and analyzed. Relationships between WOB, drilling rate of penetration (ROP), depth

of cut (DOC), and drilling cutting size were determined. Results show increase of ROP and DOC with increasing WOB. Results also show that cutting sizes increase with the increase of WOB and they can exhibit the material anisotropy. Such result can assist in a better planning of drilling in shale to enhance drilling performance, especially in deviated wells.

4.1. Introduction

With the increasing interest by oil and gas companies in comprehensively understanding shale, in particular oil shale and shale gas as it plays an important role in unconventional reservoir exploration and production, intensive laboratory studies on shale come to play major role. Numerous laboratory studies have been focused on shale characterization and determining anisotropy % and type. However not much emphasis was put on relationships between drilling performance and rock anisotropy as function of bedding orientation. The work of this paper focuses on investigating shale anisotropy through oriented drilling and drill cuttings analysis with comparison to artificial rocks (RLM). Also, to evaluate drilling performance in both rock types. An intensive work on RLM isotropy determination through multi-testing-methodologies was carried by Abugharara et al., (2016) reported that the tested RLM is isotropic rocks and was selected for further studies including the work of this paper. Many field, laboratory, and numerical studies were conducted to study the physical and mechanical properties of the anisotropic rocks and the fracture modes and propagation. Alharthi. (1998) reported that most of sedimentary and metamorphic rocks show some degree of anisotropy. In general, shale is characterized to be anisotropic Sodergeld et al. (2011). Lashkaripour. (2000) and Crawford et al. (2012) indicated that shale strength is also anisotropic. In particular the strength as, mechanical property of shale and wave velocities of shale were investigated by Fjaer et al. (2013), Ambrose et al. (2014), Simpson et al, (2014), and Mighani et el. (2016). Those studies

observed that shale strength estimated by UCS, CCS, and BTS is the highest perpendicular and parallel to bedding, but it decreases towards 45° and 30°. Wave velocities, on the other hand are highest when propagating parallel to bedding, lowest when propagating perpendicular to bedding and medium when propagating in 45°. Anisotropy and drilling ROP relationship was also investigated. Brown et al. (1981), Boualleg et al. (2007), Karfakis et al. (2007), Park et al. (2013), and Thuro et al. (2008) reported the influence of rock anisotropy on hole deviation tendency and drilling ROP. Thuro et al. (2008) concluded using PFC2D that drilling progress and ROP are highest when drilling perpendicular to bedding and decreases with the decrease of the angle between bedding plane and drilling direction until reaching the lowest when drilling parallel to bedding. Altindag. (2003) reported that drilling ROP can be estimated by means of coarseness index and mean particle size, where Pfeleider. (1953) indicated that a relationship between cutting size and shape with ROP was observed. However, as a main part of this paper, a new approach of a relationship between the ROP and cutting sizes as a function of rock anisotropy and rock orientation was investigated.

One of the latest studies that included intensive field and laboratory studies conducted by Drilling Technology Laboratory (DTL) at Memorial University of Newfoundland, Canada, started in 2014, also involved shale study.

In September 2014, DTL conducted drilling field trials during which three wells of about 120 m of each were drilled penetrating different shale formations. The formation dipping angle was about 12 deg. It was estimated before drilling though a comprehensive surface survey reported by Reyes et al. (2015). The drilling operations was rotary drilling and the drilling mode varied between conventional and vibrational drilling. Several types of drill bits including PDC, TSP and roller cone bits were used. The drilling performance was investigated as a function of drill

bit type, depth, penetrated formation type, drilling mode, etc. Collected drilling cuttings were analyzed as well. A geological cross-section of the drilling site was constructed.

For the laboratory studies, samples were cut from numerous shale rocks that were collected from an adjacent exposed formation in the drilling site that was estimated to be drilled in all wells after determining the dipping and the strikes of the formations and was confirmed by cutting analysis. Due to the challenge faced in obtaining shale core samples, a suggested method by Mele'ndez-Marti'nez, (2014) was followed to determine wave velocities for oriented samples and for physical characterization.

In general, samples of RLM and R-Shale were prepared, physically and mechanically characterized, and drilled in three main orientations (0° , 45° and 90°). The data obtained by this analysis provides a direct link between standard approaches for assessing material anisotropy and the effects of anisotropy on drilling performance.

4.2. EXPERIMENTAL EQUIPMENT AND PROCUDRE

4.2.1 Physical measurements

The main technique for measuring the physical properties practiced in this paper is the ultrasonic method. The objective of this is to evaluate the anisotropy structure of the tested material. Such physical anisotropy determination by the ultrasonic method can be analyzed with other anisotropy data obtained by mechanical tests (Sec. 2.3) and drilling experiments (Sec. 2.4). Compressional wave (V_p), and shear wave (V_s) velocities and densities were recorded for samples of different rock types before conducting the mechanical or drilling experiments. The recorded waves were measured with respect to different orientations. Moreover, the dynamic elastic moduli of RLM were calculated according to ASTM D2845-08. (2008). Figure 36 shows the average recorded V_p , V_s , and measured density of RLM samples in three different

directions. Figure 37 shows the dynamic elastic moduli of all tested samples of RLM. For RLM samples, the obtained V_p and V_s were about the same in all directions. This similarity in wave measurements can be taken as an indication of the isotropy of the tested RLM samples. Other mechanical measurements and drilling tests and cutting analysis support this observation.

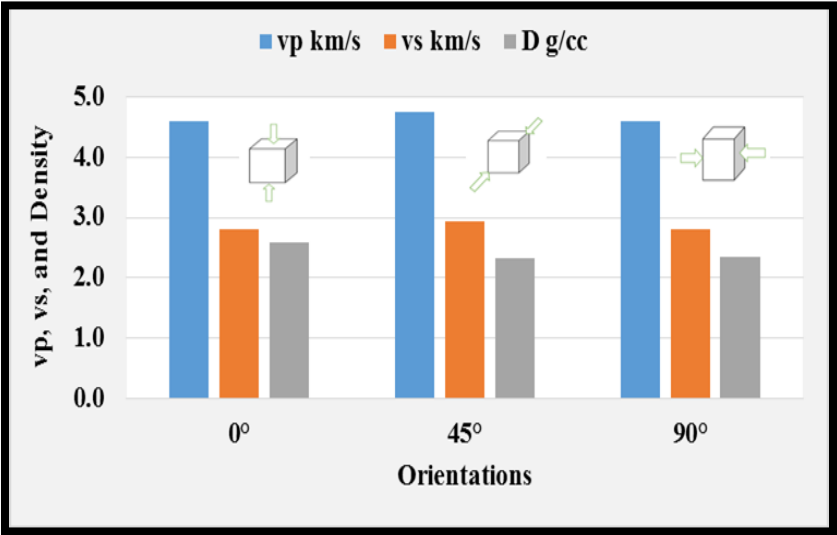


Figure 36. Oriented density and wave velocity measurements of RLM

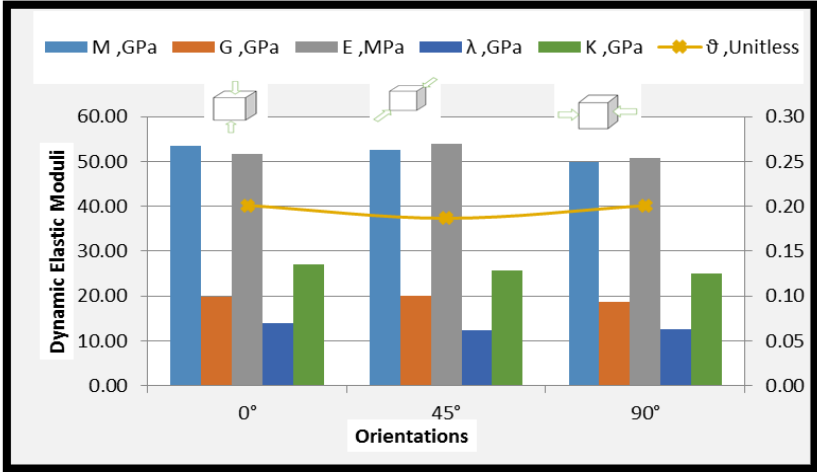


Figure 37. The oriented dynamic elastic moduli of RLM

Table 7 provides a summary of averaged measured values of V_p , V_s and Density of RLM. It also provides the mean values of RLM dynamic elastic moduli including M: Compressional

wave Modulus: modulus of rigidity, ν : Poisson's ratio, K: bulk modulus, E: Young's modulus of elasticity, and λ : Lamé's constant

Orientation	vp	vs	D	M	G
	km/s	km/s	g/cc	GPa	GPa
0°	4.60	2.80	2.58	53.54	19.83
45°	4.76	2.94	2.32	52.55	20.09
90°	4.60	2.81	2.35	49.85	18.65
Orientation	ν	K	E	λ	
	Unitless	GPa	MPa	GPa	
0°	0.20	27.10	51.62	13.88	
45°	0.19	25.76	53.94	12.37	
90°	0.20	24.99	50.88	12.56	

Table 7. Mean values of oriented Vp, Vs, density, and dynamic elastic moduli of RLM

Wave velocities were also determined for R-Shale samples in the three orientations. However, due to limited samples of shale, the dynamic elastic constants will be conducted on more samples for future work for accuracy and confirmation. In the meantime, the wave velocities exhibit the anisotropy of R Shale samples. Figures 38 and 39 show the recorded Vp and Vs and the measured density of two sets of R-Shale samples

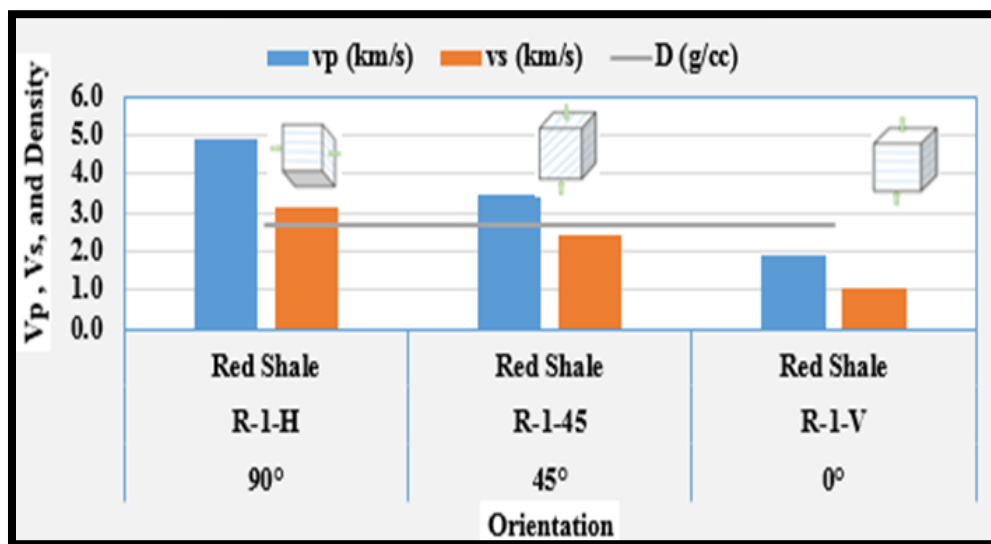


Figure 38. Oriented density and wave velocity measurements of R-Shale-1

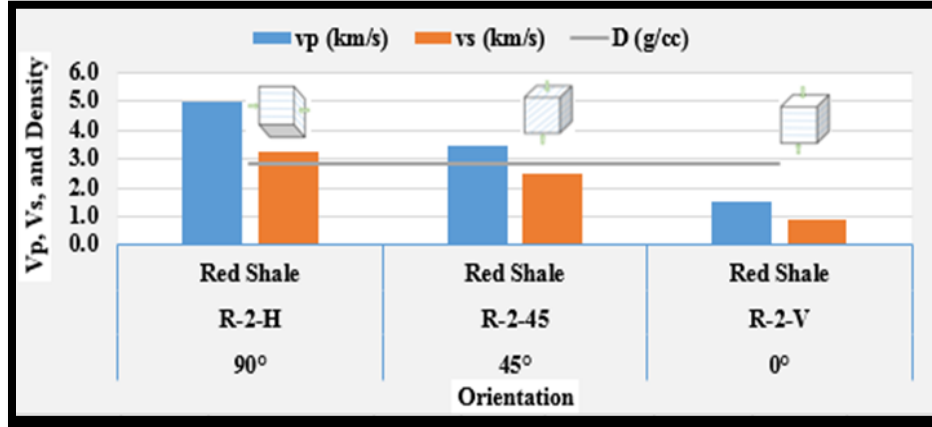


Figure 39. Oriented density and wave velocity measurements of R-Shale-2

Table 8 summarizes the mean values of Vp, Vs, and density of R-Shale samples.

Orientation	Spec.#	vp (km/s)	vs (km/s)	D (g/cc)
90°	R-1-H	4.92	3.16	2.71
45°	R-1-45	3.49	2.45	2.71
0°	R-1-V	1.89	1.05	2.71
90°	R-2-H	5.01	3.22	2.81
45°	R-2-45	3.49	2.45	2.81
0°	R-2-V	1.48	0.87	2.81

Table 8. Mean values of oriented Vp, Vs, and density of two R-Shale samples1, and 2, respectively.

For evaluating the Transversely Isotropy (TI) of R-Shale, multi measurements were taken on several R-Shale samples that were cut from same larger rock. Most of the measurements were taken parallel to bedding to confirm the shale Vertically Transversely Isotropy (VTI). The measured Vp and Vs in directions parallel to a bedding of R-Shale in various locations are summarized in table 9. Figure 40 shows all values of Vp and Vs measured parallel to R-Shale bedding in various positions on parallel faces and the mean values of Vp and Vs, top and bottom; respectively. Figure 41 shows the tested R-Shale samples and the positions of the measurements.

Spec.#	Spec. rock type	Faces set #	All values		Mean values	
			Vp	Vs	Vp	Vs
			(km/sec)		(km/sec)	
R-Shale-1	H1-1'	1-1'	4.93	3.19	4.86	3.16
	H2-2'	1-1'	4.93	3.25		
	H3-3'	1-1'	4.79	3.08		
	H4-4'	1-1'	4.79	3.13		
R-Shale-2	H1-1'	1-1'	5.14	3.18	4.86	3.11
	H2-2'	1-1'	4.61	3.04		
	H3-3'	1-1'	4.61	3.04		
	H4-4'	2-2'	4.94	3.14		
	H5-5'	2-2'	4.94	3.14		
	H6-6'	2-2'	4.94	3.14		
R-Shale-3	H1-1'	1-1'	4.84	3.19	4.87	3.19
	H2-2'	1-1'	4.84	3.26		
	H3-3'	1-1'	4.84	3.26		
	H4-4'	2-2'	4.97	3.07		
	H5-5'	2-2'	4.86	3.16		
	H6-6'	2-2'	4.86	3.21		

Table 9. All and mean values of the measured Vp and Vs of several R-Shale samples in directions parallel to bedding in various locations.

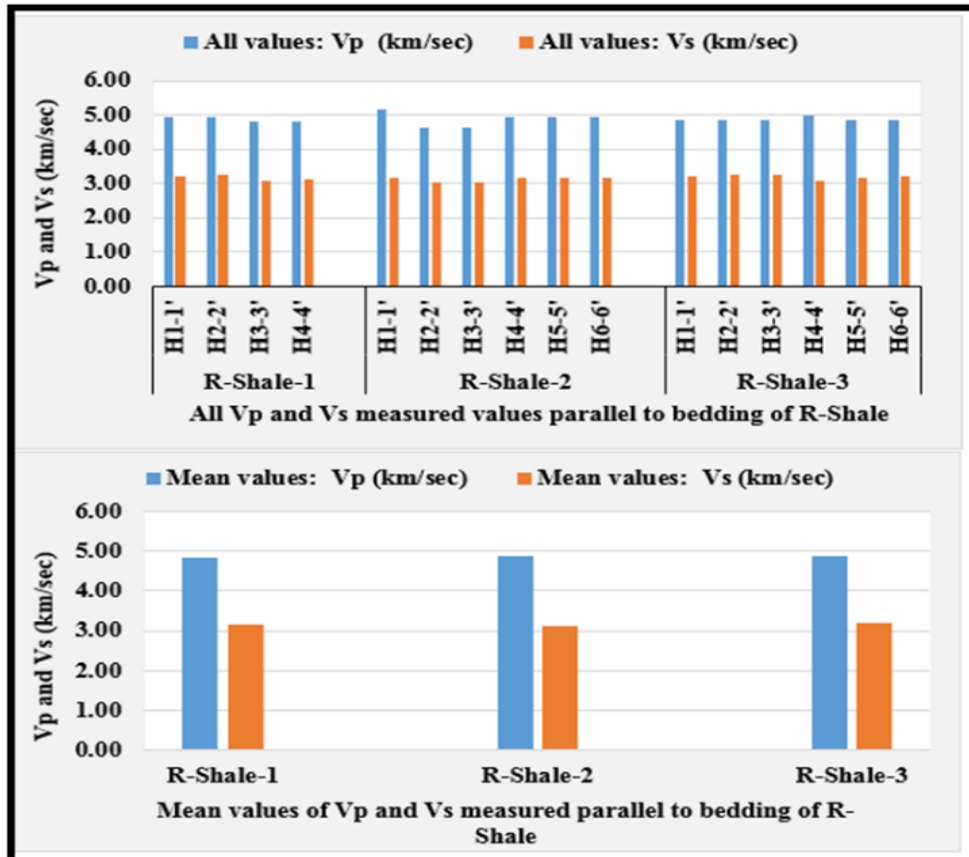


Figure 40. All and mean values of Vp and Vs measured in parallel direction to R-Shale bedding.

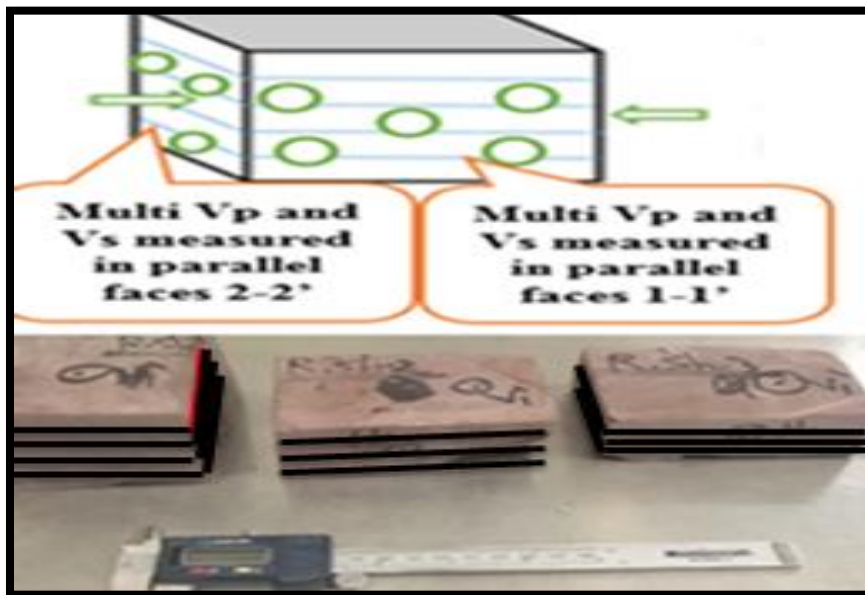


Figure 41. Multi measurements of Vp and Vs in two sets of parallel faces in parallel direction to R-Shale bedding.

4.2.3 Mechanical measurements

For RLM samples, the indirect (disk splitting) tensile test according to ASTM D3967-08. (2008) was performed to estimate the tensile strength (σ_t). The test was conducted on disks cut from ~ 2-inch cylindrical specimens cored in different orientations. Figure 42 shows the average values of the tensile strength (σ_t) of RLM in the three denoted orientations.

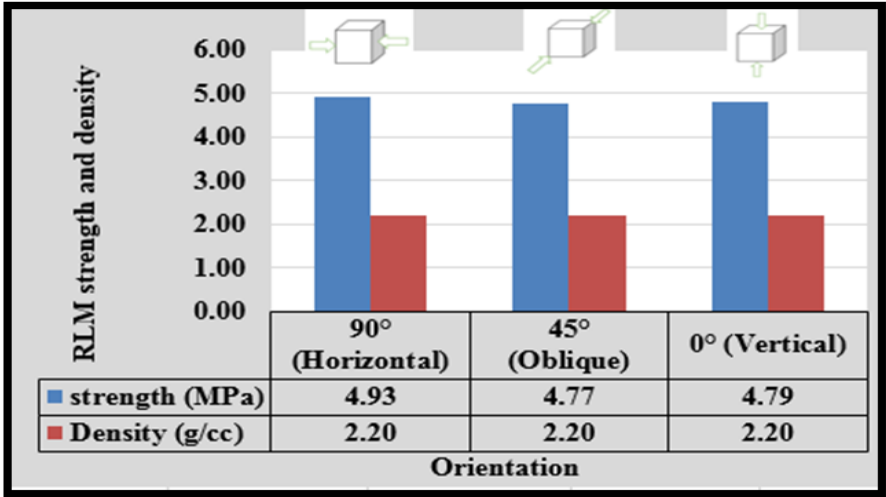


Figure 42. Mean values of oriented (σ_t) of RLM by splitting test.

Figure 43 shows the RLM disks in different orientations before and after splitting cut from ~ 2-inch samples cored from 4-inch RLM cylinders as source of the disks, and the splitting apparatus (Modified point load apparatus). The average σ_t values of ~ 4.8 MPa was obtained in all orientations.

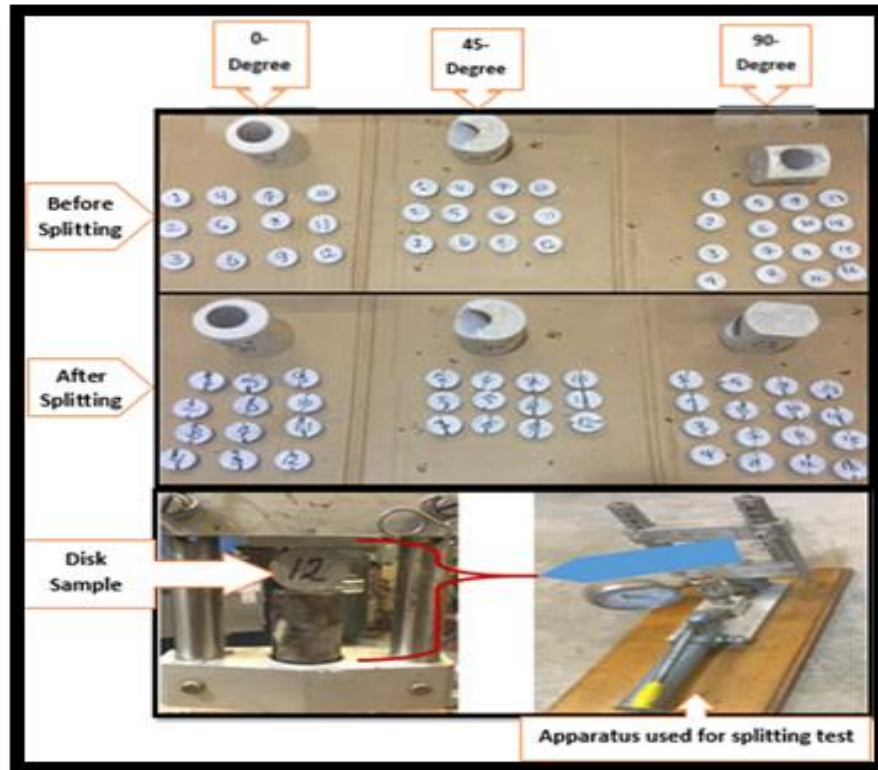


Figure 43. RLM samples before and after test and splitting test apparatus

For R-Shale, the point load index (PLI) test was performed on irregular lump samples following ASTM D5731-08. (2008). The samples were tested only vertically as a result of difficulties associated with obtaining samples in other orientations to perform this test. Figure 44 shows R-Shale samples for the physical characterization and for point load index test in tow states; before and after failure, respectively

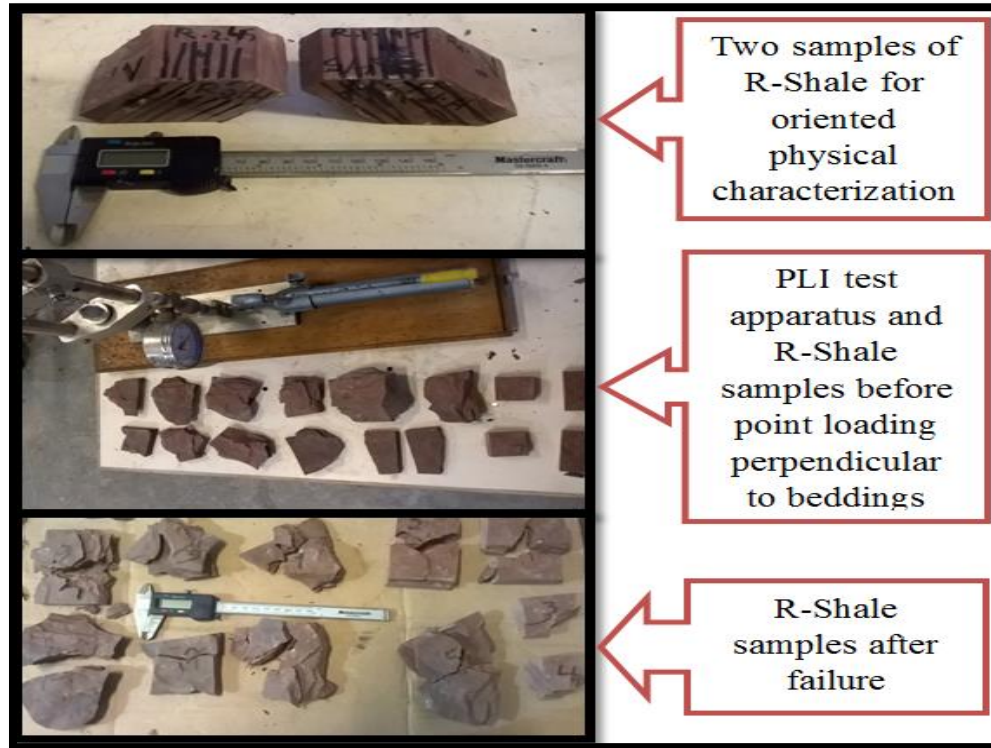


Figure 44. R-Shale samples for oriented physical characterization and point load test.

Table 10 contains the estimated UCS values of R-Shale samples obtained by point load perpendicular to bedding. The mean value of the PLI = 2.7MPa.

Result of PLI test conducted on R-Shale samples perpendicular to beddings						
Ref.	Orientation	Test type	Is	UCS	Is avg	UCS avg
1	Vertical "0° "	Lump	4.03	88.72	2.68	58.87
2			3.13	68.84		
3			2.47	54.36		
4			3.38	74.29		
5			1.53	33.72		
6			1.60	35.16		
7			2.18	48.02		
8			3.16	69.46		
9			2.60	57.22		

Table 10. Summary of PLI test values of R-Shale samples

4.2.4 Lab. Drilling experiments

4.2.4.1 Lab drilling apparatus

Lab drilling experiments were performed using a lab scale drill rig shown in figure 45. The drill bit used was a 35-mm dual cutter PDC bit. The drilling tests were conducted under atmospheric pressure. The water flow rate of 18 L/min was utilized to clean-off the drilled hole and to remove the cuttings towards the cutting collection system.

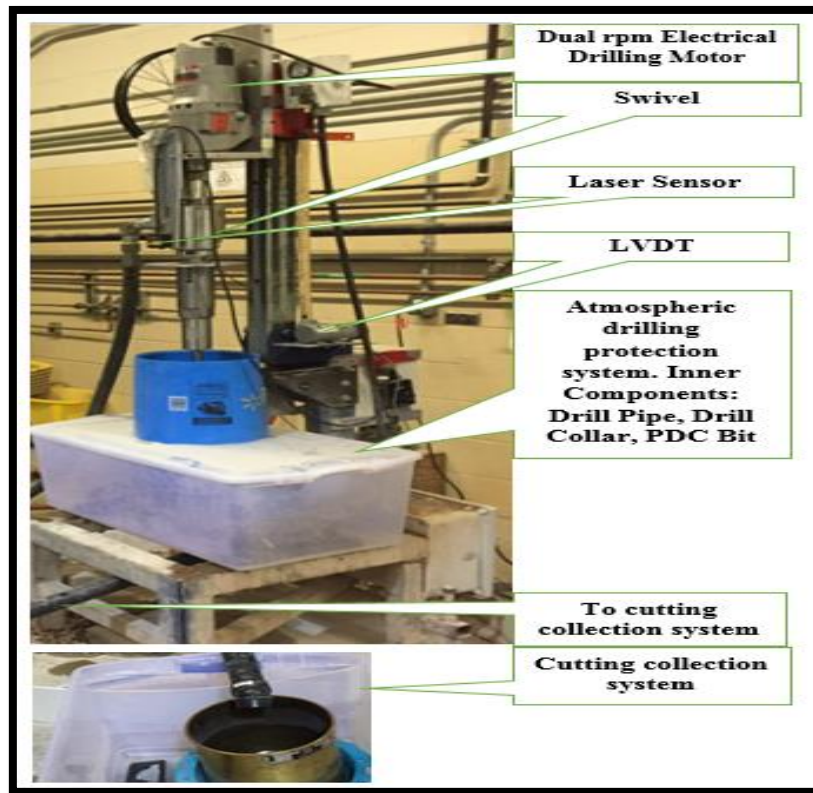


Figure 35. Lab scale conventional drill rig

4.2.4.2 RLM and R-Shale samples preparation for drilling experiments

RLM samples were cast in one direction (vertical direction). They were cut in three directions and drilled accordingly afterwards. On the other hand, as the R-Shale samples are laminated structure they are weak and easy to split when being drilled, in particular when cut into small samples. To avoid splitting R-Shale, the cut samples were stabilized by casting them in cement.

Hence, the samples were drilled afterwards according to the desired orientation. Figure 46, 47 shows the RLM and R-Shale samples after drilling in different orientations.



Figure 46. RLM and R-Shale samples after drilling in different orientations

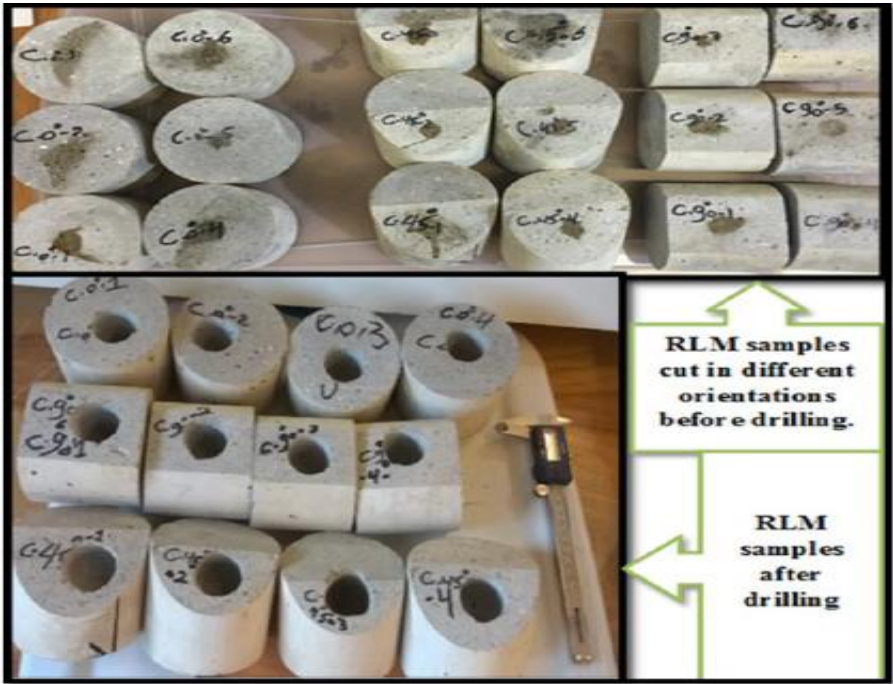


Figure 47. RLM samples before and after drilling

4.2.4.3 Drilling cuttings' collection

While drilling, a 75 μ -m (0.0030 inch) sieve was used. Cutting samples of all drilled RLM and R-shale samples in the designated orientations were collected. A standard pre-sieving procedure for drying was followed. Sieves varying between 850 μ -m and 75 μ -m were used for cuttings size analysis. There are two points to emphasize in this study. First, the cutting size increases with the increase of the ROP. Second, the relationship between ROP and cutting size should be the same in all directions when drilling a homogeneous (isotropic) material and varies when drilling a heterogeneous (anisotropic) material. The obtained drill cuttings analysis results (Sec. 3.1.2) supported the assertion that drilling an isotropic material is orientation independent. However, drilling in R-Shale is orientation dependent. Therefore, achieving high ROP in drilling in shale may require selection of the best orientation as well trajectory. Figure 48 shows the cutting samples and cutting sieving apparatus.

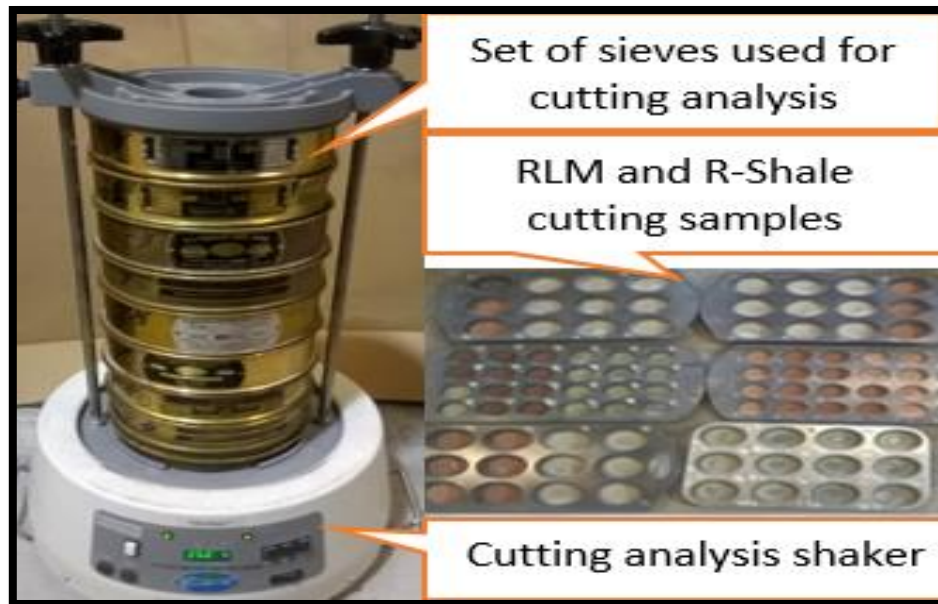


Figure 48. Cutting samples and cutting sieving apparatus

4.3. Lab experiments results

4.3.1 Drilling performance

During drilling, different sensors were used to measure various drilling parameters; including a laser sensor to measure axial vibration to evaluate the bit-rock interaction, and LVDT to measure drill bit displacement. A DAQ system utilizing LabVIEW was used to record the data. ROP and DOC were calculated and plotted versus WOB.

4.3.1.1 WOB vs. ROP and DOC

To provide WOB, several steel plates are used to feed the suspended weight. Summary of WOB, calculated ROP, and DOC is displayed in table 11.

Rock Type	Rotation	Drilling Flow Rate ~ 18 (L/min)					
		WOB(kg)	75.00	108.61	142.23	175.85	209.46
RLM	0°	ROP (m/hr)	2.55	6.35	9.53	7.49	8.35
		DOC (mm/rev)	0.19	0.50	0.80	0.50	0.67
		ROP (m/hr)	3.63	5.44	14.42	6.35	9.98
RLM	45°	DOC (mm/rev)	0.28	0.43	1.01	0.46	0.68
		ROP (m/hr)	3.63	6.60	7.56	7.71	8.29
RLM	90°	DOC (mm/rev)	0.23	0.50	0.53	0.54	0.58
		ROP (m/hr)	5.13	7.68	11.49	14.48	20.54
R-Shale	0°	DOC (mm/rev)	0.35	0.52	0.77	0.97	1.38
		ROP (m/hr)	2.06	2.40	3.39	5.55	11.03
R-Shale	45°	DOC (mm/rev)	0.16	0.18	0.24	0.39	0.76
		ROP (m/hr)	3.43	3.43	7.01	10.44	17.12
R-Shale	90°	DOC (mm/rev)	0.23	0.23	0.47	0.70	1.15

Table 11. Drilling parameters of WOB, ROP and DOC for RLM and R-Shale

The revolutions per minute (RPM) were determined by using the laser sensor. Figures 49 and 50 show the relationships between WOB and ROP in three orientations of RLM and R-Shale, respectively

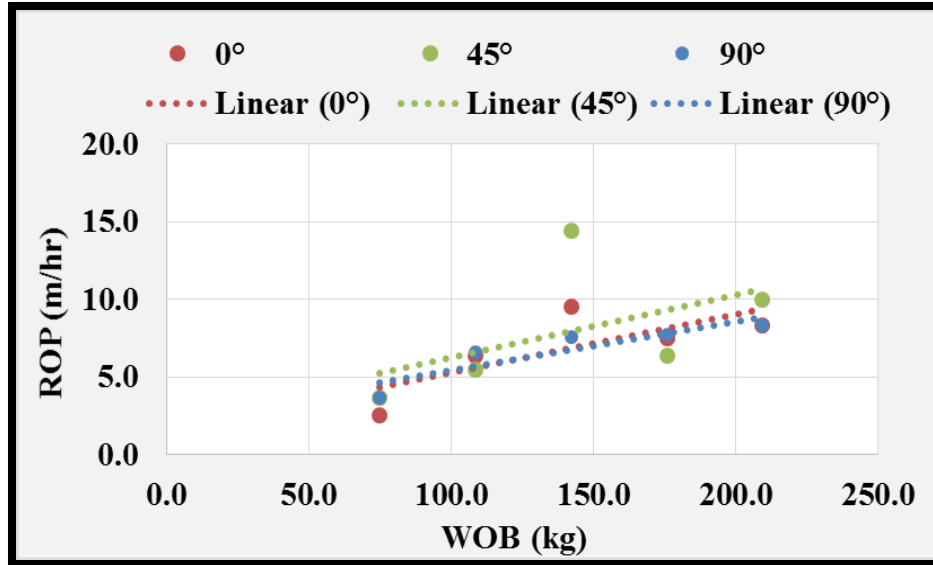


Figure 49. Oriented relationship between WOB and ROP of RLM

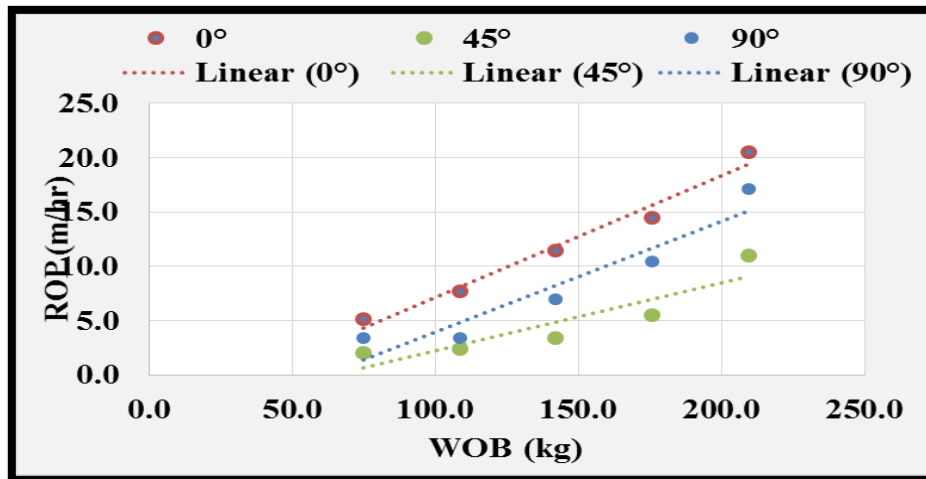


Figure 50. Oriented relationship between WOB and ROP of R-Shale

4.3.1.2 Cutting size analysis

The collected cuttings were in small volumes; however, most of the sieving analysis procedure was according to ASTM C136/C136M-14, 2014. The set of sieves used in cutting analysis included the following mesh sizes in mm: 0.85, 0.63, 0.59, 0.42, 0.25, 0.212, 0.177, 0.166, 0.15, 0.09, and 0.075

The results of the cutting analysis can be summarized as follows:

- For RLM, the cutting size distribution in % follows same trend when drilling in different orientations. Such matching in size distribution confirms the anisotropy of the drilled rocks.
- Similar matching trends were noticed in low WOB: (W1=75kg) as well as in high WOB: W9=209 kg.
- Drilling in RLM as an isotropic rock is orientation independent. Figure 51 (top and bottom) shows the distribution of cuttings collected from drilling RLM.
- For R-Shale, the cutting size distribution in % follows same trend when drilling in different orientations. Such matching in size distribution confirms the anisotropy of the drilled rocks.
- Such mismatching trends were noticed in low WOB: (W1=75kg) and in high WOB: W9=209 kg.
- Drilling in R-Shale as an anisotropic rock is orientation dependent. Figure 52 (top and bottom) shows the distribution of cuttings collected from drilling R-Shale.

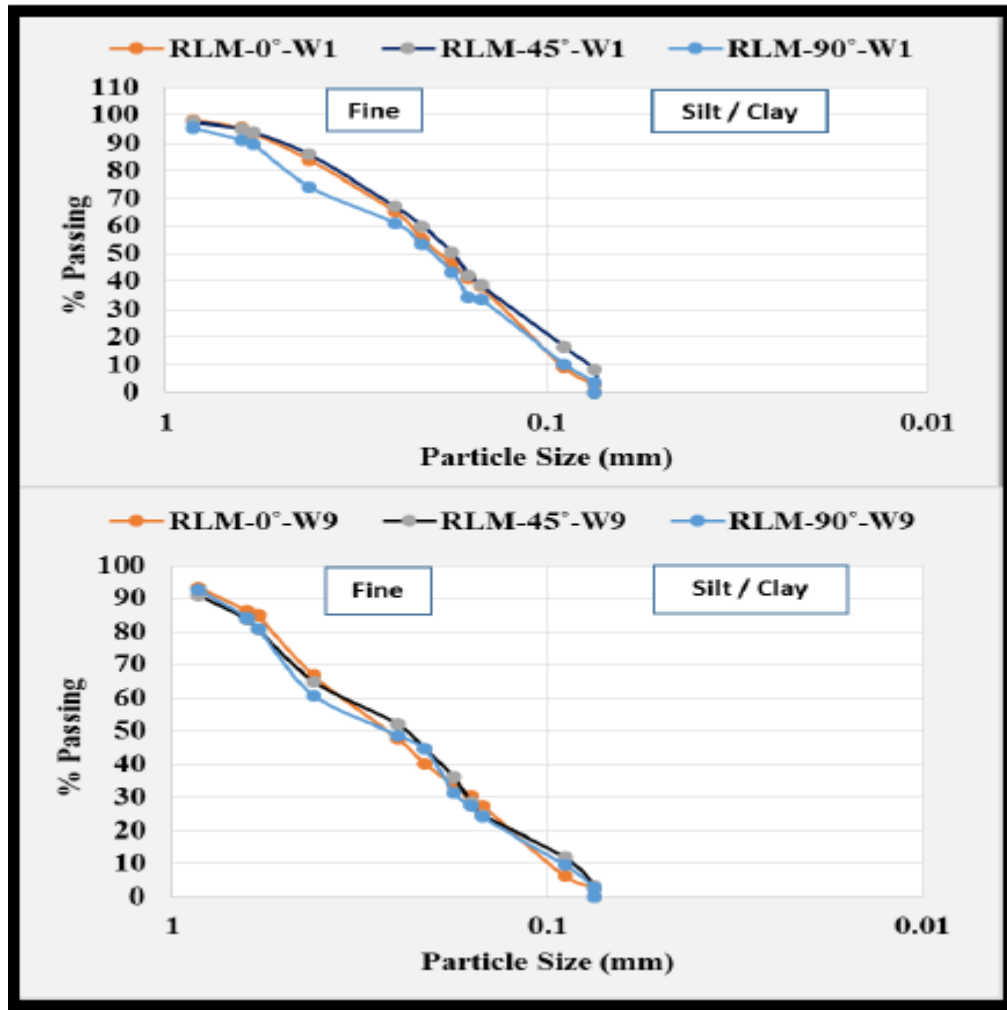


Figure 51. Cutting size analysis with the increase of WOB in drilling RLM in the three orientations 0°, 45°, and 90°. Figures show matching distribution confirming isotropy of RLM.

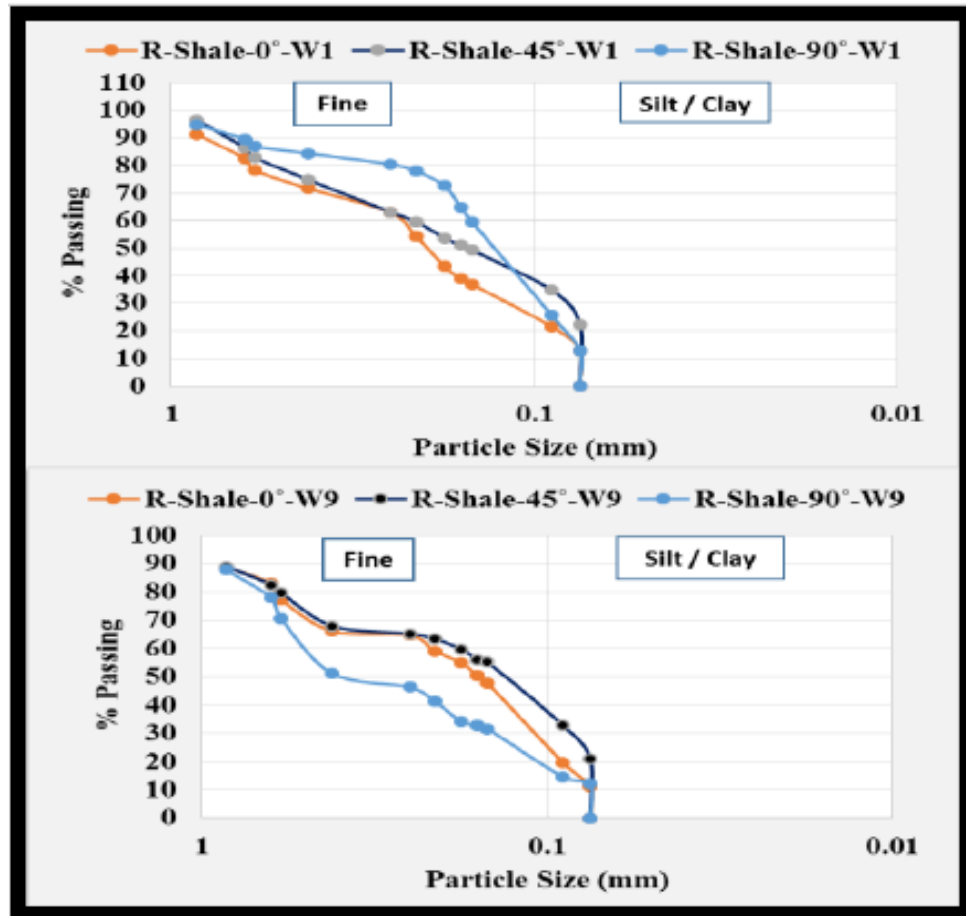


Figure 52. Cutting size analysis with the increase of WOB in drilling RLM in the three orientations 0°, 45°, and 90°. Figures show mismatching distribution confirming isotropy of RLM

4.6. Conclusions

Several physical and mechanical measurements and drilling tests were conducted as work of this paper. Conclusions of those measurements and tests are summarized as follows:

- Physical measurements using ultrasonic method conducted on RLM showed material isotropy, where same applied measurements conducted on R-shale showed material anisotropy.
- In particular, beside R-shale anisotropy exhibition, oriented V_p and V_s through R-shale in three different angles in couple samples exhibited special anisotropy of Vertically

Transversely Isotropy (VTI). Investigation of such VTI has started using more angles representing more orientations of cores and cupped shaped samples will be reported in future publications.

- However, multi V_p and V_s measurements have been taken in parallel direction to R-Shale's bedding and showed same values of VTI.
- Mechanical measurements through indirect tensile tests conducted on disks cut from cylindrical samples cored in different orientations of RLM showed the RLM isotropy. Where PLI test was only conducted in perpendicular direction to R-shale bedding represents R-shale strength in this direction. R-shale strength determination in other directions to be conducted for R-shale anisotropy or VTI confirmation are under investigation and will be reported in future publications.
- Laboratory drilling experiments were conducted under constant water flow rate and rotary speed under atmospheric pressure. Recorded data of drill bit travel; bit-rock interaction through axial motion and vibration, as well as the actual rpm while drilling was all recorded by utilizing precise sensors. Such obtained data assists in calculating ROP and DOC. ROP and DOC are plotted against WOB.
- ROP, DOC, as well as the cutting size % obtained from RLM exhibit same trend with respect to orientations confirming the isotropy of RLM.
- ROP, DOC, and the cutting size % obtained from R-Shale exhibit various trends with respect to different orientations proposing R-Shale anisotropy.

Chapter 5

PFC-2D Numerical study of the influence of passive vibration assisted rotary drilling tool (pVARD) on drilling performance enhancement

This chapter is the paper “PFC-2D Numerical study of the influence of passive vibration assisted rotary drilling tool (pVARD) on drilling performance enhancement”. A. Alwaar and A. Abugharara concerted and conducted the simulation, analysed the data, and wrote the paper with C. Hurich, S. Butt, suspended the research, edited the paper. thus, submitted it to American Rock Mechanics Association in June 17-22, 2018, Madrid, Spain. The Figure numbers and references are altered to coordinate the designing rules set out by Memorial University of Newfoundland as compared with the original manuscript published in the conference proceeding.

ABSTRACT:

The objective of this work is to evaluate the influence of the implementing the downhole Passive Vibration Assisting Rotary Drilling (pVARD) Tool on enhancing drilling performance using a numerical study utilizing a Particle Flow Code (PFC-2D). The work is comprised of a numerical study of a simulation using the PFC-2D on an experimental work described in ARMA 15-492 (Rana et al, 2015). The numerical study was performed to validate the experimental work following the steps, procedure, and conditions performed in the laboratory work.

The numerical study of the laboratory work involves not only the evaluation of drilling rate of penetration (ROP), but it also includes the Depth of Cut (DOC) of the bit cutters and the Mechanical Specific Energy (MSE). This numerical work also includes comparison study of

drilling performance under various configurations of the pVARD tool, which represents a controlled downhole vibration against the rigid drilling configuration that represents the conventional rotary drilling. The pVARD configurations involves pVARD low spring compliance, medium spring compliance, and high spring compliance. The drilling output parameters of DOC, MSE, and ROP are then studied and analyzed in all pVARD and non-pVARD configurations.

Likewise of the experimental work, the result of the numerical simulation approves the experimental work and it indicates the positive effect of utilizing the downhole pVARD on improving ROP. The drilling performance enhancement is also supported by the DOC and the MSE result.

5.1. INTRODUCTION AND BACKGROUND

Field and laboratory drilling experiments approved the positive effect of the employment of pVARD on enhancing ROP Rana et al (2015), Zhong et al (2016). Akbar. (2011).

Research describes the efficient drilling of oil and gas wells in various ways. One way includes reduction of the non-productive time (NPD) by extending the downhole tools' lives, preventing damaging drill bit as a result of encountered downhole lateral and stick/slip vibrations, improving the downhole drillstring mechanical behavior, reducing downhole frictions in non-vertical wells, and ultimately enhancing ROP by inducing downhole axial vibrations Rana et al (2015), Zhong et al (2016). Abtahi. (2011) and Gee et al (2015)

PFC-2D has been used as an applicable method to simulate drilling performance Zhong et al (2016), Akbar. (2011), Wilson. (2017) and Carrapatoso. (2013). Various conditions of pressure, rock properties, flow rates vibration and non-vibration modes were applied during implementing

PFC-2D studies for numerical drilling investigations Zhong et al (2016). Babatunde. (2011), and Akbar. (2011)].

The enhancement of the drilling ROP can be achieved through numerous ways. The conventional way of improving the ROP can be reached by manipulating with the inputs of the drilling parameters including drill mud flow rates, rotary speeds, rotary torque, and weights on bit (WOB). However, the increase of the above drilling parameters can negatively impact the drilling performance if not applied optimally. For example, an intensive increase of the WOB could cause buckling of the drill string. Also, the intensive increase of the rotary rpm and torque could damage the teeth of the drill bit associated with a high DOC when using a polycrystalline diamond compact (PDC) bit that follows rock shear fracture mode. Considering the fact that the increase of each of the above parameters can only be entered at the top of the drill string and would be transmitted through the entire drill string to reach the drill bit.

The unconventional method to improve the drilling ROP can be achieved by utilizing the available, moderate, and practical inputs of the drilling parameters at the drill bit by tools installed as part of the Bottom hole assembly (BHA). One approach of increasing the ROP by this method is by implementing the downhole pVARD tool Zhong et al (2016).

pVARD tool was designed at the Drilling Technology Laboratory (DTL) in Memorial University of Newfoundland, St. John's, Canada. The pVARD tool was also tested to study its influence on drilling performance applying numerous drilling conditions. The drilling conditions included pressure, flow rates, rotary speeds, formation strengths, formation orientations in laboratory and field scales. Under the above drilling conditions, the pVARD tool was approved to play an important role in improving the drilling performance. This paper validates the results of improving ROP of the field and laboratory work published in ARMA

15-492 (Rana et al, 2015) by employing a comparison study between the experimental study with the simulation study using PFC-2D.

5.2. DESCRIPTION OF PWARD

pWARD tool has numerous advantages. One of its main functions is to allow the drilling string to have some axial movement with different magnitudes based on the equation of bit-rock-interaction. The axial movements that the pWARD tool has is controlled by the strength of the contained springs of the tool components that produce the pWARD compliance magnitude. The range of the spring compliance has a relationship with the strength of the rock being drilled and therefore it governs the operation range of the tool.

The three main configurations of the pWARD tool that are analyzed in this paper includes sets of low compliance, medium compliance, and high compliance, which represent a high magnitude of low spring strength, a medium magnitude of medium spring strength, and a low magnitude of high spring strength; respectively.

With the additions of the various drilling conditions that the pWARD tool was tested for that were mentioned in the introduction section, the field and laboratory pWARD tool was also experimentally tested under different applications and configurations included the above three sets mentioned above.

Table 13 summarizes the parameters and their magnitudes that were implemented in the PFC-2D simulation study of the pWARD.

5.3. STUDIED PARAMETERS

The parameters included in the analysis are the same in the experimental work as well as in the numerical work. They involve the followings:

1. Input Drilling Parameters (IDP):

- Different Bottomhole Pressure (BHP).
- Different Weights on Bit (WOB).
- Three configurations of PVAR D versus Rigid.

2. Output Drilling Parameters (ODP):

- Drilling Rate of Penetration (ROP)
- Depth of Cut (DOC).
- Mechanical Specific Energy (MSE).

Property	Magnitude
Ratio of Maximum to Minimum Ball Size	1.8
Parallel Bond Shear Strength	44e6 Pa
Parallel Bond Normal Strength	44e6 Pa
Minimum Ball Radius	0.35e-3 m
Ball and Bond Elastic Modulus	44e9 Pa
Ratio of Normal to Shear Stiffness	2.5
Ball-Ball and Ball-Wall Friction	0.5
Density	2650 kg/m ³
Porosity	18 %
Normal Damping Ratio	0.2
Shear Damping Ration	0.2
Local Damping Ratio	0.5
Unconfined Compressive Strength (UCS)	55 MPa
Young Modulus	40 GPa

Table 12. Summary of PFC-2D parameters and their magnitudes.

Figure 53 shows the drilling procedure of PFC-2D. It also shows the cutter, weight configurations applied, and region of study in the PFD-2D study. The three balls displayed in Fig. 53 represent the static weight on bit, the spring stiffness for each pVARD configuration, and the damping.

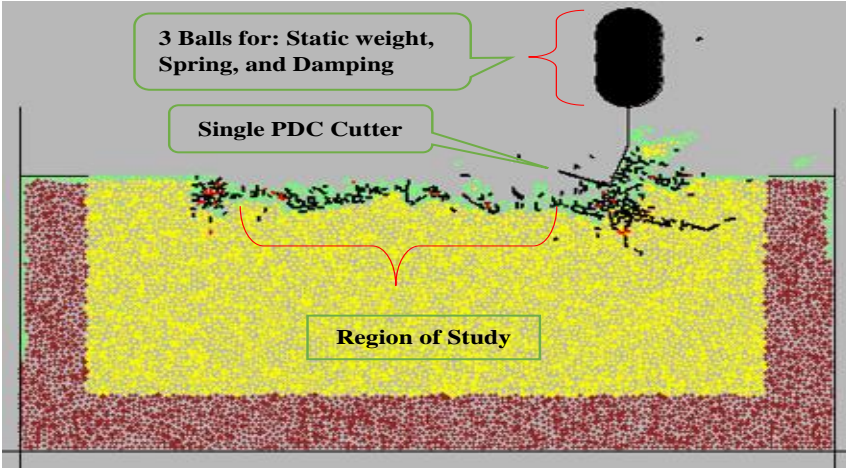


Figure 43. Description of the numerical study of the drilling process using PFC-2D, including weight on bit in case of PVAR

BHP was another factor implemented in the PFC-2D simulation. The purpose of this is to evaluate the influence of the BOP on drilling performance using pVARD Versus. rigid drilling. The result of the effect of BOP on the drilling performance is shown in Fig.54

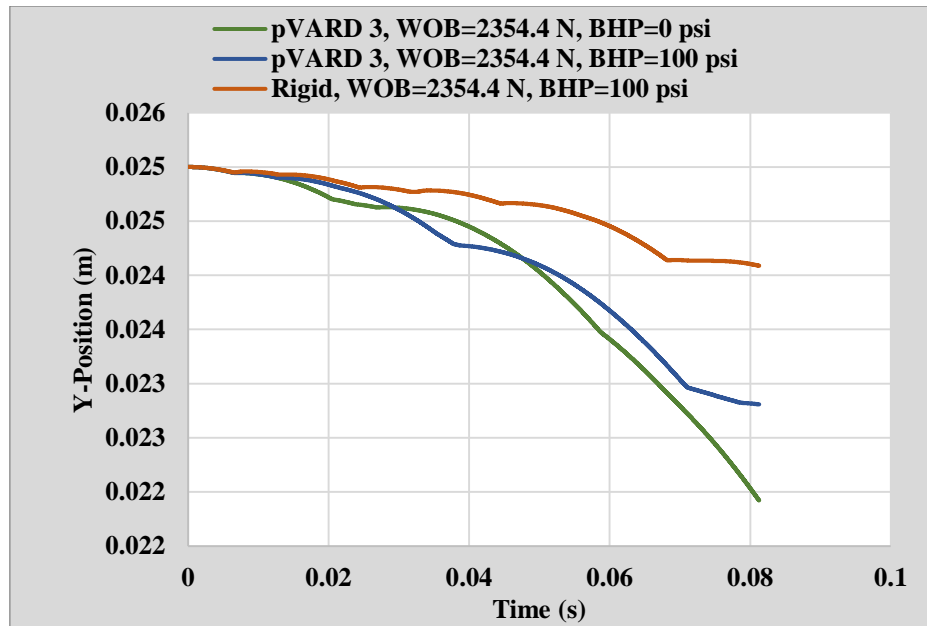


Figure 54. One set of PFC-2D output using rigid drilling for different BHP and same WOB=2354.4N.

5.4. RESULTS

The following method of data analysis adopts the graphical display of the results, in which there is comparison analysis between pVARD PFC-2D numerical study and the experimental result obtained from ARMA 15-492 (Rana et al, 2015). The comparison study is based on a double-parameter-analysis with respect to their drilling ROP, which means that the analysis is referenced to the drilling performance as well as a multiple parameter analysis. However, the drilling performance is represented by a pre-analyzed ROP. The pre-analysis is based on the associated DOC; if the DOC is greater than the depth of the chamfer of the bit cutter, then the drilling results are in the accepted range and they are considered to be used for the study. The depth of the chamfer in the PDC cutter used for the experimental work is 0.15 mm. Since we use the same PDC bit used by Hossein Khorshidian, (2012). He reported the related specifications for this PDC bit. Drilling data of the PFC-2D is considered all valid and all included in the analysis with reference to DOC due to that no chamfer is considered in the design

of PDC-2D cutter. Table 14 contains the DOC data, based on which the drilling performance is analyzed and classified.

After determining the valid drilling data to be included in the analysis based on the DOC, the study proceeded for more data evaluation including the ROP and MSE. Figure 55 shows one example of the comparison study of the simulation and the experimental results of ROP using the 3rd pVARD configuration. The result of this study shows good agreement between the two ROP results obtained experimentally and numerically.

Drilling Mode	Depth of Cut	
	EXPERIMENT	SIMULATION
pVARD 1	0.281	0.333
	0.815	0.557
	0.856	0.698
	1.080	1.320
	1.200	2.320
pVARD 2	0.350	0.357
	0.465	0.601
	0.754	1.064
	1.110	1.490
	1.002	2.348
pVARD 3	0.440	0.403
	0.674	0.674
	0.842	1.090
	1.049	1.380
	1.200	2.400
RIGID	0.262	0.303
	0.414	0.357
	0.445	0.439
	0.786	0.524
	0.766	0.911

Table 14. Summary of DOC result in PFC-2D and laboratory work.

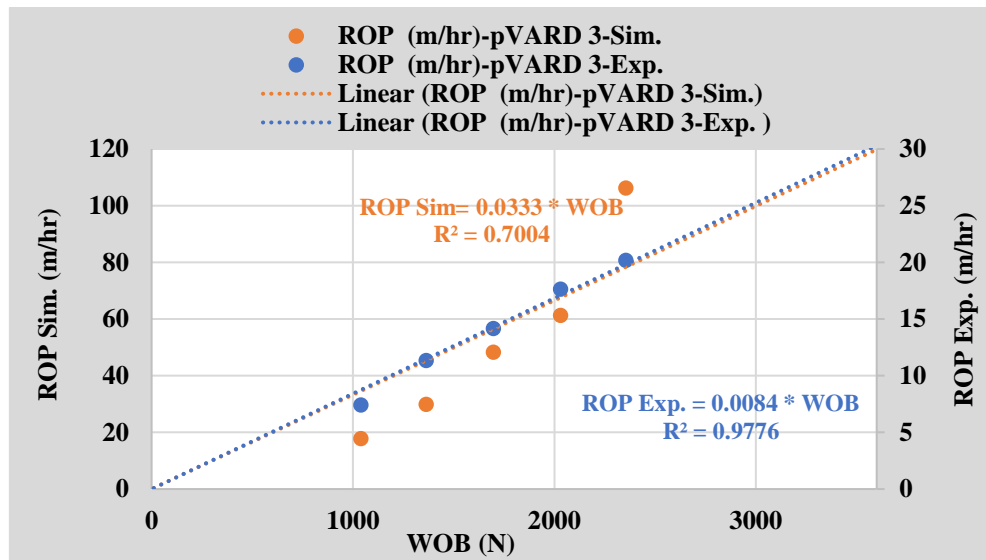


Figure 55. One example of data comparison between simulation and experimental work using the 3rd pVARD configuration.

5.4. Double parameter analysis

In this analysis, in each individual drilling configurations, two drilling parameters were analyzed with the drilling ROP, including DOC and MSE. Figures 56, 57, and 58 show the analysis of the drilling performance based on the study of ROP and DOC. The figures show that DOC was directly proportional to ROP. Figures 59, 60, 61, and 62 show the analysis of the drilling performance based on the study of ROP and MSE in 5 different WOBs using the three pVARD configurations vs. Rigid drilling in the numerical study, in which MSE was reversely proportional to ROP.

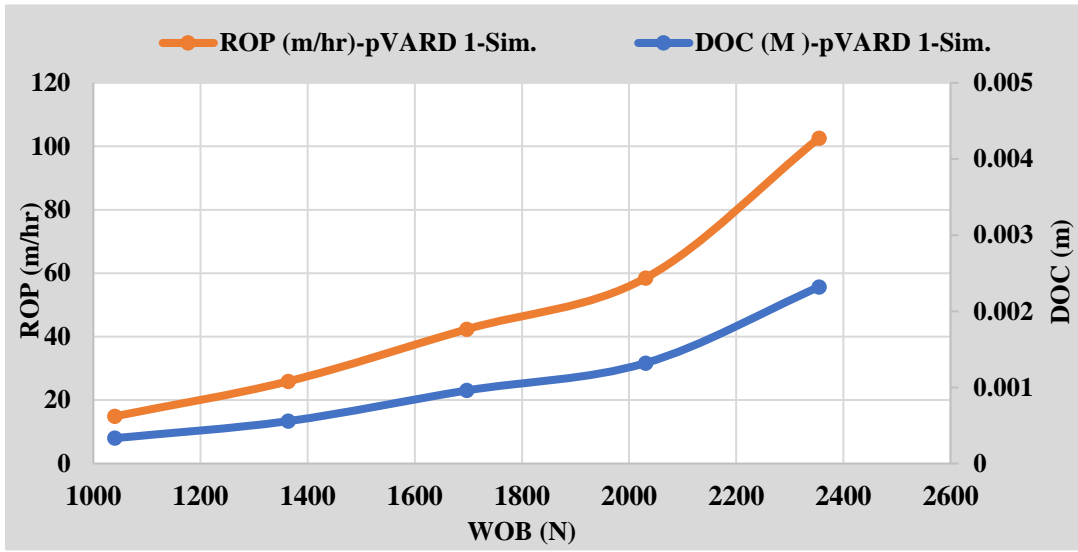


Figure 56. ROP, DOC vs WOB for simulated pVARD 1

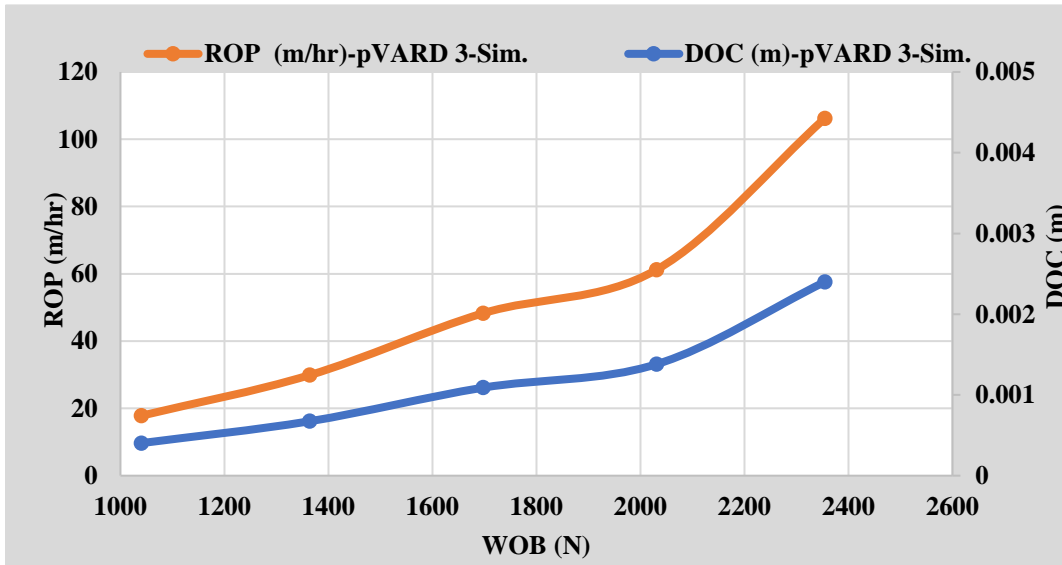


Figure 57. ROP, DOC vs WOB for simulated pVARD 2

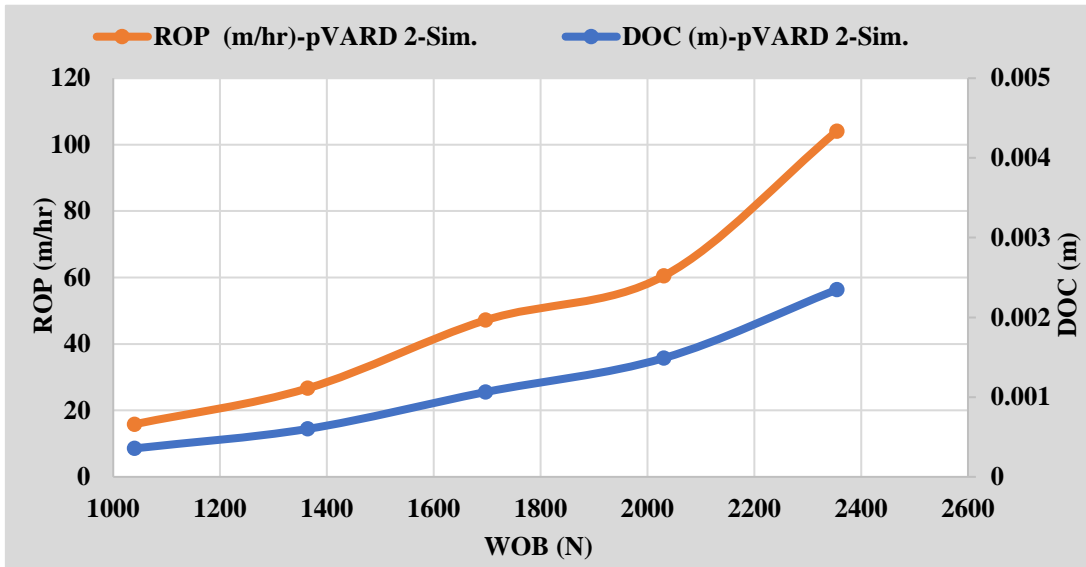


Figure 58. ROP, DOC vs WOB for simulated pVARD 3

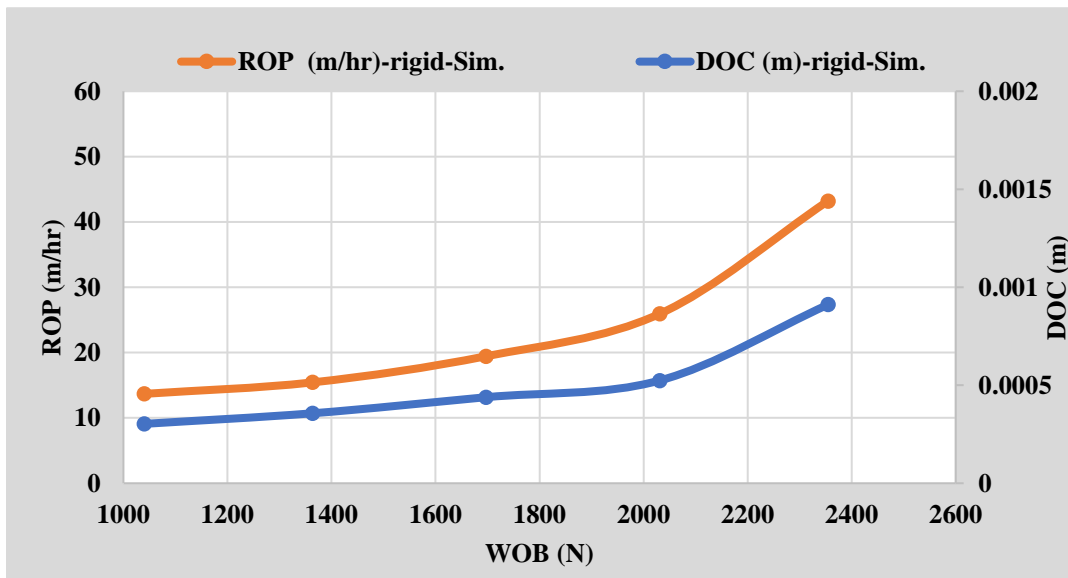


Figure 59. ROP, DOC vs WOB for simulated RIGID

Results of figures 56 through 63 show good agreement between ROP, DOC, and MSE in all drilling tests of pVARD vs. rigid and experimental work vs. simulation.

Figures 56 to 59 show the relationship between ROP and DOC in the simulation work by PDC-2D. These figures show that ROP is directly proportional to DOC showing the positive influence of the increase of DOC on ROP.

Figures 60 to 63 show the relationship between ROP and MSE in the simulation work by PDC-2D. These figures show that ROP is reversely proportional to MSE, showing the positive influence of the reduction of MSA on the efficient drilling performance through ROP.

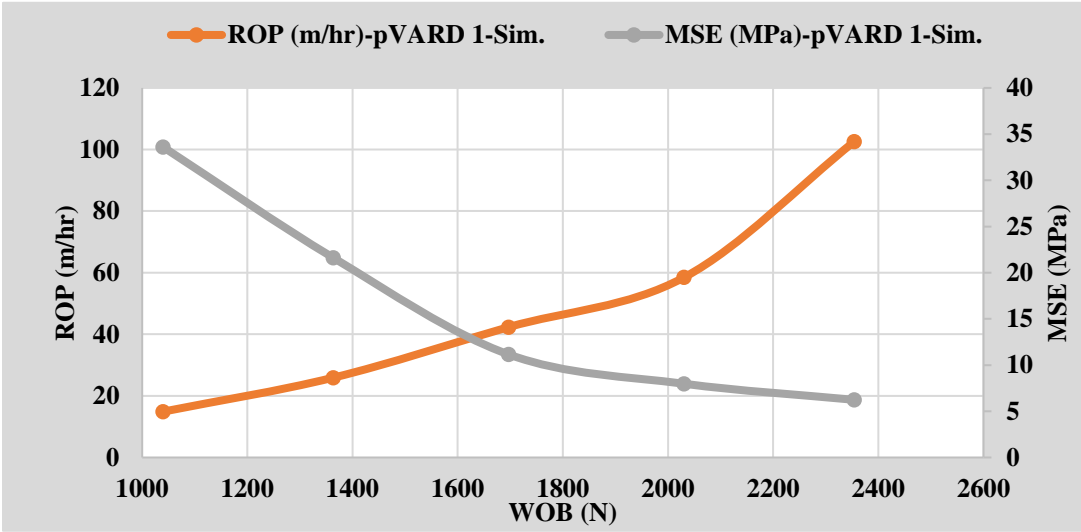


Figure 60. ROP, MSE vs WOB for simulated pVARD1.

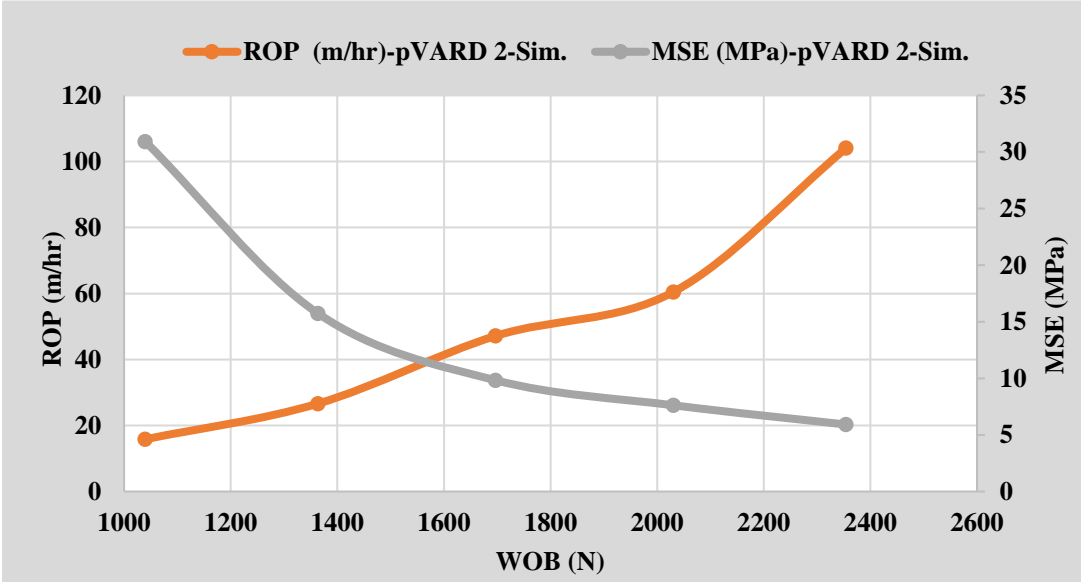


Figure 61. ROP, MSE vs WOB for simulated pVARD 2

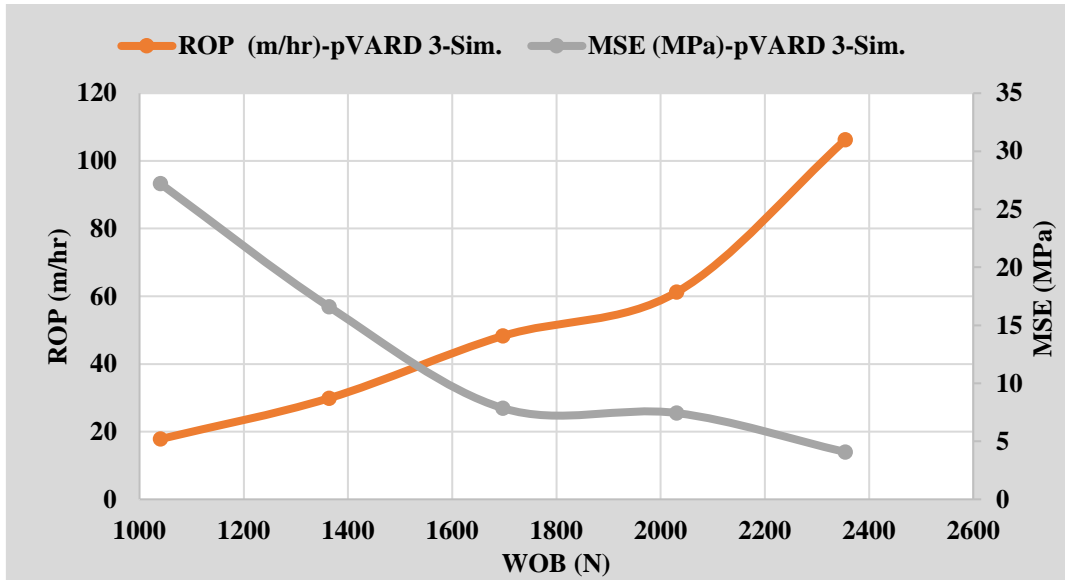


Figure 62. ROP, MSE vs WOB for simulated pVARD 3

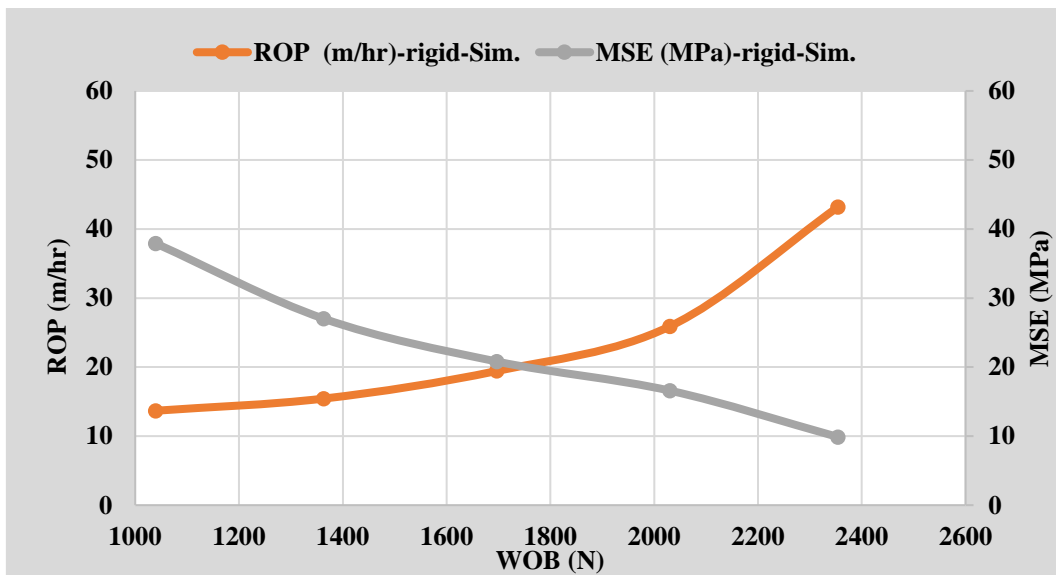


Figure 63. ROP, MSE vs WOB for simulated RIGID

5.5. Multiple parameter analysis

In this analysis, all drilling results of ROP, DOC, and MSE were analyzed together using different drilling modes of pVARD and rigid based on experimental and simulation. Figures 64 and 65 show the comparison results of ROP in different drilling modes experimentally and numerically, respectively.

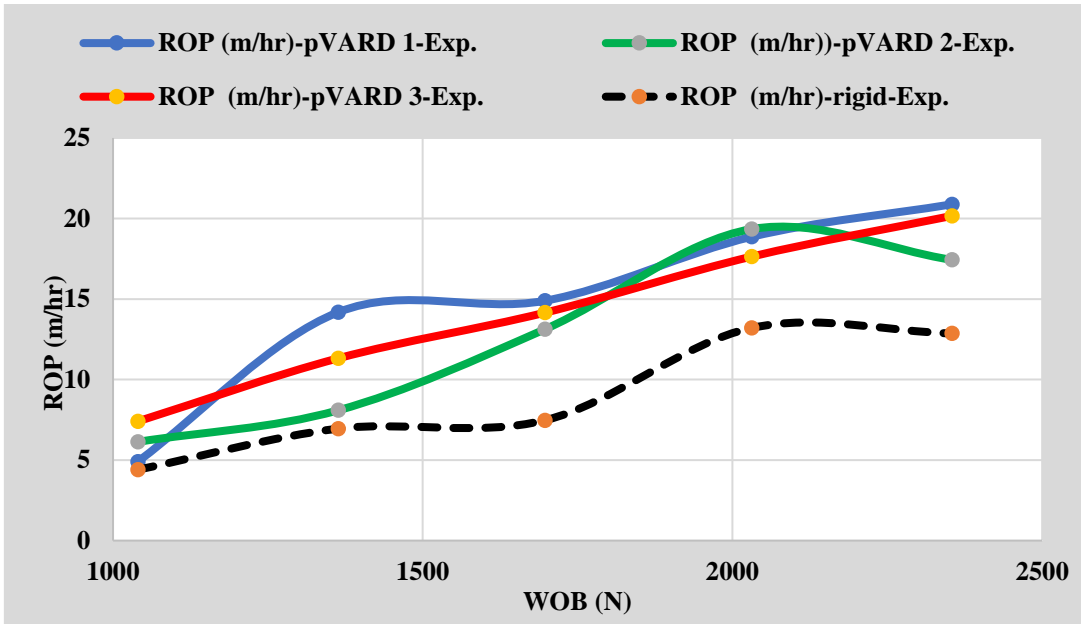


Figure 64. Compared experimental ROP in all drilling modes of pVARD and rigid.

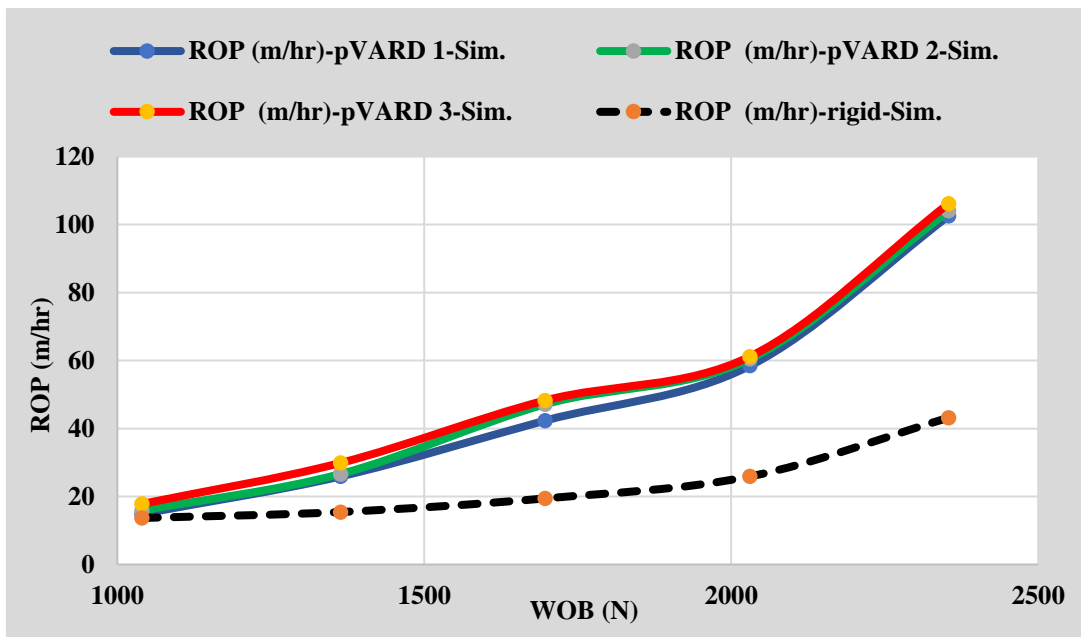


Figure 65. Compared simulated ROP in all drilling modes of pVARD and rigid.

Figures 66 and 67 show the comparison results of DOC in different drilling modes experimentally and numerically, respectively.

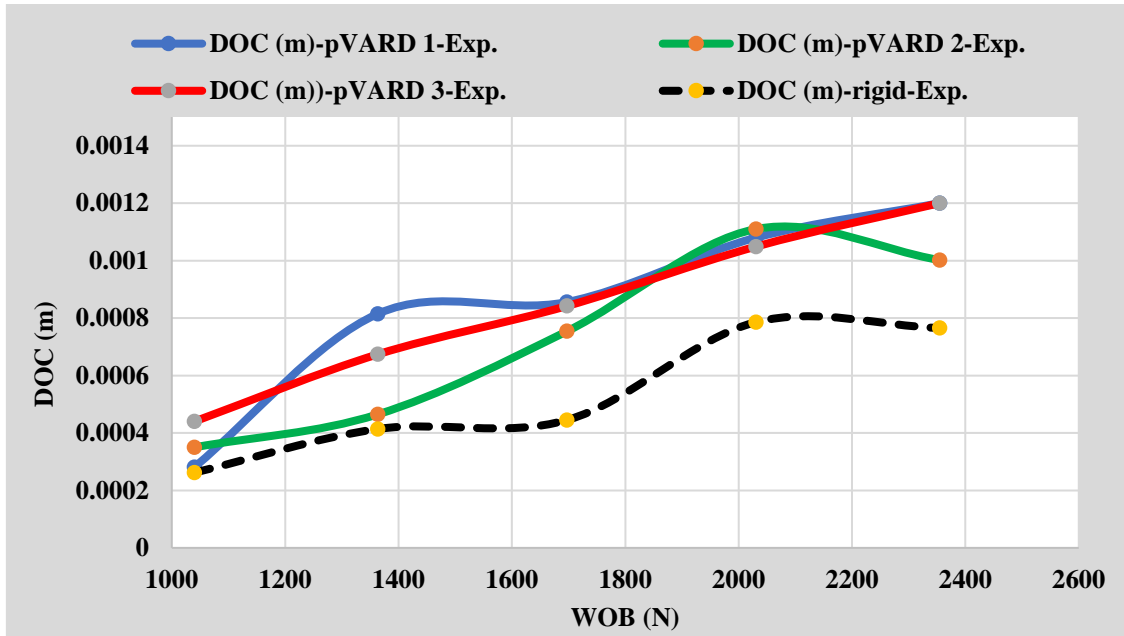


Figure 66. Compared experimental DOC in all drilling modes of pVARD and rigid.

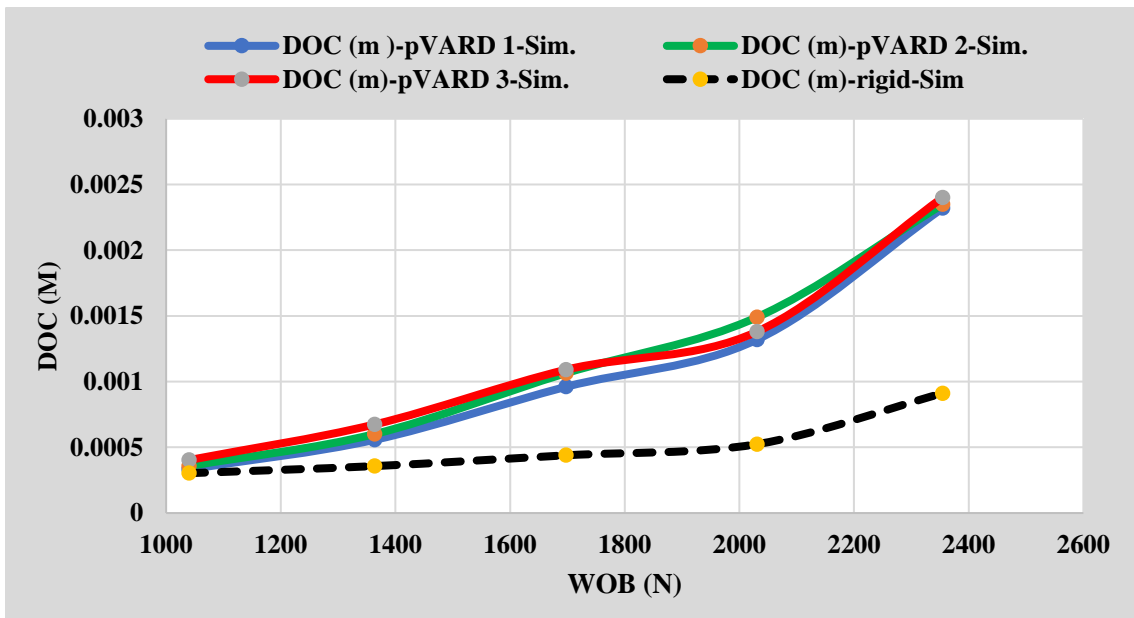


Figure 67. Compared simulated DOC in all drilling modes of PVARD and rigid.

Figures 68 and 69 show the comparison results of MSE in different drilling modes experimentally and numerically, respectively.

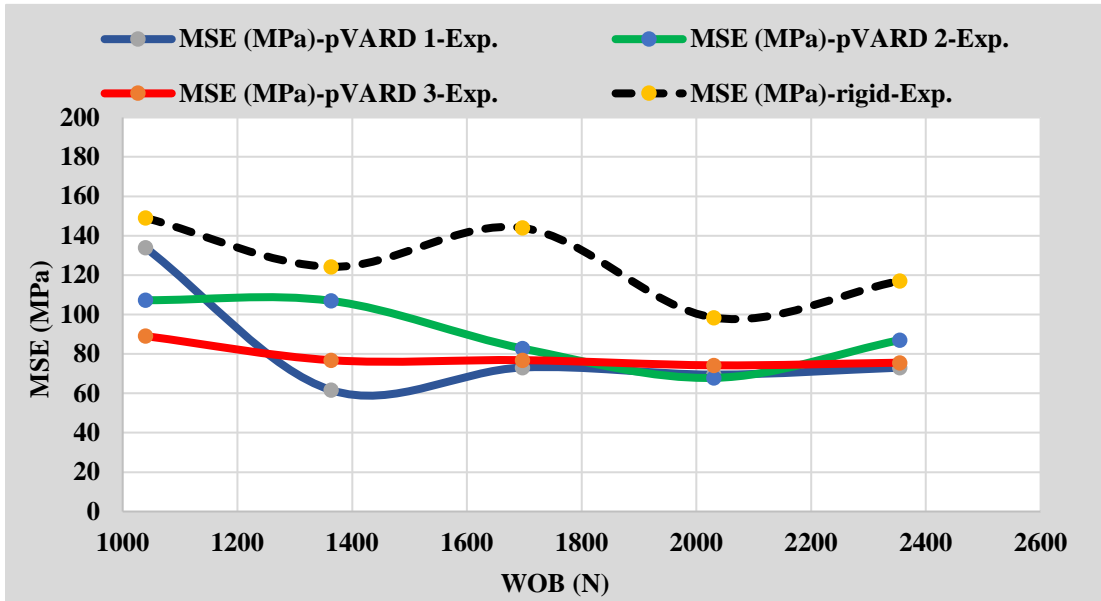


Figure 68. Compared experimental MSE in all drilling modes of pVARD and rigid.

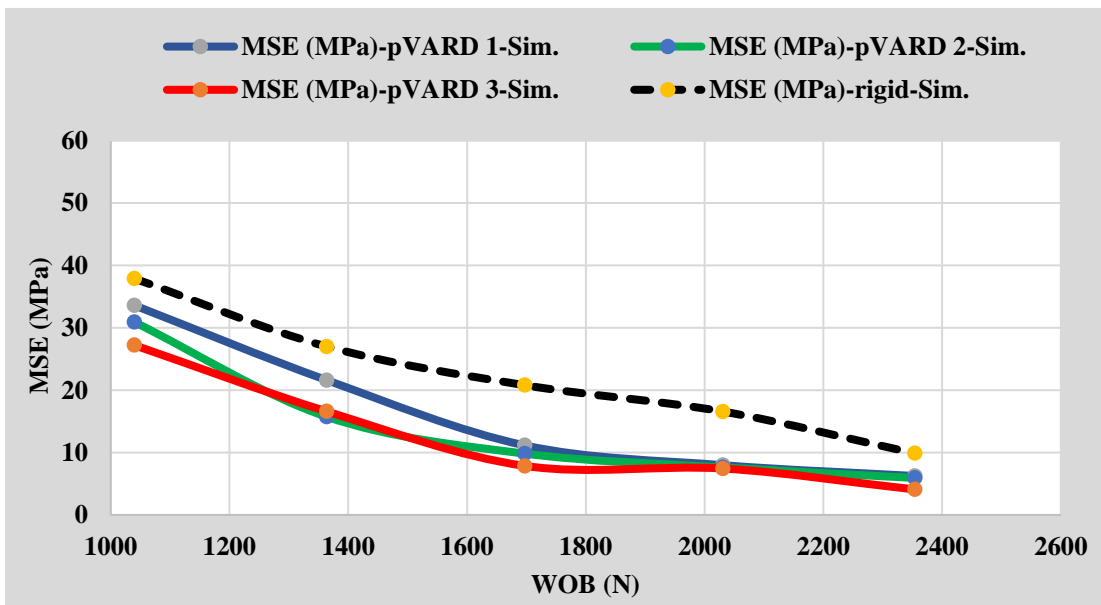


Figure 69. Compared simulated ROP in all drilling modes of pVARD and rigid.

Figure 70 shows the combined result of ROP experimentally vs. numerically. The result shows that ROP is always higher in all pVARD configurations versus rigid drilling in both experimental and numerical work. Figure 71 shows the combined result of MSE vs WOB experimentally for PDF 2D. numerically. The result shows that MSE is always lower in all pVARD configurations versus rigid drilling in both experimental and numerical work. The

result of figures 70 and 71 confirms the positive influence of pVARD on enhancing drilling performance as proved by field and laboratory, and numerical work.

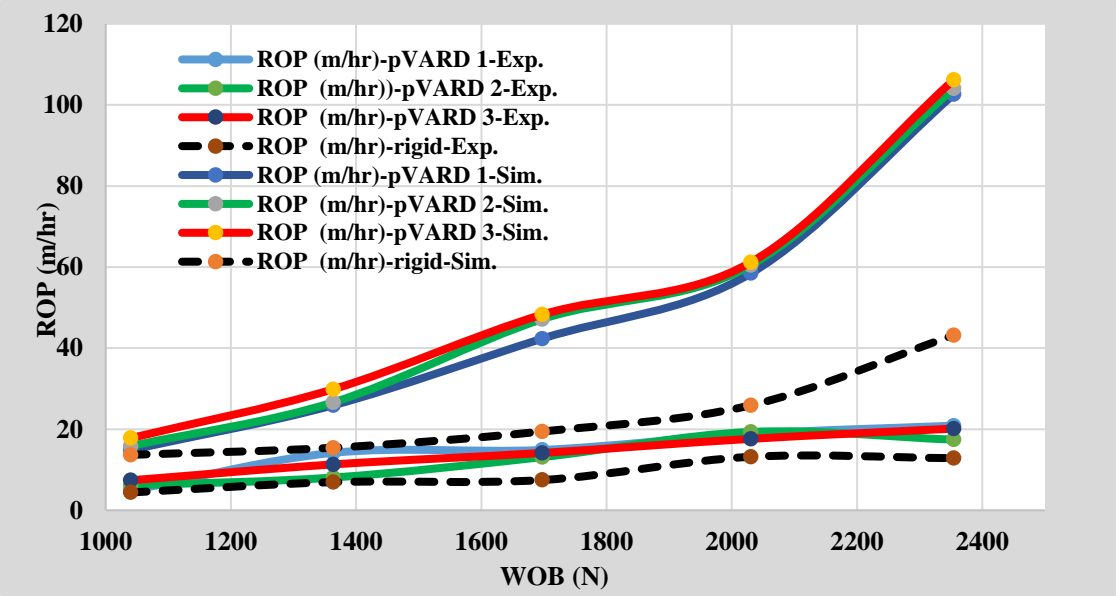


Figure 70. Compared result of ROP vs WOB for all drilling modes of experimental work vs. PFC-2D numerical work.

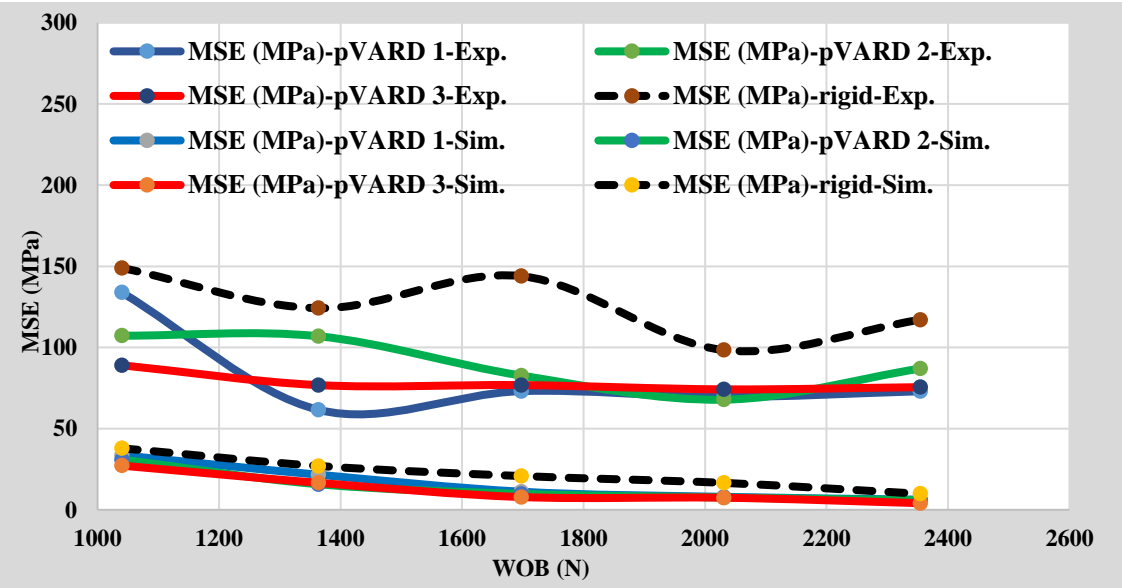


Figure 71. Compared result of MSE vs WOB for all drilling modes of experimental work vs. PFC-2D numerical work.

DISCUSSION

PFC-2D was used for simulating and validate the experimental work described above.

As shown in all figures of the double parameter section, the drilling ROP increases with the increase of DOC. This was found in all drilling tests of the experimental and the simulation. Also, the drilling ROP was found to be increasing with the decrease of the MSE. This is found in all drilling tests of the experimental and the simulation as well.

As shown in all figures of the multiple parameter section (Fig. 56 to Fig.63), the combined relationships between ROP, DOC, and MSE were found to have good agreements in all drilling modes in experimental and simulation when applying all drilling modes, including the three sets of pVARD and rigid.

As the drilling ROP increases with the increase of WOB, all ROP results from the numerical and experimental work were found to have good agreement and were increasing with the increase of WOB. In figure 64, the result of the simulated ROP was found to be the lowest in the rigid drilling compared to all pVARD configurations, which was good validation to the experimental work of the ROP shown in Figure 65. This confirms the positive influence of implementing pVARD on enhancing drilling performance.

Based on that the increase of DOC causes an increase of the drilling ROP, all DOC relationships were found to have good agreement and their increase found to result increase of ROP numerically and experimentally. In figure 66, the simulated DOC was found to be the lowest in the rigid drilling compared to all pVARD sets that had good agreement and validated the experimental results of the DOC displayed in figure 67.

As MSE has a reverses relationship with the drilling ROP and that its decrease while increasing the drilling ROP is a sign of an efficient drilling performance, all MSE results were found to be decreasing with the increase of ROP. In Figure 68, the simulated MSE result was

found to be the highest in the rigid drilling compared to all pVARD configurations confirming the positive influence of implementing pVARD on enhancing the drilling performance.

The drilling parameters mentioned above and evaluated experimentally and numerically in various drilling settings supported enhancing the drilling performance when using pVARD tool.

SUMMARY

The numerical study using the PFC-2D software conducted on the experimental work published in ARMA 15-492 (Rana et al, 2015) can be summarized in the following points:

- The numerical study supports the experimental work in approving the positive influence of PVARD on drilling performance enhancement.
- Involving more drilling parameters including DOC and MSE supported the comparison study and strengthen the validation work of both the simulation and the experimental results.

As the PFC-2D was the software used for data validation, it showed good agreements between all studied drilling parameters.

Chapter 6 Conclusion and Future Work

6.1. Conclusion

This research work has shown that single Polycrystalline Diamond Compact (PDC) cutter-rock interaction models have strong potential for resolving issues related to full bit-rock interaction. The research has also offered insight on factors leading to rock failure due to PDC bit action. Both experimental and numerical simulations provided reasonably similar outcomes, further supporting the validity of these strategies. The ROP, DOC, along with the corresponding effective WOB were analyzed, with the findings for the physical, mechanical, and drilling measurements indicating consistency in values. This outcome points to the isotropy of the rocks used in the test and also confirms that the tests were bias-free in relation to drilling orientation. After the collection and analysis of drilling cuttings, any relationships found between DOC, ROP and WOB were investigated, revealing that increased WOB leads to increases in DOC and ROP. The findings indicate as well that increased WOB results from increases in cutting sizes, again underscoring the material's anisotropy. These outcomes can help engineers and site managers form better plans for shale drilling that will result in better drilling performance, particularly in situations where the wells are deviated.

With increased WOP leading to increased drilling ROP, the ROP findings in both the experimental and numerical studies showed good agreement. In comparison with pVARD configurations, simulated ROP results were the lowest in rigid drilling scenarios, which provided reasonable validation for the ROP experimental work. It also verifies the positive effect of employing the pVARD tool for improving drill performance. Including other drilling parameters (e.g., MSE and DOC) further assisted in validating the work. In fact, the software

employed in the data validation (PFC2D) showed good agreement between all drill parameters used in the study.

6.2. Future Work.

The work of this theses will be taken as baseline for physical and mechanical measurements and drilling tests under various levels of pressures of well bottom-hole pressure while drilling and confining pressures while conducting the confined compressive strength (CCS) tests. The future work will, also be extended to cover some anisotropic rocks such as shale and new baseline for anisotropic materials will be proposed.

Medium-strength rock, which is similar to red shale in the CBS NL field trail and DTL concrete samples, was used in the PFC simulation. Future simulations could include lower- or higher-strength rock as well as other types of software (e.g., PFC3D or FDEM simulation software) for simulating bit-rock interactions.

References

- Aadnoy, B. C. (2009). Wellbore Measurement: Tools, Techniques, and Interpretation. In *Advanced Drilling and Well Technology*. Texas: SPE, 544-556.
- Abtahi, A. B. (2011, January 1). Wear Analysis and Optimization on Impregnated Diamond Bits in Vibration Assisted Rotary Drilling (VARD). American Rock Mechanics Association. The 45th US Rock Mechanics / Geomechanics Sym.
- Akbari, B. B. (2011, January). Dynamic Single PDC Cutter Rock Drilling Modeling and Simulations Focusing on Rate of Penetration Using Distinct Element Method. In 45th US Rock Mechanics/Geomechanics Symposium, San Francisco, CA (pp. 11-379).
- Al-Harhi, A. A. (1998). Effect of planar structures on the anisotropy of Ranyah sandstone, Saudi Arabia: *Engineering Geology*, 50, no. 1-2, 49-57,[http://dx.doi.org/10.1016/S0013-7952\(97\)00081-1](http://dx.doi.org/10.1016/S0013-7952(97)00081-1).
- Altindag, R. (2003). Estimation of penetration rate in percussion drilling by means of coarseness index and mean particle size. *Rock Mechanics and Rock Engineering*. 36(4):323-332.
- Amadei, B. (1996). Importance of anisotropy when estimating and measuring in situ stresses in rock ,*Int. J. Rock Mech. Min. Sci.&Geomech. Abstr.*,33(3), 293-325.
- Ambrose, J. Z.-R. (2014). Failure of shales under triaxial compressive stress. American Rock Mechanics Association, the 48th US Rock Mechanics/Geomechanics Symposium in Minneapolis, MN, USA, 1-4 June 2014.
- Ashley, D. X. (2001). "Extending BHA Life with Multi-Axis Vibration Measurements." SPE/IADC Drilling Conference. Amsterdam, 2001.

ASTM C136/C136M-14. (2014). Standard test method for sieve analysis of fine and coarse aggregates. Astm International, West Conshohocken, PA, 2014, www.astm.org.

ASTM D5731-08. (n.d.). Standard test method for determination of the point load strength index of rock and application to rock strength classifications, astm international, west conshohocken, PA, 2014, www.astm.org.

ASTM Standard D2845. (2008). “Standard Test Method for Laboratory Determination of Pulse Velocities and Ultrasonic Elastic Constants of Rock,.” *ASTM International, West Conshohocken, PA, www.astm.org* .

ASTM Standard D4543. (2008). “Standard Test Method for Preparing Rock Core as Cylindrical Test Specimens and Verifying Conformance to Dimensional and Shape Tolerances,.” *ASTM International, West Conshohocken, PA, www.astm.org* .

ASTM Standard. (2012). “Standard Test Method for Indirect Tensile (IDT) Strength of Bituminous Mixtures,.” ASTM International, West Conshohocken, PA, 2012, www.astm.org.

Azar J., S. G. (2007). *Drilling Engineering*. Tulsa, Oklahoma.

Babatunde O.Y. (2011). *The Effects Of Varying Vibration Frequency And Power On Efficiency In Vibration Assisted Rotary Drilling*, Final MEng. Thesis, Memorial University of Newfoundland, St. John’s, NL, Canada. November, 2011.

Biligin N, D. M. (2006). Dominant rock properties affecting the performance of conical picks and the comparison of some experimental and theoretical results. *International Journal of Mining Engineering*, 43(1): 139–156.

Birch, F. (1961). The Velocity of Compressional Waves in Rocks to 10 Kilobars, Part 2. *Journal of Geophysical Research*, (66), pp. 2199-2224.

Boualleg, R. S. (2007). Effect of rocks anisotropy on deviation tendencies of drilling systems. 11th Congress of the International Society for Rock Mechanics, pp. 1221-1224. Taylor and Francis Group, London, ISBN: 978-0-415-45084-3.

Bourgoyne, A. M. (1986). *Applied Drilling Engineering*. Richardson, Texas, USA: Society of Petroleum Engineers.

Bowden, A. J.-B. (1998). "Point Load Testing of Weak Rocks with Particular Reference to Chalk", *Quarterly Journal Engineering Geology*. 31, (2), pp. 95-103.

Bowman S.D. (2007). Technical Note: A New, Highly Portable Point Load Test Device for Extreme Field Areas," *Environmental and Engineering Geoscience*, XIII, (1), pp.69-73.

Brown, E. R. (1977). Shear strength characteristics of Delabole slates. In *Proceedings of the conference rock engineering*, Newcastle upon Tyne (pp.33-51).

Carrapatoso, C. d. ((2013, January 1).). Simulation of single cutter experiments in evaporite using the discrete element method. In *ISRM International Symposium-EUROCK 2013*. International Society for Rock Mechanics and Rock Engineering.

Chappell, B. A. (1990). Moduli stress dependency in anisotropic rock masses. *Mining Science and Technology*, 10(2), 127-143.

Chen, S. L. (n.d.). (2002, March 1). Field Investigation of the Effects of Stick-Slip, Lateral, and Whirl Vibrations on Roller-Cone Bit Performance. Society of Petroleum Engineers. doi:10.2118/76811-PA.

- Cho, J. K. (2012). Deformation and strength anisotropy of Asangneiss, Boryeong shale, and Yeoncheon schist, *Int.J.Rock Mech.&Min.Sci.*,50(12), 158-169.
- Copur H, B. N. (2003). A set of indices based on indentation tests for assessment of rock cutting performance and rock properties[J]. *The Journal of the South African Institute of Mining and Metallurgy*, , 103(9): 589— 599.
- Crawford, B. R. (2012). Shear strength anisotropy in fine-grained rocks. American Rock Mechanics Association, the 46th U.S. Rock Mechanics/Geomechanics Symposium, ARMA, 12-290.
- D5731, A. S. (2008). “Standard Test Method for Determination of the Point Load Strength Index of Rock and Application to Rock Strength Classifications,” ASTM International, West Conshohocken, PA, 2008, www.astm.org.
- D7012, A. S. (2014). “Standard Test Methods for Compressive Strength and Elastic Moduli of Intact Rock Core Specimens under Varying States of Stress and Temperatures,” ASTM International, West Conshohocken, PA, 2014, www.astm.org.
- Dan, D. H. (2013.). Brazilian tensile strength tests on some anisotropic rocks. *International Journal of Rock Mechanics and Mining Sciences*, (58), 1-7.
- Debecker, B. A. (2013). Two-dimensional discrete element simulations of the fracture behaviour of slate. *International Journal of Rock Mechanics and Mining Sciences*, 61: p. 161-170.

- Detournay, E. A. (1962). A phenomenological model for the drilling action of drag bits. *International Journal of Rock Mechanics and Mining Sciences & Geomechanics Abstracts*, Volume 29, Issue 1, pp 13-23.
- Detournay, E. R. (2008). Drilling response of drag bits: Theory and experiment. *International Journal of Rock Mechanics and Mining Sciences*, Volume 45, Issue 8, pp 1347–1360.
- Dubinsky, V. H. (1992). *Surface Monitoring of Downhole Vibrations: Russian, European, and American Approaches*. European Petroleum Conference. Cannes, France: Society of Petroleum Engineers.
- Dunayevsky, V. A. (1993). Dynamic Stability of Drillstrings Under Fluctuating Weight on Bit. *SPE Drilling and Completion* 8 (2), Volume 8, Issue 2, pp 84-92: Society of Petroleum Engineers.
- Dupriest, F. E. (2005). *Maximizing Drill Rates with Real-Time Surveillance of Mechanical Specific Energy*. SPE/IADC Drilling Conference. Amsterdam, The Netherlands: Society of Petroleum Engineers.
- Duveau, G. S. (1988). Assessment of some failure criteria for strongly anisotropic geomaterials. *Mechanics of Cohesive-Frictional Materials*, 3(1), 1–26.
- Elnahas, A. (2014). *Experimental investigation of the effect of axial vibration generated by pressure pulses on drilling performance* Doctoral dissertation, Memorial University of Newfoundland st john's,NL,Canada.
- Evans, I. (1984). , "A theory of the cutting force for point-attack picks." *International Journal of Mining Engineering* 2, no. 1 (1984): 63-71.

- Fjær, E. A.-M. (2013). Strength anisotropy of Mancos shale. American Rock Mechanics Association, the 47th US Rock Mechanics/Geomechanics Symposium in San Francisco, CA, USA, 23-26 June 2013.
- Garner, N. (1967). Cutting Action of a Single Diamond Under Simulated Borehole Conditions. *Journal of Petroleum Technology*, Volume 16, Issue 7, pp 937-942: Society of Petroleum Engineers.
- Gatlin, C. M. (2013). Mechanical Anisotropies of Laminated Sedimentary Rocks. *Society of Petroleum Engineers Journal*, 5(01), 67–77.
- Gee, R. H. ((2015, March 17).). Axial Oscillation Tools vs. Lateral Vibration Tools for Friction Reduction- What’s the Best Way to Shake the Pipe? Society of Petroleum Engineers. The SPE/IADC Drilling Conferen.
- Gerbaud, L. M. (2006). PDC Bits: All Comes From the Cutter/Rock Interaction. IADC/SPE Drilling Conference, Miami, Florida, USA: Society of Petroleum Engineers.
- Gharibiyamchi, Y. (2014). Evaluation and characterization of hydraulic pulsing drilling tools and potential impacts on penetration rate (Doctoral dissertation, Memorial University of Newfoundland).
- Glowka, D. (1989). Use of Single-Cutter Data in the Analysis of PDC Bit Designs: Part 1- Development of a PDC Cutting Force Model. *Journal of Petroleum Technology*, Volume 41, Issue 8, pp 850 - 859.
- Goktan, R. M. (1997). A suggested improvement on Evans’s cutting theory for conical bits, *Proceedings of fourth symposium on mine mechanization automation*, 1 (1997) 57-61.

- Hentz, F. D. (2004). Discrete Element Modelling Of Concrete Submitted To Dynamic Loading At High Strain Rates, *Computers and Structures*, vol. 82, pp. 2509–2524,.
- Horino, F. (1970). A method for estimating strength of rock containing planes of weakness (Vol. 7449). US Dept. of Interior, Bureau of Mines, USA.
- Hornby B.E. (1998). Experimental laboratory determination of the dynamic elastic properties of wet, drained shales." *Journal of Geophysical Research: Solid Earth* 103, no. B12 (1998): 29945-29964.
- Inc., I. C. (2008). Particle Flow Code Manual 4th edition.
- ISRM. (1885). Commission on Testing Methods, Suggested Method for Determining the Point Load Strength (Revised. *Int. Journal Rock Mech. Min. Sci. and Geomech. Abstr.*, (22), pp. 51-60.
- ISRM. (1981). "Rock Characterization, Testing and Monitoring,. ISRM Suggested methods, Pergamon press,Oxford, UK.
- Mendoza, I. G. (2010). Discrete element modeling of rock cutting using crushable particles, presented at the 44th U.S. Rock mechanics symposium and 5th U.S./Canada Rock mechanics symposium, Salt Lake City, UT, USA.
- Jinghan Zhong, J. Y. (2016). DEM simulation of enhancing drilling penetration using vibration and experimental validation. In *Proceedings of the 49th Annual Simulation Symposium* (p. 12). Society for Computer Simulation International.
- Johnston, J. E. (1995). Seismic anisotropy of shales: *J. Geophys. Res.*, 100, 5991–6003.

- Karfakis, M. A. (1987). Technical Note: Effects of rocks lamination anisotropy on drilling penetration and deviation. *Int. J. Rock Mech. Min. Sci. and Geomech. Abstr.* Vol. 24, pp.371-374, 1987, United Kingdom.
- Khorshidian, H. B. (2014). .Influence of High Velocity Jet on Drilling Performance of PDC bit under Pressurized Condition, 48th US Rock Mechanics/GeoMechanics Symposium, Minneapolis, MN, USA.
- Khorshidian, H. M. (24-27 June 2012). “The Role of Natural Vibrations in Penetration Mechanism of a single PDC cutter”, ARMA 12-09, Proceedings of 46th US Rock Mechanics/Geomechanics Symposium, Chicago, IL, US, .
- Kolle, J. (2004). HydroPulse Drilling, Final Report. Retrieved 18 Feb. 2014 from http://www.netl.doe.gov/technologies/oil-gas/publications/.../Final_34367.pdf.
- Larsen, L. (2014). *Larsen, Lena. "Tools and techniques to minimize shock and vibration to the bottom hole assembly.*
- Lashkaripour, G. A. (2000). Strength anisotropies in mudrocks: *Bulletin of Engineering Geology and the Environment*, 59, no. 3,195-199, <http://dx.doi.org/10.1007/s100640000055>.
- Ledgerwood, L. (2007). PFC modeling of rock cutting under high pressure conditions in 1st Canada-US Rock Mechanics Symposium.
- Lekhnitskii, S. (1963). *Theory of elasticity of an anisotropic body*, Holden- Day.Mas Ivars, D., Pierce, M.E., Darcel, C., Reyes-Montes, J., Potyondy, D.O., Young, P.R. and Cundall,

- P.A., 2011, The synthetic rock mass approach for jointed rock mass modelling. *Int. J. RockMech.& Min.Sci.*, 48(2),219-44.
- Lesage, M. F. (1988). Evaluating Drilling Practice in Deviated Wells with Torque and Weight Data”, *SPE Drilling Engineering*, September 1988.
- Li, H. (2011). Experimental investigation of the rate of penetration of Vibration Assisted Rotary Drilling. Master's dissertation, Memorial University of Newfoundland, St. John's,NL ,Canada.
- Li, H. B. (2010). Experimental Investigation of Bit vibration on rotary drilling Penetration rate” ARMA 10-426, 44th US ROCK Mechanics Symposium and 5th US-Canada Rock Mechanics Symposium, Salt Lake City.
- Lisjak, A. E. (2014). Numerical Modelling of the Anisotropic Mechanical Behaviour of Opalinus Clay at the Laboratory-Scale Using FEM/DEM. *Rock Mechanics and Rock Engineering*, 47(1): p. 187-206. .
- Maurer, W. C. (1962). (The Perfect - Cleaning Theory of Rotary Drilling. *Journal of Petroleum Technology*, Volume 14, Issue 11, pp 1270-1274: Society of Petroleum Engineers.
- McCray, W. a. (1959). *Oil Well Drilling Technology*. Oklahoma: University of Oklahoma Press, Norman In USA , pp 351-356.
- Melaku, M. T. (2007). Velocity anisotropy of shales and sandstones from core sample and well log on the Norwegian continental shelf (Doctoral dissertation, Dissertation, University of Oslo)..

- Mele'ndez-Marti'nez, J. (2014.). Elastic properties of Sedimentary rocks, Edmonton, AB: University of Alberta.
- Mensa-Wilmot, G. L. (2010). Drilling Efficiency and Rate of Penetration: Definitions, Influencing Factors, Relationships, and Value. In IADC/SPE Drilling Conference and Exhibition. Society of Petroleum Engineers,.
- Mighani, S. S. (2016). Observations of tensile fracturing of anisotropic rocks. Society of Petroleum Engineers. SPE Journal, doi:10.2118/2014-1934272-PA.
- Mohammed Fayez, A. D. (2012). Investigation of drillstring vibration reduction tools." .
- Mozaffari, M. (2013). Comprehensive simulation of single PDC cutter penetration using distinct element modeling (DEM) methods,2013 Master's thesis, Memorial University of Newfoundland, St. John's, NL ,Canada .
- Nasseri, M. K. (2003). Anisotropic strength and deformational behavior of Himalayan schists. International Journal of Rock Mechanics and Mining Sciences, . 40(1): p. 3-23.
- Nur, V. L. (1992). Petrophysical classification of siliciclastics for lithology and porosity prediction from seismic velocities: Bulletin of the American Association of Petroleum Geologists, 76, 1295-1309.
- Omid, A. (2008). "Innovations in Rotary Drill Bit Design to Reduce Vibration and Improve Durability. (2008).
- Onyia, E. C. (1988). "Relationships between Formation Strength, Drilling Strength, and Electric Log Properties," the 63rd Annual Conference and Exhibition of the Society of Petroleum Engineers, Houston, 2-5 October.

- Park, B. (2013). Discrete element modeling of transversely isotropic rock. American Rock Mechanics Association, the 47th US Rock Mechanics/Geomechanics Symposium in San Francisco, CA, USA, 23-26 June 2013.
- Payne, M. A. (1995). Drilling Dynamic Problems and Solutions for Extended-Reach Operations. In *Drilling Technology PD-volume 65*, ed. J.P. Vozniak, 191-203. New York: ASME.
- Pessier, R. D. (2011). Hybrid Bits Offer Distinct Advantages in Selected Roller-Cone and PDC-Bit Applications. *SPE Drilling & Completion*, Volume 26, Issue 1, pp 96-103.
- Pfleider, E. A. (1953). Research on the cutting Cutting Action of the Diamond Drill Bit. *Mining Eng. 5*: 187-195.
- Pietruszczak, S. L. (2002). Modelling of inherent anisotropy in sedimentary rocks. *International Journal of Solids and Structures*, 39(3), 637–648.
- Pixton, D. a. (2010). New-Generation Mud-Hammer Drilling Tool, Annual report. Retrieved 24 Nov. 2010 from: <http://www.netl.doe.gov/KMD/cds/Disk28/NG2-2.PDF>.
- Potyondy, D. O. (2004). A Bonded-Particle Model For Rock," *Int. J. Rock Mech. Min. Sci.*, 41, 1329-1364.
- Rahman, R. (2015). Development and Interpretation of Downhole Data from Downhole Vibration Monitoring Tool. Faculty of Engineering and Applied Science. St. John's, Newfoundland, Canada:
- Ramamurthy, T. (1993). Strength and Modulus Responses of Anisotropic Rocks. *Compressive Rock Engineering*,(1), pp. 313-329, Pergamon press, Oxford.

- Rana, P. A. (June- 1 July, 2015). Experimental and Field Application of Passive-Vibration Assisted Rotary Drilling (p-VARD) Tool to Enhance Drilling Performance. To be published in proceedings of 49th US Rock Mechanics / Geomechanics Symposium held in San Francisco, CA, USA, 28.
- Ranman K E. (1985). A model describing rock cutting with conical picks[J]. *Rock Mechanics and Rock Engineering*, , 18(2): 131 – 140.
- Reich, M. H. (1995). Drilling Performance Improvements Using Downhole Thrusters. *Society of Petroleum Engineers, January 1*, doi:10.2118/29420-MS.
- Reyes, R. K. (2015). Cuttings Analysis for Rotary Drilling Penetration Mechanisms and Performance Evaluation in ARMA 15-764 Memorial University of Newfoundland, St. John's, NL, Canada.
- Rezapour, A. (2015). Modeling of Mechanical Behaviour of Anisotropic Rocks (Doctoral dissertation).
- Richard, T. D. (2002). Influence of bit-rock interaction on stick-slip vibrations of PDC bits. SPE Annual Technical Conference and Exhibition. San Antonio, Texas: Copyright 2002, Society of Petroleum Engineers Inc.
- Sandford, M. R. (1974). Intrinsic shear strength of a brittle, anisotropic rock—I. *International Journal of Rock Mechanics and Mining Sciences & Geomechanics Abstracts*, 11(11), 423–430.
- Schamp, J. E. (2006). Torque Reduction Techniques in ERD Wells”, SPE/IADC 98969 presented at the SPE/IADC Drilling Conference, Miami, Florida, February 2006. .

- Schen, A. E.(2005, January 1). Optimization of Bit Drilling Performance Using a New Small Vibration Logging Tool. Society of Petroleum Engineers. doi:10.2118/92336-MS.
- Schlumberger. (2017). PDC Smith Bits Data Sheet. Retrieved from www.slb.com/pdc.
- Schmalhorst, B. (1999). Dynamic Behaviour of a Bit-Motor-Thruster Assembly. *SPE Paper 52823, SPE/IADC Drilling Conference, March*.
- Sellami, H. F. (1989). The Role of In-situ Rock Stresses And Mud Pressure on the Penetration Rate of PDC Bits. Rock at Great Depth, Maury & Fourmaintraus (eds), ISBN 9061919754, pp769-779.
- Simpson, N. D. (2014). Failure mechanics of anisotropic shale during Brazilian tests. American Rock Mechanics Association, the 48th US Rock Mechanics/Geomechanics Symposium in Minneapolis, MN, USA, 1.
- Sondergeld, C. A. (2011). Elastic anisotropy of shale: The leading Edge, 30, 324-331, <http://dx.doi.org/10.1190/1.3567264>.
- Soroush, H. (2003). “Evaluation of Some Physical and Mechanical Properties of Rocks Using Ultrasonic Pulse Technique and Presenting Equations between Dynamic and Static Elastic Constants. *International Society for Rock Mechanics, Technolog*.
- Speer, J. W. (1959). A Method for Determining Optimum Drilling Techniques. Gulf Coast Drilling and Production Meeting. Lafayette, Louisiana, USA: Society of Petroleum Engineers.
- Strack, P. C. (1979). A Discrete Numerical Model For Granular Assemblies. *Geotechnique*, 29:47–65,.

- Taylor, M. M. (1996). High penetration rates and extended bit life through revolutionary hydraulic and mechanical design in PDC drill bit development, SPE 36435. Society of Petroleum Engineers, Inc. , 191-204.
- Thuro, K. A. (2008). Fracture propagation in anisotropic rocks during drilling and cutting, Geomechanics and Tunnelling, Volume 1, Issue 1, PP. 8–17, 2008.
- Tien, Y. A. (2001). A failure criterion for transversely isotropic rocks. International Journal of Rock Mechanics and Mining Sciences. 38(3): p.399-412.
- Tsidzi, K. (1997). Propagation Characteristics of Ultrasonic Waves in Foliated Rocks. International Association of Engineering Geology,(56), pp. 103-113.
- Tutluoglu, L. (1984). Mechanical rock cutting with and without high pressure water jets. University Microfilms International, Ann Arbor, MI, PhD dissertation, Berkeley: University of California, Berkeley.
- Unlu, T. K. (2004). Effect of transverse anisotropy on the Hoek–Brown strength parameter “mi” for intact rocks. International Journal of Rock Mechanics and Mining Sciences, 41(6), 1045–1052.
- Vernik L. (1997). Predicting porosity from acoustic velocities in siliciclastics: a new look: Geophysics 62, 118-128.
- Wang, Z. (2002). Seismic anisotropy in sedimentary rocks, part 2: Laboratory data: Geophysics, 67, 1423–1440,.
- Wang, Z. (2002). Seismic anisotropy in sedimentary rocks, part 1: A single-plug laboratory method: Geophysics, 67, 1415–1422,.

Wells, M. M. (2008). Bit Balling Mitigation in PDC Bit Design. IADC/SPE Asia Pacific Drilling Technology Conference and Exhibition. Jakarta, Indonesia: Society of Petroleum Engineers.

Wikipedia Shi, G. (1989). Wikipedia Shi, G, Discontinuous deformation analysis – A new numerical model for the statics and dynamics of deformable block structures, 16pp. In 1st U.S. Conf. on Discrete Element Methods, Golden. CSM Press: Golden, CO, .

Wilson, J. K. (2017, March 14).). Inducing Axial Vibrations in Unconventional Wells: New Insights through Comprehensive Modeling. In SPE/IADC Drilling Conference and Exhibition. Society of Petroleum Engineers.

Xia, M. Z. (2009). Experimental Study And PFC Modelling Of Failure Process Of Brittle Rock Under Uniaxial Compression. 43rd U.S. Rock Mechanics Symposium & 4th U.S. – Canada Rock Mechanics Symposium. Asheville, North Carolina: American .

Babatunde O,Y. (2011). Investigation of the effects of vibration frequency on rotary drilling penetration rate using diamond drag bitUS Rock Mechanics / Geomechanics Symposium held in San Francisco, CA, June 26–29,.